AUTOMATIC CLASSIFICATION OF WOODEN CABINET DOORS USING COMPUTER VISION

by

Bin Yuan

Thesis submitted to the Faculty of the

Virginia Polytechnic Institute and State University

in partial fulfillment of the requirements for the degree of

Master of Science

in

Electrical Engineering

APPROVED:

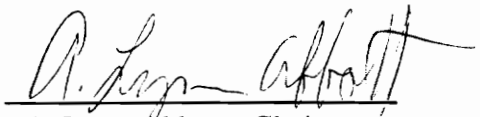

A. Lynn Abbott, Chairman

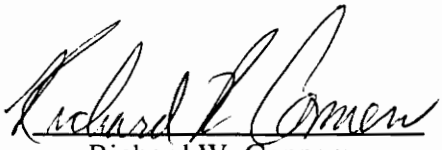

Richard W. Conners

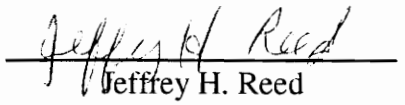

Jeffrey H. Reed

November, 1994

Blacksburg, Virginia

c.2

AUTOMATIC CLASSIFICATION OF WOODEN CABINET DOORS USING COMPUTER VISION

by

Bin Yuan

Committee Chairman: A. Lynn Abbott

Electrical Engineering

(ABSTRACT)

This thesis describes the use of computer vision techniques for distinguishing wooden components in a manufacturing environment. The components considered here are kitchen cabinet doors, which are produced in many different styles and sizes, and travel on a conveyor at 30 feet per minute. An automatic classification system has been developed which can classify doors reliably. The system includes a host computer with video digitizer, two laser sources, and three video cameras to obtain profile images. This thesis describes the careful design of illumination and sensing geometry, the profile-based feature extraction process, and the classification method. The system exists as a laboratory prototype, and has been successfully tested with a large number of samples.

Acknowledgements

I would like to thank my advisor, Dr. A. Lynn Abbott, for his invaluable guidance and encouragement throughout this project, and the patience and support he has given me throughout the development of this thesis. I would also like to thank Dr. Conners and Dr. Reed for their helpful advice and for being on my committee. I am grateful to Skip Landes from American Woodmark for the information he provided concerning the cabinet door classification. I wish to thank the graduate students of the Spatial Data Analysis Laboratory and the faculty and staff of the Electrical Engineering Department for making my stay at Virginia Tech both rewarding and enjoyable. Those I especially wish to thank are Farooq Bari for his suggestions on this project, and Loretta Estes for her administrative assistance. Most of all, I want to thank my family for their unlimited understanding and support during my study in the U.S.

TABLE OF CONTENTS

1. INTRODUCTION 1
1.1. Motivation 1
1.2. Background 2
1.3. Objective 3
1.4. Contributions of this research 4
1.5. Outline of thesis 5
2. PROBLEM DESCRIPTION AND PROPOSED SOLUTIONS 6
2.1. Production environment 6
2.2. Problem description 7
2.3. Mathematical representation 10
2.4. Proposed solution for automated classification 12
2.5. Assumptions 17
3. PREVIOUS WORK 19
3.1. Image acquisition 19
3.2. Image processing 23
3.2.1. Thinning 24
3.2.2. Template matching 25
3.2.3. Edge detection 26
3.3. Previous work on shape descriptors 27
3.3.1. Moment based shape descriptors 28
3.3.2. Template matching 28
3.3.3. Feature based shape descriptors 29
3.3.4. Summary 30
4. PROFILE CLASSIFICATION 31
4.1. Overview 31
4.2. Profile extraction 31
4.3. Preprocessing steps 33

4.4. Profile classification by template matching 37
4.4.1. Database 37
4.4.2. Mathematical representation of template matching 38
4.4.3. Summary 38
4.5. Feature based profile classification 39
4.5.1. Feature extraction 40
4.5.2. Feature based profile classification 45
4.5.3. Summary 45
5. NOISE SENSITIVITY ANALYSIS FOR EDGE DETECTORS 47
5.1. Noise model and edge detection method 47
5.2. Edge detectors 49
5.3. Noise sensitivity analysis 54
5.4. Effect of filter length on edge detector performance 59
5.5. Conclusion 61
6. REMAINING CLASSIFICATION TASKS 63
6.1. Overview 63
6.2. Remaining classification 64
6.2.1. Panel height 64
6.2.2. Door size 64
6.2.3. Panel shape 65
6.2.4. ER-type doors 70
6.3. Database 73
6.4. Door classification station 75
6.5. Door classification procedure 77
7. PERFORMANCE AND FUTURE ENHANCEMENTS 80
7.1. Classification system performance 80
7.2. Future enhancements 82
8. SYSTEM INSTALLATION AND CALIBRATION 85

8.1. Overview 85
8.2. Installation procedure 86
8.3. Calibration of camera orientation 90
8.4. Tolerance of conveyor belt speed 91
9. CONCLUSION 97
REFERENCES 98
APPENDIX A. PROFILE CLASSIFICATION USING CURVE FITTING 100

LIST OF FIGURES

Figure 2-1. Current layout of production facility 6
Figure 2-2. A typical cabinet door 7
Figure 2-3. Illustration of square and cathedral panel shapes 8
Figure 2-4. Partial profile of door 10
Figure 2-5. Outside and inside profiles for AWC doors currently in production 13
Figure 2-6. Illustration of horizontal profile and vertical profile 14
Figure 2-7. Illustration of structured light projected on a cabinet door 16
Figure 2-8. Image of door under laser source 16
Figure 3-1. One possible image geometry to determining height dimension with structured light 22
Figure 4-1. Illustration of profile extraction using structured light 32
Figure 4-2. Example profile images 33
Figure 4-3. Profile processing steps 34
Figure 4-4. Thresholded profile image in a two dimensional space 36
Figure 4-5. Replacement of dropout points 37
Figure 4-6. Profile processing and classification by template matching 39
Figure 4-7. Features used for profile classification 40
Figure 4-8. Twelve profile images with plateau corners detected 42
Figure 4-9. A decision tree for profile classification 46
Figure 5-1. Processing steps in edge detection 48
Figure 5-2. Example profile 49
Figure 5-3. Example profile curve, style 3S 51
Figure 5-4. Results obtained by low-pass filtering the profile 52
Figure 5-5. Results obtained by filtering the profile using 7-point edge detector 53
Figure 5-6. Canny edge detector with filter length 7 56
Figure 5-7. Results obtained from canny edge detector on profile style 3S 59
Figure 5-8. Canny edge detector with length 19 and $\sigma^2 = 0.001$ 60

Figure 5-9. Comparison of Canny edge detector and difference-of-boxes filter with filter length 19 61
Figure 6-1. Classification of panel shape 65
Figure 6-2. Illustration for panel shape analysis 67
Figure 6-3. New approach for panel shape classification 69
Figure 6-4. Sample images to illustrate panel shape classification 71
Figure 6-5. Sample images to illustrate classification of ER-type 72
Figure 6-6. Door style classification station 76
Figure 6-7. Classification of door styles and sizes 79
Figure 7-1. Illustration of misclassification among profile groups 1K, Y2, and Y2 81
Figure 7-2. An "unknown" square panel door 82
Figure 8-1. Door classification stand 87
Figure 8-2. Equipment location and installation measurement 89
Figure 8-3. Calibration program flow chart 92
Figure 8-4. Example images during calibration of profile camera 93
Figure 8-5. Example images from sideview camera 94

LIST OF TABLES

Table 5-1. Non-normalized result using edge detector [1 1 1 0 -1 -1 -1] 57
Table 5-2. Non-normalized result using edge detector [2 1.5 1 0 -1 -1.5 -2] 57
Table 5-3. Non-normalized result of Canny edge detector with $\sigma^2 = 0.00003$ 58
Table 5-4. Non-normalized result of Canny edge detector with $\sigma^2 = 0.0002$ 58
Table 8-1. Equipment list 86
Table A-1. Result from second order polynomial curve fitting 103
Table A-2. Result from third order polynomial curve fitting 103
Table A-3. Result from fourth order polynomial curve fitting 104

Chapter 1

Introduction

1.1 Motivation

In recent years, computer vision technology has been adopted in many industrial applications. Computer vision borrows from human vision principles to automate such tasks as visual inspection, object recognition, and robot control. Machine vision, which is a computer vision with an industrial flavor, involves both image processing and pattern recognition. It can be defined as the process of extracting information from visual sensors to enable machines to make manufacturing decisions.

Modern manufacturing processes have increasing needs for automatic decision making based on visual information. The widespread use of robotics and CAD in industry provides a need for an automated process of acquiring and using visual information in digital form. At the same time, social, industrial, and economic changes mandate a need to increase productivity, provide better traceability of parts, and improve levels of quality and reliability in the finished product. A great deal of effort has been expended in recent years in adapting machine vision system to these tasks. Advances in computer technology, sensing devices, image processing, and pattern recognition have resulted in better and cheaper industrial visual inspection equipment, and making it feasible to apply the

technology in manufacturing environments. In particular, machine vision has come to play a major role in such tasks as inspection, measurement, and process control.

Compared with the human visual system, machine vision systems are more consistent at making quantitative measurements and decisions. After a system has been developed, it will perform with a high degree of repeatability. A machine vision system is not subject to fatigue or distractions, and the established level of performance will be constant, for all practical purposes, for the entire operating life of the equipment. Human vision is more adaptable, but can be greatly impacted by fatigue, environmental factors, and physical and mental condition. Since quality control is so important in today's manufacturing environment, it is important to use machine vision whenever possible to boost productivity.

This thesis describes one industrial application of machine vision. It is the use of computer vision techniques for the automated classification of wooden cabinet doors. The thesis describes the careful design of illumination and sensing geometry, the profile-based feature extraction process, and the classification method. The system is among the first to apply computer vision methods to finished wooden component identification in the forest products industry.

1.2 Background

American Woodmark Corporation (AWC), based in Winchester, Virginia, is a manufacturer and distributor of kitchen cabinets and vanities. One of their plants

manufactures finished wooden doors, door frames, and other components that are shipped to other AWC plants for assembly. Over the past few years, the number of component types produced by AWC has increased dramatically. Currently, more than 9000 distinct component classes are produced on 3 modern assembly lines.

The recent expansion in the product line has led to significant problems in classification and inventory handling. As each component leaves the assembly line, it is manually identified, and shelved, where it remains until requisitioned by an assembly plant. Because of the enormous number of component types which can leave the conveyor belt, and since many of them are similar in appearance, it is very difficult for the human eye to accurately distinguish similar looking cabinet doors and door frames. Furthermore, it is impossible to memorize the identification code for each component. Therefore, the classification task has become very tedious, labor intensive, and error prone.

In order to improve this process, increased automation is needed. This thesis describes a system that has been developed at the Spatial Data Analysis Laboratory at Virginia Tech to automate this difficult classification problem. The system utilizes machine-vision techniques to determine the style and size of cabinet doors. It will significantly simplify the classification process, and improve productivity.

1.3 Objective

The major goal of this research has been to develop a system that can classify cabinet doors that are produced by American Woodmark Corporation. The resulting system should sense components on a conveyor and derive an identification code for any

AWC door. The system should be accurate, and should preferably classify something as "unknown" rather than assign an incorrect code. The system should be capable of operation with conveyor speeds of 30 feet per minute. Finally, the system should be expandable to permit the addition of new styles.

1.4 Contributions of this research

The system developed in this research is one of the first computer vision system to classify finished wooden components. The major contributions of this research are as follows:

1. The entire cabinet door product line, including all available door styles and sizes, has been carefully analyzed. All the features necessary for classification have been specified, and a classification strategy has been developed.

2. A door classification station has been designed and constructed. This has involved the careful design of illumination and sensing geometry, construction of camera mounts, and development of a camera calibration program.

3. A technique for acquiring profile images using structured light has been developed. Profile based feature extraction has been implemented in door style classification. A method has been developed to reduce the profile processing complexity from 2-D to 1-D.

4. Different edge detectors have been analyzed for detection, localization, and noise sensitivity. Plateau endpoints have been effectively and accurately detected in the

presence of noise by applying bi-directional edge detection using a simple difference-of-boxes filter.

5. Software for the classification system has been developed. The system has been extensively and successfully tested at the factory conveyor rate of 6 inches/second. A duplicate system will be installed in the factory in the near future.

1.5 Outline of thesis

This thesis describes the design and implementation of an automatic classification system. Chapter 2 presents the problem description and proposed solutions. Chapter 3 presents a review of previous work related to this research. Chapter 4 discusses profile classification using both template matching and a feature based approach. Chapter 5 analyzes the noise sensitivity of edge detectors that were considered here. Chapter 6 describes the remaining tasks in door classification, and discusses the final classification system. Chapter 7 describes the performance of the final classification system, and proposes future enhancements. Chapter 8 describes the system installation and calibration, and Chapter 9 presents a summary of the thesis. Finally, there is an Appendix on profile classification using a curve fitting approach.

Chapter 2

Problem Description and Proposed Solutions

2.1 Production environment

As described in Section 1.2, American Woodmark produces doors and other components of kitchen cabinets. Components which will form the exposed portion of cabinets must be carefully finished. After assembly, they are placed on conveyors for final sanding and painting. For efficient painting, different component types are mixed on conveyors as shown in Figure 2-1. Finished units are transferred manually to inventory.

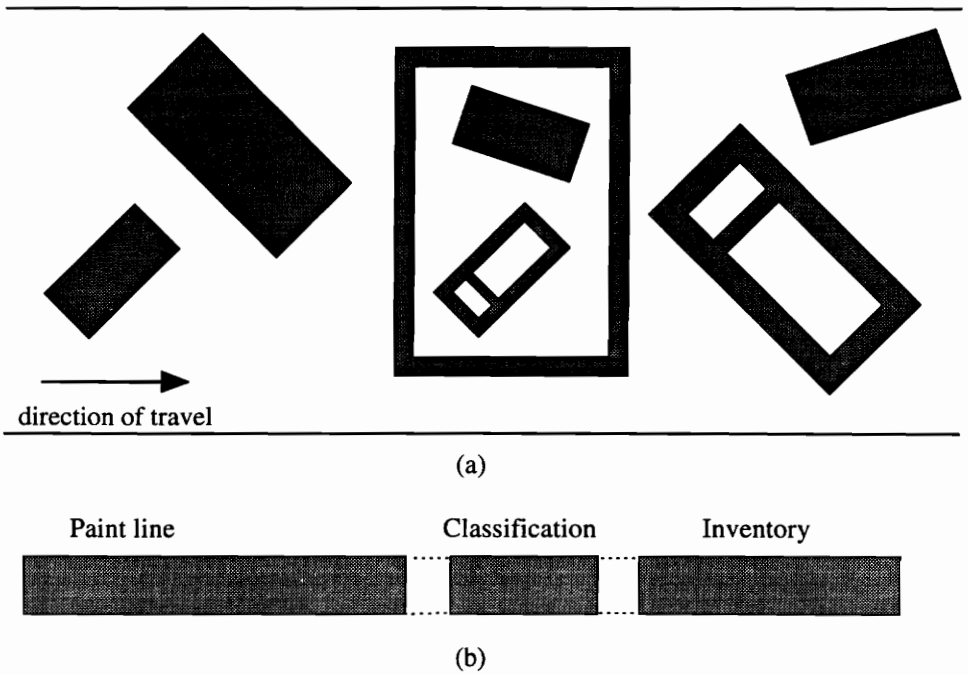

Figure 2-1. Current layout of production facility. (a) Top view of paint-line conveyor, which is about 5 feet in width. Cabinet doors(solid rectangles) and frames are mixed on the line. (b) The production lines produce finished components that are identified and shelved manually. Each paint line is approximately 100 feet in length. The goal of this research is to automate the classification operation.

In recent years, manufacturers have dramatically increased the number of product styles. The result is that manual identification has become particularly tedious, labor-intensive, and prone to error. In order to improve this process and reduce cost, increased automation is needed.

2.2 Problem description

Cabinet doors are formed by joining four molded wooden pieces around a central panel, as illustrated in Figure 2-2. Different door types are distinguished by shape, size, color, and species. The shape of a door determines its *style code*, and its size (overall height and width) determines a *size code*. This thesis is concerned with the identification of style and size codes for cabinet doors.

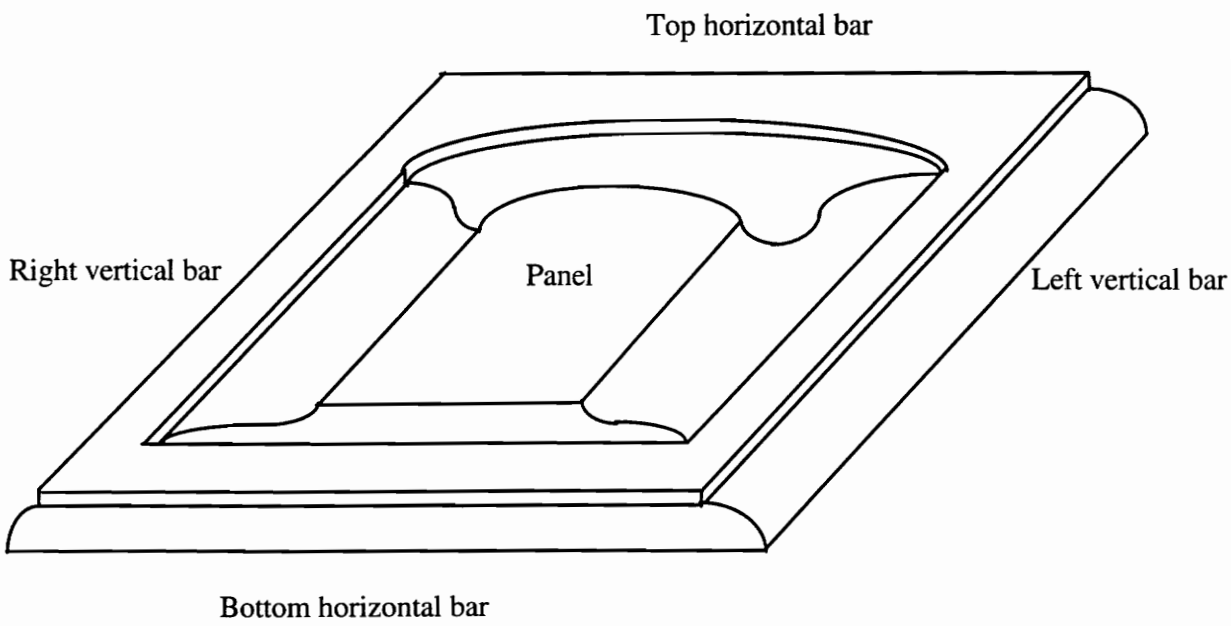

Figure 2-2. A typical cabinet door. Four interlocking bars are joined around a central panel.

A door's size is determined by its overall width and height. The components considered here can range in width from 6.875" to 33.75", and the height can range approximately from 10.0" to 49.25". Doors fall into three groups based on the amount of hinged-side overlay of the doors onto the supporting frames; within each group, the width and height increase in steps of 1.5". A total of 60 different sizes are possible within each group.

The style of a door is determined by its unique combination of outside profile, inside profile, panel profile, and panel shape, as described below.

Panel shape. The top horizontal piece of a door can be *square* or *cathedral* (curved), as shown in Figure 2-3.

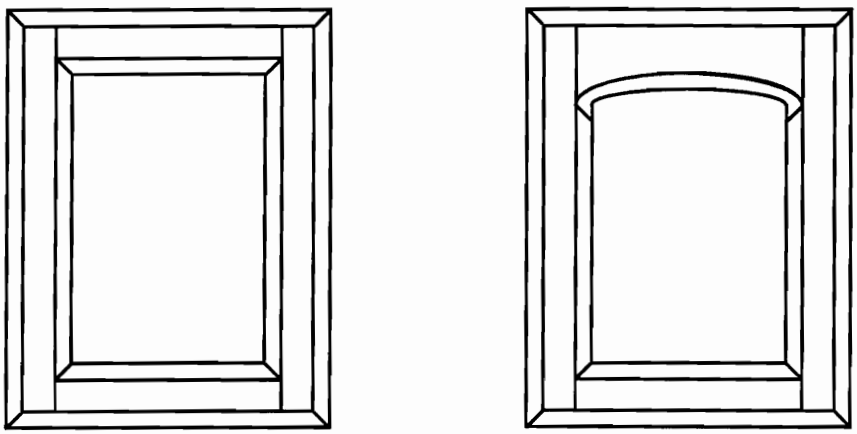

Figure 2-3. Illustration of (a) square and (b) cathedral panel shapes. A cathedral door has a curved top horizontal piece. The amount of curvature varies with different door styles and with different sizes.

Outside and inside profiles. The profile of a door refers to the shape of the door's cross-section. The *outside profile* lies at the outside edge of the door. It is

separated from the *inside profile* by a horizontal *plateau* region, as described in Figure 2-4. All profiles are defined by product designers using piecewise circular arcs and linear segments. AWC currently produces 7 distinct outside profiles and 8 distinct inside profiles. (This description does not include ER-type doors, which are described below.)

Panel profile. The central panel may be *flat* or *raised* as illustrated in Figure 2-4. A flat panel is simply a thin wooden section at the center of the door. A raised panel is thin near its outer edge, but "bulges" outward as it leaves the inside profile of the surrounding bars. Some of the "doors" do not have a central panel, and are defined as *door frames*. AWC currently produces 6 distinct panel profiles, not considering missing and flat panels.

ER-type doors. Most doors have the same outside profile along the entire perimeter of the door. ER-type doors are different in that one vertical side has a square outside profile (a right-angle cut), as shown in Figure 2-4(c).

If all possible combinations of the above features were produced, the number of door types would be very large. In practice, AWC has combined particular sets of inside, outside, and panel profiles with particular panel shapes to form a total of 28 style designations. If all 28 styles were available in 60 sizes each, then 1680 classes would result.

Figure 2-5 illustrates the twelve possible outside and inside profiles that are currently in production. Notice that for some profile combinations, several style codes are listed. In these cases, panel shape and panel profile are used to distinguish them.

2.3 Mathematical representation

A door style can be described by its *horizontal profile* and *vertical profile,* as illustrated in Figure 2-6. A horizontal profile is defined to be a horizontal cross-section of a door, with width W; a vertical profile is defined to be a vertical cross-section of a door, with height H. Figure 2-6(a) shows a horizontal profile, represented by $h_H(x)$, and Figure 2-6(b) is a vertical profile, represented by $h_V(y)$. L_0 is the length of the outside profile. The thickness of a door is T, and is the same for all doors.

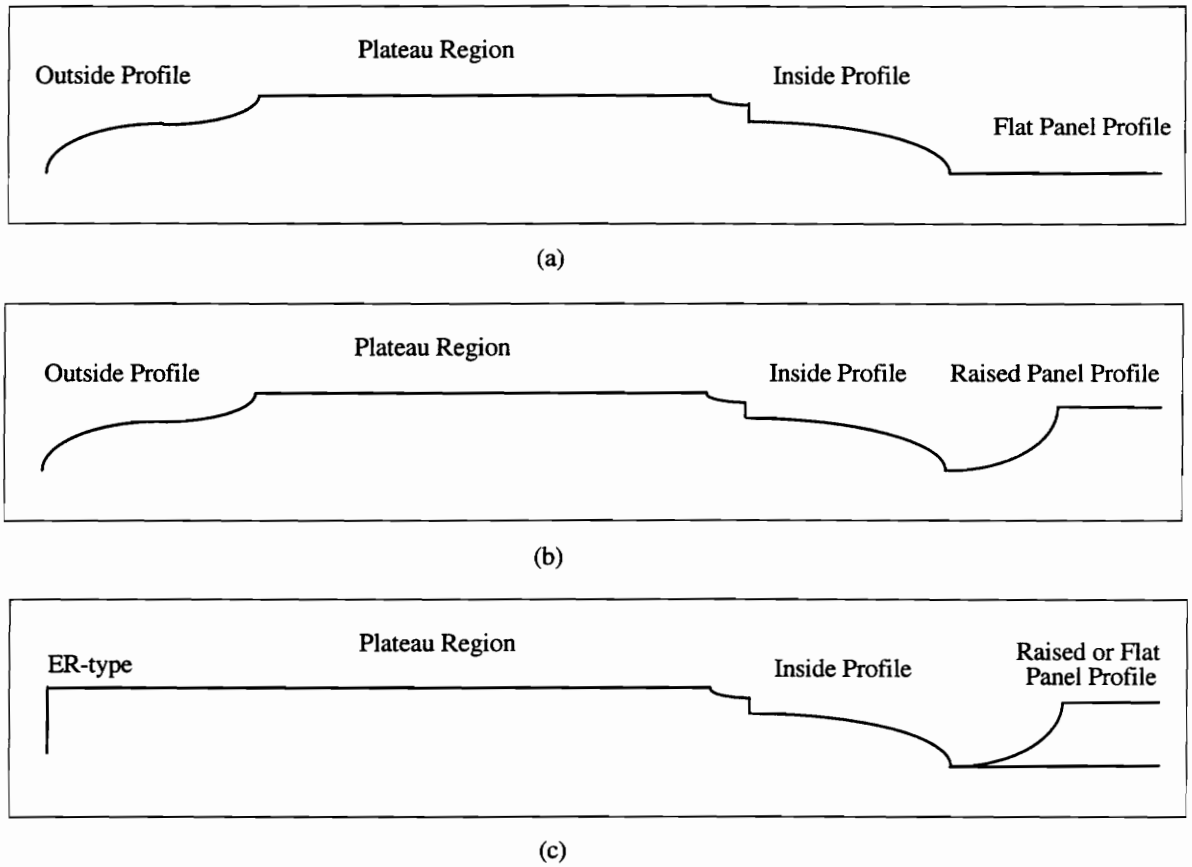

Figure 2-4. Partial profile of door. The left of the figure corresponds to the left edge of a door. The vertical bar of the door is distinguished by its outside profile, plateau, and inside profile. This is attached to a panel, which may be (a) flat or (b) raised. An ER-type door has a square outside profile, as shown in (c). The square profile appears only at the left or right side of the door, but not both.

These two profiles, observed at appropriate locations on a door, are sufficient to distinguish each door style and size from all others. The objective of this research is to characterize the profiles and obtain a set of features that can be detected and mapped to a style code and size code. This is illustrated as follows:

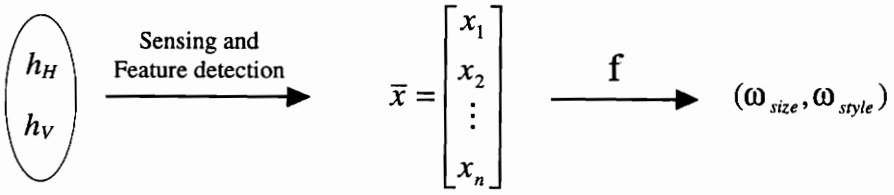

Let $\bar{x} \in \mathbb{R}^n$ represent an n dimensional feature vector that can be extracted from an observed profile. The function $\mathbf{f} : \mathbb{R}^n \longrightarrow \Omega_{size} \times \Omega_{style}$ maps a given feature vector to a style code ω_{style} and size code ω_{size}. The sets Ω_{style} and Ω_{size} represent the style and size codes, along with the designation "unknown".

This research has concentrated on determining the feature vectors $\bar{x}$ that can be mapped to the given style and size code. At the same time, the research has focused on developing techniques for detecting these features from actual doors.

The following relationships assist in determining style codes from profiles. Most doors are symmetrical, so that a non-ER type door satisfies

$$h_H(x) = h_H(W - x), \qquad \text{for } 0 \le x \le W \tag{2-1}$$

An ER-type door satisfies

$$h_H(x) = h_H(W - x), \qquad \text{for } L_0 < x < (W - L_0) \tag{2-2}$$

but we have

$$h_H(x) = T, \qquad \text{for } 0 \le x \le L_0 \text{ or } W - L_0 \le x \le W \qquad (2\text{-}3)$$

A square panel satisfies

$$h_V(y) = h_V(H - y), \qquad \text{for } 0 \le y \le H \qquad (2\text{-}4)$$

but for a cathedral panel, (2-4) is not satisfied.

The approach that has been adopted is to decide which of the twelve profiles is present; decide whether the panel shape is cathedral or square from $h_V(y)$ by using EQ. 2-4; decide whether the panel is raised, flat, or empty from $h_H(x)$; decide ER-type from $h_H(x)$ by using EQ. 2-3; and decide height and width of the door. Finally, these features are mapped to door style and size code with a look-up table. Notice that not all combinations of features are currently under production. In this case, the system will assign an "unknown" ID.

2.4 Proposed solution for automated classification

In order to classify cabinet doors automatically, all of the features described above need to be examined by a computational system. One of the best potential solutions to this problem is to use computer vision techniques.

The suggested approach for determining panel profile, panel shape, panel height, and door width is to use structured light. One laser source is used to generate a fan-shaped plane of light, as illustrated in Figure 2-7. It is positioned above the conveyor belt so that this plane of light intersects the conveyor belt perpendicular to its direction of travel. This causes a bright red stripe to appear on the components which pass directly

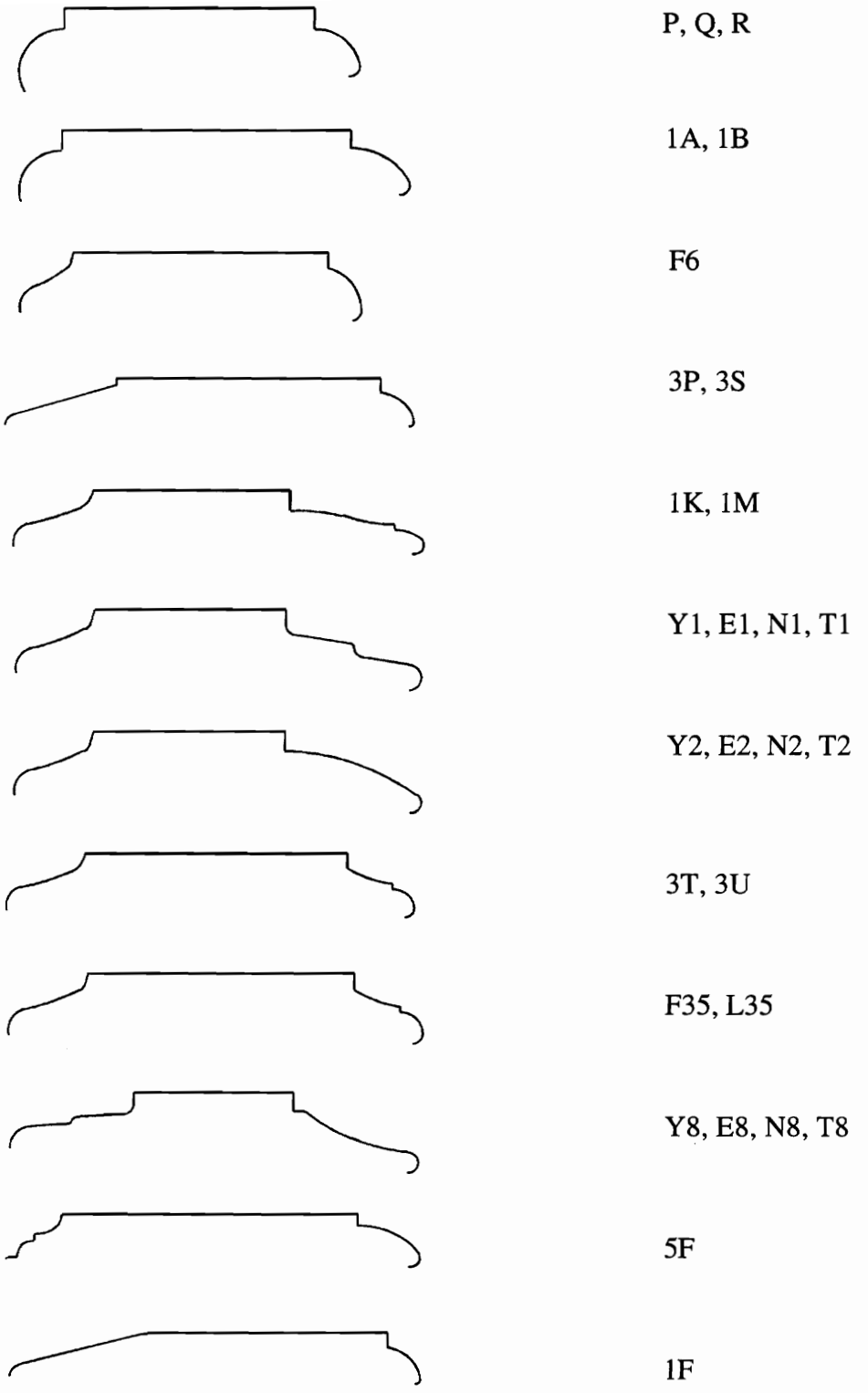

Figure 2-5. Outside and inside profiles for AWC doors currently in production. Outside profiles are shown at the left, and inside profiles are shown at the right. Styles are drawn to scale. Style codes for each profile are given. All of these except 3P and 3S were generated with AutoCAD. If several style codes are given for one profile, panel shape and panel profile are used to distinguish them.

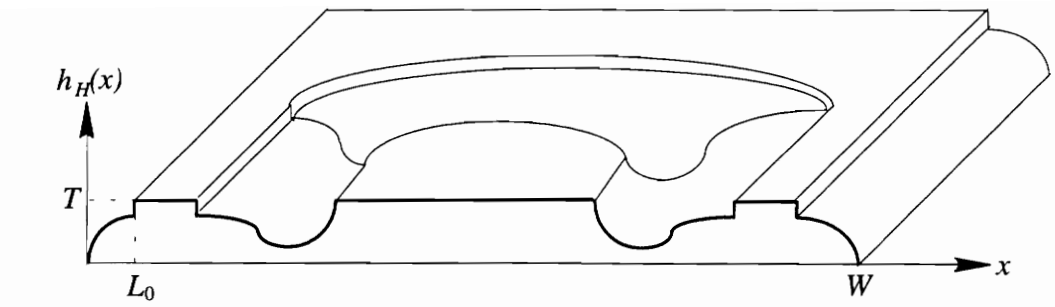

(a)

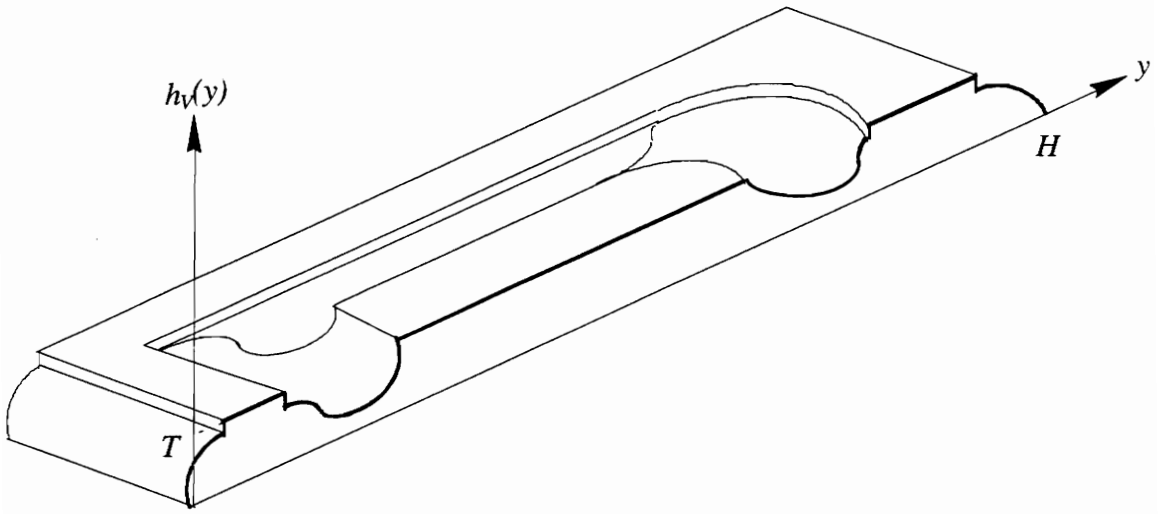

(b)

Figure 2-6. Illustration of horizontal profile and vertical profile. (a) Horizontal profile of a non-ER door with raised cathedral panel. The width of the door is *W*. (b) A vertical profile of the same door. The height of the door is *H*.

under the laser source. The laser light projected onto the cabinet door highlights the horizontal profile, and generates a characteristically different curve for each possible profile. This is illustrated in Figure 2-8, which shows a door lying horizontally under a laser source. A second laser source (not shown) projects a laser stripe parallel to the direction of movement, and highlights the vertical profile of the door.

Three cameras are proposed for this station. All of them are mounted above the conveyor belt which carries the components to be classified. The first, called the "overview" camera, is positioned to provide a view of almost the entire width of the door. The second provides a close-up image of the profiles along one side of the component. It is called the "profile" camera. The third camera provides a side view of the vertical profile. It is called the "side" camera.

The profiles of the door cause the laser stripe to appear curved in the image. Using the overview camera, the classification system can detect the edges of the door, which provide a measurement of the door's width. The profile camera provides a higher resolution image of the outside, inside, and panel profiles. This higher resolution is needed to differentiate the subtle difference in profile shapes. The side camera is used to determine panel shape (square or cathedral).

A darkroom environment is required to exclude most ambient light. The reason for this is to provide high contrast for the laser stripe. Black curtains can be used for this purpose.

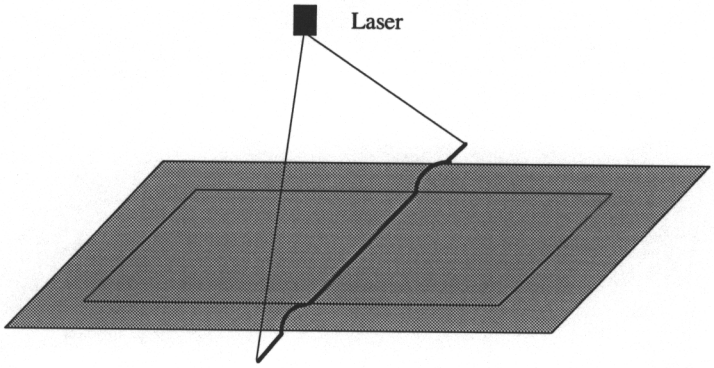

Figure 2-7. Illustration of structured light projected on a cabinet door. The laser source is positioned above the door and generates a fan-shaped plane of light.

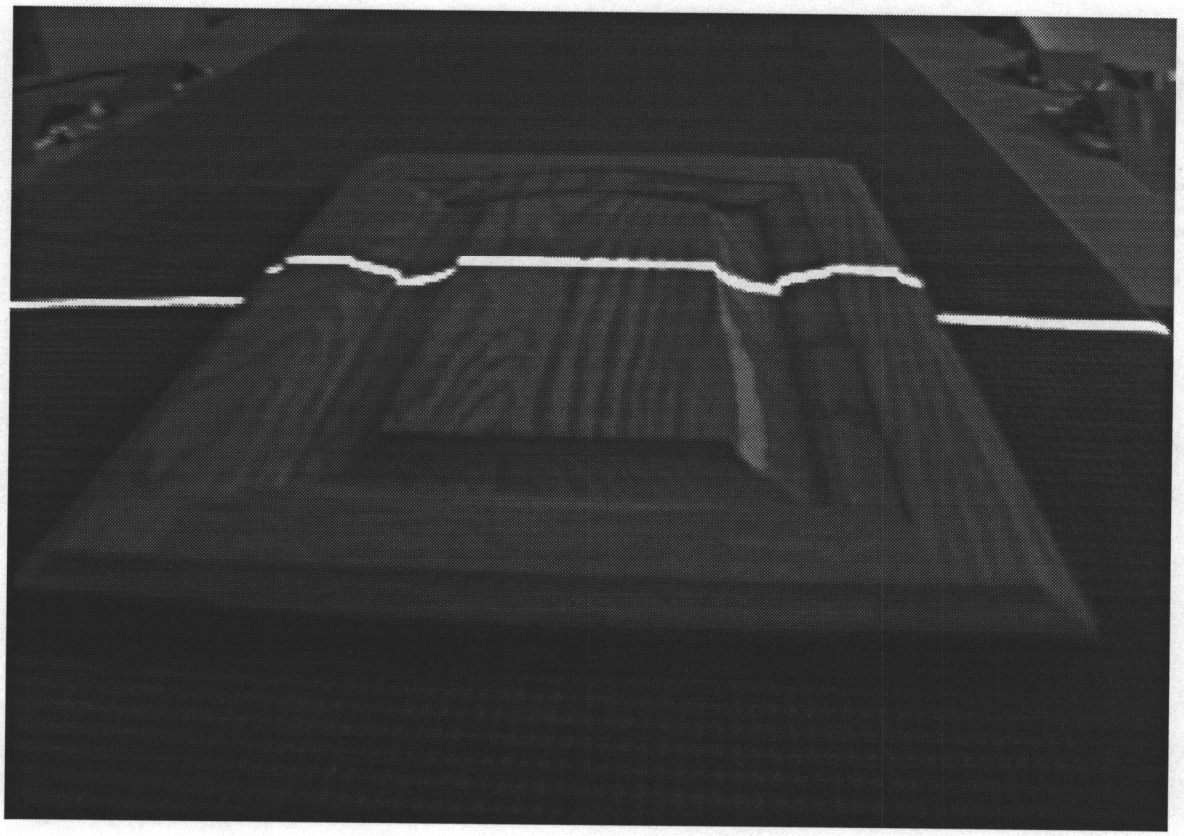

Figure 2-8. Image of door under laser source. The laser stripe highlights the profile of the door. This is style 1K, which has a raised panel. The bottom of the door is near the camera.

Two photoelectric sensors are needed to trigger image acquisition for the side camera. One sensor is also used to detect the beginning and end of the door. Since the conveyor speed is known, the height of door can be measured by the time which elapses as the door passes through the sensor.

A host computer is needed to control the entire process, and serves as an image processing unit. The laboratory system uses a 486-based PC with adequate memory, disk capacity, and expansion slots for a frame grabber and accelerator card. The frame grabber is connected to all three cameras to acquire and process images. This frame grabber is capable of selecting one of the cameras at a time automatically.

This proposed solution has been implemented, and extensively tested. Details are described in Chapter 4 and Chapter 6. The resulting system automatically classifies all existing styles with high accuracy.

2.5 Assumptions

Like most machine vision systems, this classification system requires well positioned, isolated objects against a clean background. To simplify the processing procedures, several assumptions have been made. Some of them are obvious, and others will be explained in later chapters.

1. Components must be placed on the conveyor belt against the alignment bar. Non-ER type doors can travel both top and bottom first. For ER type doors, the alignment must be along the side which contains the characteristic profile.

2. The speed of the conveyor belt is used to calculate the height of the cabinet door. It should be constant within a certain tolerance range. This is described and calculated in Chapter 8.

3. The surface of the conveyor belt must be flat within the classification station. A curved surface will result a variation in height map of the profile. Details are given in Chapter 7.

4. Components must be separated by at least 24 inches on the conveyor.

Chapter 3

Previous Work

The last chapter has described the componments of interest, and proposes a method for automatic classification. This chapter is concerned with image acquisition techniques and shape description methods that are needed to implement the method.

The most difficult problem in this research is profile analysis. For many of the inside, outside, and panel profiles, the differences are very subtle. For this application, the structured-light approach seems to be the best method to obtain three-dimensional information for profile analysis. Recognition is possible by adopting a representation scheme that reduces a shape to a small number of shape descriptors, and then classifying the shape according to the values of these descriptors.

3.1 Image acquisition

A machine vision system may be viewed in terms of the two main functional components: image acquisition and image processing. Image acquisition transforms light energy from a physical object into a set of digitized data which can be used by the processing unit of the system. The imaging system must reduce noise, prevent blur, optimize contrast between parts of interest and the background, and emphasize those features which are relevant to the inspection. The primary objectives are to acquire a

quality representation of the object under inspection, and to reduce the complexity of subsequent image processing. Image acquisition involves the design of illumination and optics, and the choice of sensors and their placement.

Illumination is a critical component in a machine vision system. It is a key parameter since it directly affects the quality of the input data. Appropriate illumination can accentuate the features on an object and result in sharp, high-contrast detail. Illumination is dictated by the application, and the properties of the object, such as geometric properties, color, background, and the data to extract from the object. It can be subdivided into three categories: back lighting; front lighting; structured lighting, as described below.

Back lighting. Back lighting is when an object is located between the light source and camera. Back lighting has the advantage that it produces high-contrast silhouette images of opaque objects. The high contrast can simplify image processing and reduces the sensitivity of the system to illumination source variations. The back lighting method is also ideally suited for tasks like the location of foreign material, voids, and fractures in transparent objects. The examination of bone fractures with x-ray plates and the measurement of heat energy leakage from a building with IR sensors are examples of this technique.

Front lighting. Front lighting employs light reflected from the object. The illumination source and the camera are both on the same side of the object. This method of

illumination is used to obtain information on surface texture or features as well as for dimensioning.

Structured light. Structured light is the use of illumination of the object with a special pattern or grid. The intersection of the object and the projected illumination results in a unique pattern depending on the shape and dimensions of the object. Vertical and horizontal distances, as well as the shape of surface features, can be measured, and surface profiles can be obtained.

Because structured light has been used in this research, a more complete description is given here. A pattern of light is projected onto an object and viewed with a single camera [1], as illustrated in Figure 3-1. When the position and angle of the source are known with respect to the camera, the position or shape of the object in space can be computed by triangulation from the distortion in the light pattern perceived by the camera. These systems can use a simple pattern such as a stationary or scanned spot of light or a line of light to produce range information.

The inspection of solder joints [2] is another system based on a structured lighting approach to obtain shape information. Stripes of light are generated and focused onto the joint's surface. The surface reflectance containing range information is detected, stripe by stripe, for the reconstruction of the surface. Defects are detected by analyzing the sequential signal. This approach has the advantage of very fast processing. A similar technique has been used in the inspection of mounted discrete components on hybrid

circuit boards [3]. The application requires the checking of components and their mounting quality.

These three types of illumination can be used together for a particular task. It is possible to combine back lighting and structured lighting in one image by simultaneously

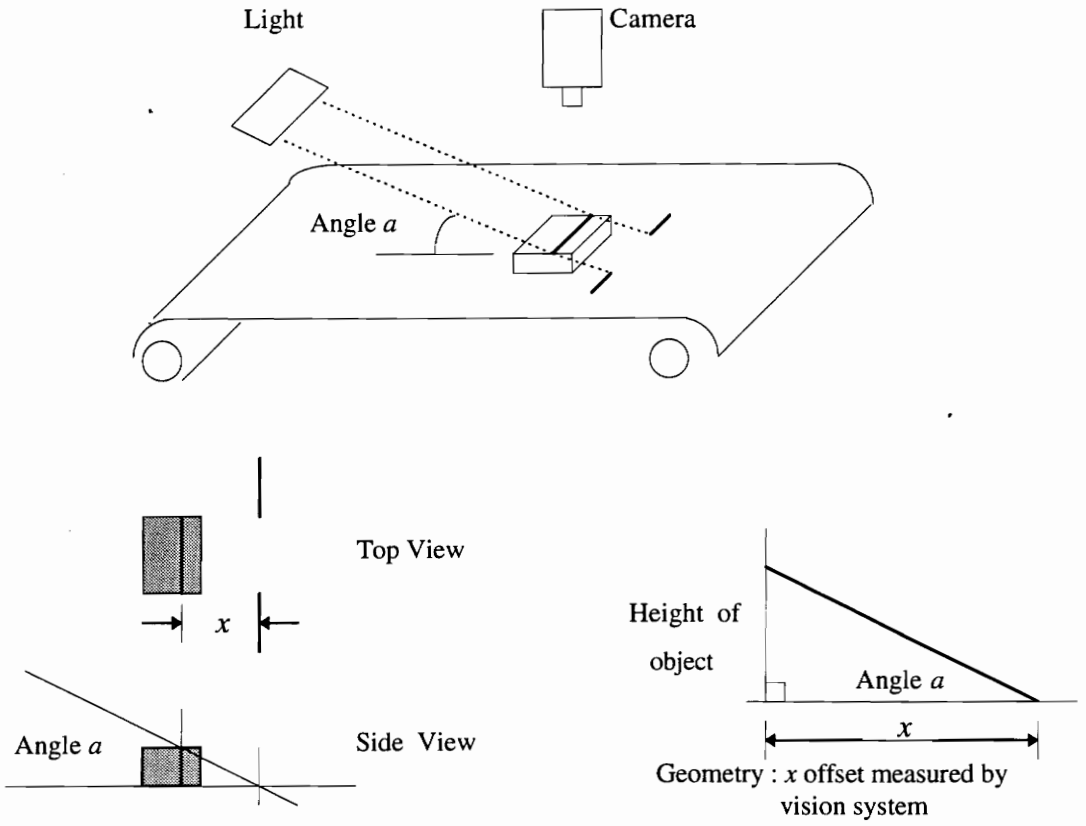

Figure 3-1. One possible imaging geometry to determining height dimension with structured light.

illuminating the object from behind and projecting a structured pattern in the front. An example of this is described in [4].

Many industrial inspection applications involve the inspection of planar (flat) objects, such as circuit boards, or labels on packages. These patterns can be well represented by models containing two-dimensional features. The inspection of three-dimensional parts requires the construction of three-dimensional models. A simple approach to this problem is the use of multiple sensors, such as a setup with a camera inspecting the top view and a second camera looking at the side. In this multisensor configuration, the model again consists of a number of two dimensional models, each describing a different view of the part.

3.2 Image processing

Since the mid-1970s, a large number of vision systems and algorithms have been developed. In many inspection applications, the first problem is to determine which feature measurements should be taken from the input image. Feature extraction is associated with low-level image processing, extracting very simple elements such as corners, edges, curves, holes, etc., along with their dimensions, locations, and orientations. These elements define geometric characteristics of a part under inspection. The process of feature extraction usually begins with the generation of a binary image from the original gray-scale image using simple thresholding. The techniques discussed here is based on a binary image, which is generated from the original gray-scale image using simple thresholding. The use of binary representation reduces the amount of data that must be handled, although such information as surface texture is lost. This section describes

related processing techniques for profile analysis, such as thinning, template matching, and edge detection.

3.2.1 Thinning

Thinning is a procedure to transform a digital binary pattern to a skeleton of unit width [5]. The operation reduces a large amount of data to a connected skeleton which is a reasonable topological representation of the object. It has many applications, such as character recognition, inspection, and shape description.

Most thinning algorithms delete from an object at each iteration; boundary pixels whose removal does not disturb the general configuration and connectivity. Some thinning algorithms, such as Medial Axis Transform [6], also guarantee that the final connected skeleton does not change or vanish, even if the iteration process continues. In other words, thinning converges to a connected skeleton which is reasonable topological representation of the object.

Many thinning algorithms have been proposed to date, they can be classified into two general types: sequential and parallel algorithms. The main difference between these two types is that sequential thinning operates on one pixel at a time and the operation depends on preceding processed results. Parallel thinning operates on all the pixels simultaneously [5,7], but it may require parallel processing hardware to realize the algorithm. Sequential thinning algorithms generally generate a better skeleton, but parallel thinning is substantially faster.

3.2.2 Template matching

Template matching is a simple filtering method for detecting a particular feature or object in an image [6]. The template is a subimage that looks just like the object to be located. A similarity measure is computed which reflects how well the image data match the template for each possible template location. The point of best match can be selected as the location of the feature.

One standard similarity measure between an image *I(x)* and template *T(x)* is the Euclidean distance *d(y)* squared, given by

$$d^2(x) = \sum_{y=-(N-1)/2}^{(N-1)/2} [I(x-y) - T(y)]^2 \qquad (x \in \mathbb{Z},\ y \in \mathbb{Z}) \qquad (3\text{-}1)$$

where N is the size of the template, an odd number; M is the size of the one dimensional profile image, and $(N+1)/2 \le x \le M-(N-1)/2$.

If the image at point x is an exact match, then $d(x) = 0$; otherwise, $d(x) > 0$. Expanding the expression for d^2, we can see that

$$d^2(x) = \sum_{y=-(N-1)/2}^{(N-1)/2} [I^2(x-y) - 2I(x-y)T(y) + T^2(y)] \qquad (3\text{-}2)$$

Notice that $\sum_{y=-(N-1)/2}^{(N-1)/2} T^2(y)$ is a constant term and can be neglected. When $\sum_{y=-(N-1)/2}^{(N-1)/2} I^2(x-y)$ is approximately constant it too can be discounted, leaving what is called the *cross-correlation* between I and T.

$$R(x) = \sum_{y=-(N-1)/2}^{(N-1)/2} I(x-y)T(y) \qquad (3\text{-}3)$$

This is maximized when the portion of the image is identical to the template.

3.2.3 Edge detection

Edges represent intensity discontinuities in an image. Enhancement of edges in an image is an important operation used in feature extraction. Edge detection requires two operations, differentiation and smoothing.

The common approaches for edge detection include [6]: (i) the use of spatial gradients, (ii) the use of the Laplacian, (iii) the use of differences of averages, (iv) matching or fitting to a prespecified pattern, (v) the detection of maxima in the image filtered by the first derivative of the Gaussian, popularized by Canny [11], or the detection of zero-crossings in the image filtered by the Laplacian of the Gaussian (LOG) [8], and (vi) the minimization of cost functions through the use of relaxation techniques such as simulated annealing and discrete relaxation [9,10]. A common drawback of most existing edge detectors is that their performance is substantially degraded in the presence of noise. This results from the fact that the effects of noise are not taken into account in the development of most of these edge detectors.

Edge detectors that are developed using approaches (v) and (vi) do consider the effects of noise in the image. But edge relaxation techniques are normally computationally complex, requiring several iterations before converging. Both Canny [11] and LOG

detectors take advantage of the noise suppressing characteristics of the Gaussian operator. Specially, the Canny edge operator can be approximated by the first derivative of Gaussian $G'(x)$, where

$$G(x) = \exp(-\frac{x^2}{2\sigma^2}) \tag{3-4}$$

The operation corresponds to smoothing an image with a Gaussian function and then computing the gradient. It is described as an optimal edge detector in the presence of Gaussian noise.

3.3 Previous work on shape descriptors

Various shape descriptors have been proposed. In general, these descriptors can be classified into two categories -- information preserving and non-preserving. Information preserving descriptors store unique information about the shape. It is possible to reconstruct a reasonable approximation of the original object from such a shape descriptor. A Fourier series or a polygonal approximation are information preserving descriptors because the original data can be represented as closely as one likes by choosing a high enough number of Fourier coefficients or polygon vertices. On the other hand, non-preserving techniques are those that do not provide a unique description of the shape. Examples of such descriptors are area (A), perimeter (P), and circularity (P^2/A). In this section, three commonly used shape descriptors are discussed. They are moment based shape descriptors, template matching, and feature based shape descriptors.

3.3.1 Moment Based Shape Descriptors

The concept of moments has its root in mechanics. It is one of the earliest information preserving techniques used and is based on scalar measurements. Alt [12] discusses the application of moment-based shape descriptors to character recognition, and derives formulas of moment based shape descriptors with location, size, and rotational invariance. A fast moment based classification algorithm called the "Delta method" was proposed by Zakaria [13]. To increase computing speed, this method uses the contribution of each row instead of individual pixels. Only the coordinates of the first pixel along with length of the chained pixels of the contour in each row are needed. It can be implemented by use of run-length codes. Another computationally efficient method of moment-based shape classification is described by Dai [14]. It is very similar to the Delta method. The algorithm is based on the double integral form of moments with the shape being considered as a continuous region. This algorithm, like the Delta method, makes use of run length codes or chain codes.

3.3.2 Template Matching

Template matching is a method of searching for an object in an image. Cross-correlation is used as one of the measures of similarity between a template and object in an image [15]. Recently, fast hierarchical matching algorithms using correlation of pyramidal structures have been proposed [16]. They are more efficient than the traditional cross-correlation techniques. The main idea of these methods is fast preliminary selection of a template's promising locations at higher levels of the search area and template pyramids,

followed by a gradual refinement at lower pyramid levels with higher resolution. To select the promising locations at the starting level, the value of the cross-correlation function is calculated for every possible location of the template in the search area. If this coefficient is higher than a given threshold value, the corresponding template location is marked as promising. The procedure is repeated at each lower pyramid level for those template locations. Most of these algorithms are designed for matching of rectangular templates.

3.3.3 Feature based shape descriptors

The basis of this method is to divide a curve into segments and then use relatively simple features to characterize the segments. The key to this method is an effective segmentation scheme. Critical points along the curve, such as discontinuities, endpoints, and intersections, also can uniquely identify a shape. Ventura and Chen [17] discuss the segmentation of two-dimensional curve contours. They give two new algorithms for this purpose and then use these algorithms in experiments on polygonal shapes. Pei and Lin [18] discussed the detection of dominant points on curves using scale-space filtering. Instead of conventional polygonal approximation algorithms, which are very time consuming, they introduce a scale space filtering method with a Gaussian kernel to detect dominant points on curves. They also proposed a new fast convolution algorithm to detect dominant points at each scale. Teh and Chin [19] detects dominant points based on angle detection. This algorithm works well on an object curve which is not corrupted with noise. However, because of its sensitivity to noise, some false dominant points will be detected due to quantization error and noise effect.

3.3.4 Summary

All three types of shape description are applicable to profile classification. Template matching is the simplest approach to this problem. But it has several limitations: large data storage, the need for precise alignment, and sensitivity to illumination and sensor conditions. The data storage requirement can usually be dealt with by careful implementation approaches. The sensitivity problem is the major drawback, and it is due to the fact that many objects do not match point-by-point, because of scaling or rotation. A feature based approach, on the other hand, is less sensitive. The extracted features are in most cases geometrical patterns such as corners, edges, holes, etc. It greatly compresses the image data for storage, and at the same time reduces the sensitivity of the input intensity data and enhances the robustness of the system.

Chapter 4

Profile Classification

4.1 Overview

Each door profile is composed of an inside profile, a plateau, and an outside profile. Profile classification is the process of examining a profile image and assigning a class designation to it. The class designation can be written p_i, where $i = 1..12$ represents one of the twelve profile shapes shown in Figure 2-5. Many of the profile shapes are subtle and difficult to distinguish, even for humans. This chapter concerns profile classification, which is the most difficult task in this research. Structured light is used to extract the profile image. Both template matching and feature-based classification are described in this chapter. Based on the results from both approaches, the preferred method is implemented in the final classification system.

4.2 Profile extraction

Cabinet doors are assumed to be aligned against the alignment bar on the conveyor. In order to characterize the profile, a laser source is used. The laser is mounted above the conveyor belt, and produces a fan-shaped plane of light. The laser stripe is perpendicular to the moving direction, and covers the entire door width, from the alignment bar to the maximum door width of about 25 inches. It intersects the moving

component on the conveyor belt to form a characteristic curve of the door. This is illustrated in Figure 4-1.

A profile camera captures a close-up view of the outside profile, plateau, inside profile, and panel profile of the door near the alignment bar. Its field of view is approximately 3.5", and its resolution is approximately 0.01 inch/pixel. Example images from this camera are provided in Figure 4-2. Notice that these profile images are not

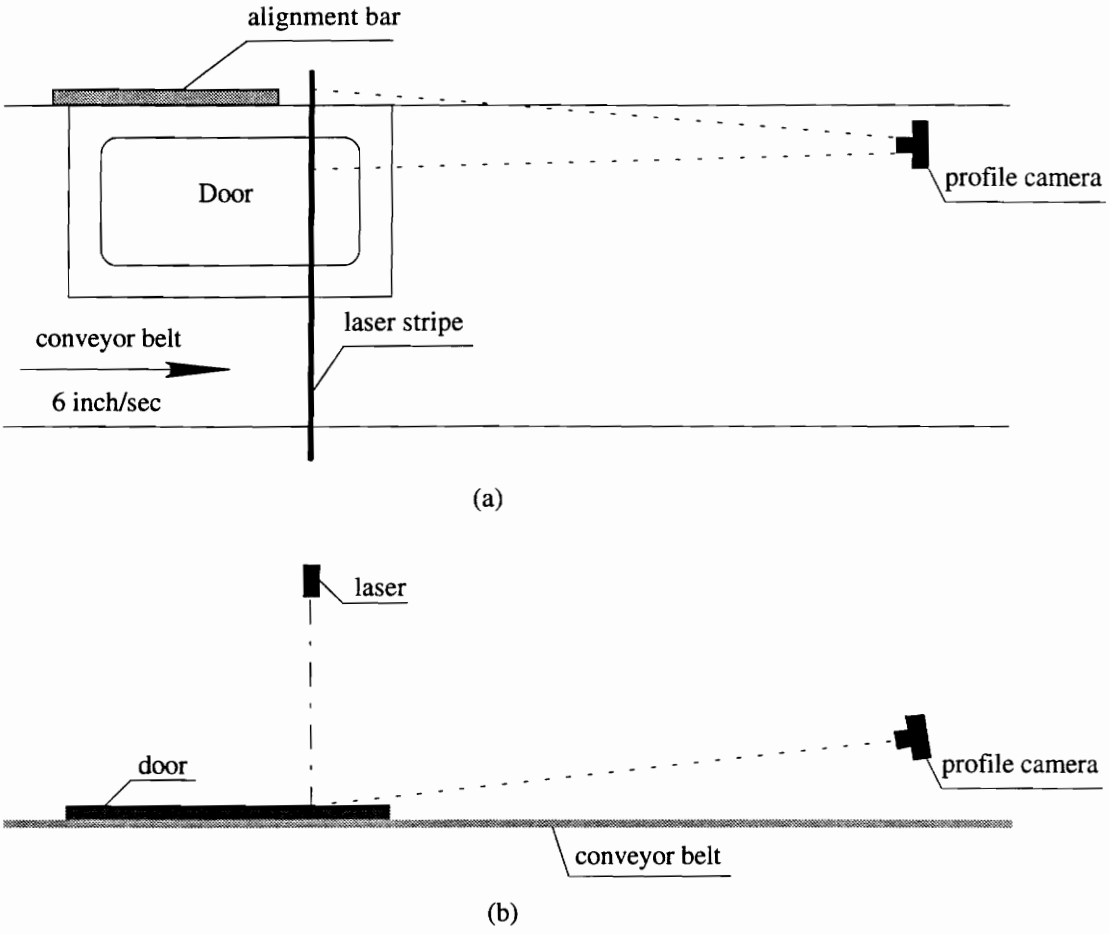

Figure 4-1. Illustration of profile extraction using structured light. (a) Top view. (b) Side view. Profile corner captures outside profile, inside profile, panel profile. Laser stripe covers entire door width of approximately 25" from the alignment bar.

simple connected regions, and their borders are not perfectly smooth. Several preprocessing steps are needed before profile classification can occur. These are described in the next section.

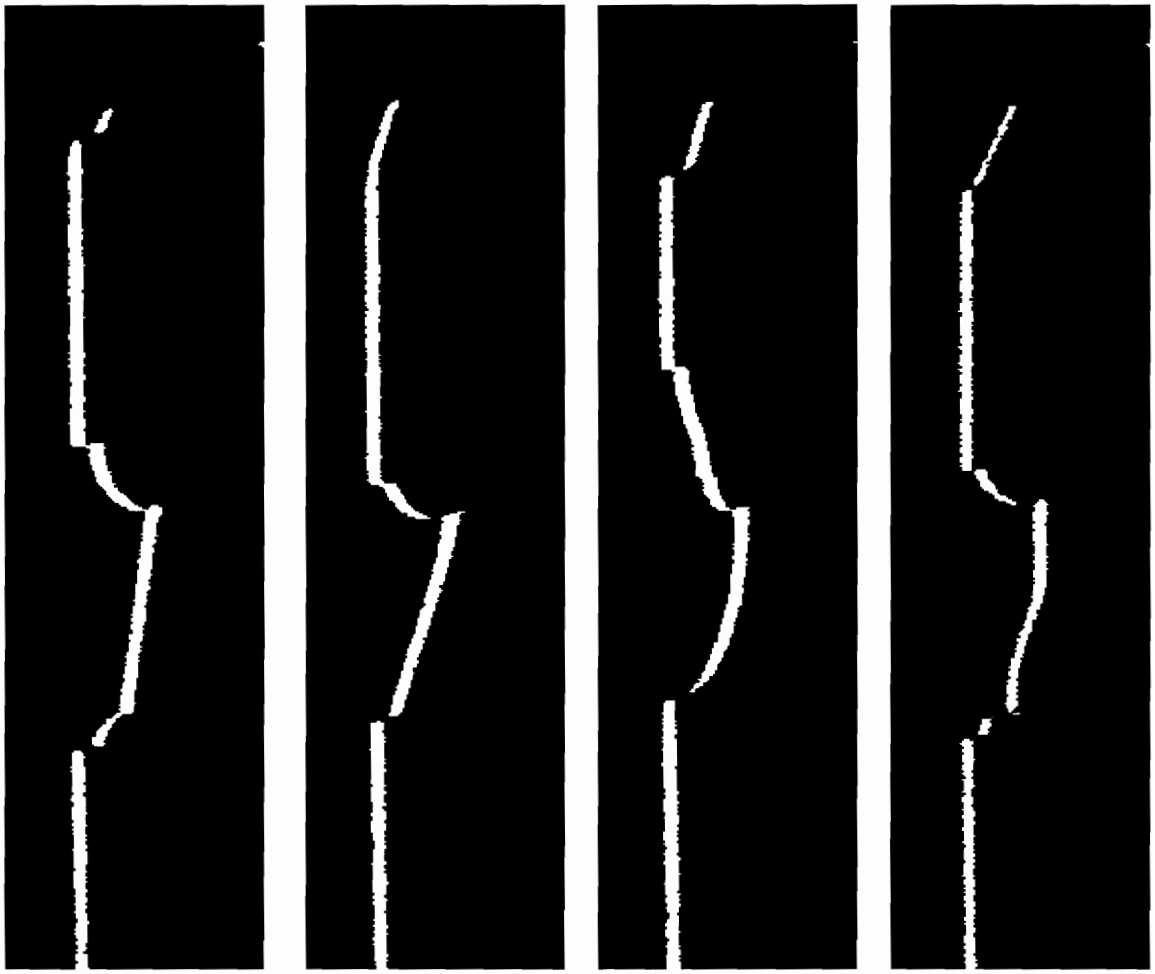

Figure 4-2. Example profile images. These were obtained using the profile comera on the door style classification stand.

4.3 Preprocessing steps

The preprocessing steps are 1) thresholding, 2) thinning, and 3) dropout replacement. These steps are illustrated for one profile image in Figure 4-3. The original

image in Figure 4-3(a) is thresholded immediately after A/D conversion using a lookup table on the frame grabber board, resulting in the binary image in Figure 4-3(b).

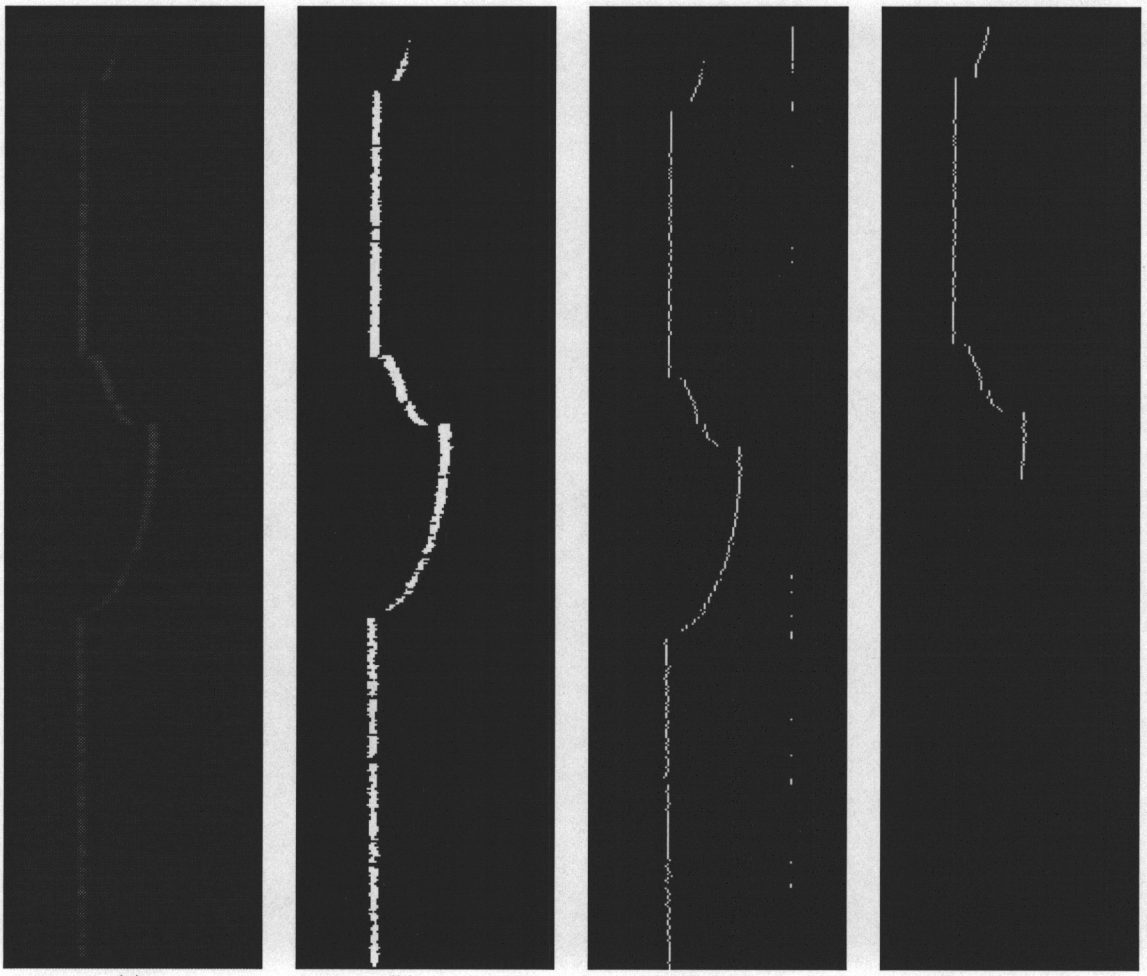

Figure 4-3. Profile processing steps. The profile style illustrated above is 3T. (a) Image from profile camera. (b) Profile image after threshold operation. (c) Profile image after thinning. Notice that some points are missing on the profile. (d) Profile image for classification. The is the profile image after missing point correction.

Thinning is a procedure to transform a binary profile to a skeleton. It reduces the amount of data and simplifies later processing. Because of the image geometry, a very simple thinning method is possible, it is described as Algorithm 4-1. The image is

processed one row at a time, from column index 1 to column index M, retaining only the midpoint of the bright profile region.

Notice that the result of thinning is not a single continuous curve. Points on the profile may be missing for several reasons, including roughness of the wood or small shadow regions on the door caused by occlusion of the laser by the molding. If there is no bright spot in a row, this thinning algorithm assumes the maximum column index M as the result. This is shown in Figure 4-3(c), in which all the missing points are located at column M.

To simplify later processing, these "dropouts" in the profile curve are replaced by their previous neighboring values as illustrated in Figure 4-5. If $p(j)$ is thinned profile, j is the row index of the missing profile point, then this dropouts replacement can be represented by

$$p(j) = p(j\text{-}1)$$

This replacement method is appropriate because 1) empirically, the maximum number of continuous missing points is no more than three; and 2) by carefully adjust the camera position, the plateau region can be placed almost at the same height level. The resulting image after dropout replacement is shown in Figure 4-3(d).

The preprocessing steps results in a one-dimensional profile curve $p(j)$, this represents the height map of the profile, where j is the row index of the original image.

Algorithm 4-1. Thinning

Let pixels inside the profile region have value 1, and outside the profile region have value 0. The entire region to be processed is a rectangular area of size L rows by M columns, as shown in Figure 4-4. The output is a thinned profile, a one-dimensional array called Thin_profile.

```
counter = 0
FOR j = 1 to L
        set Profile_start = False
        FOR i = 1 to M
                IF pixel value is 0
                        IF Profile_start is FALSE
                                increase counter by 1;
                        ELSE
                                break out of i loop
                        ENDIF
                ELSE
                        set Profile_start = TRUE
                        increase counter by 0.5
                ENDIF
        END FOR
        Thin_profile[j] = (int) counter;
END FOR
```

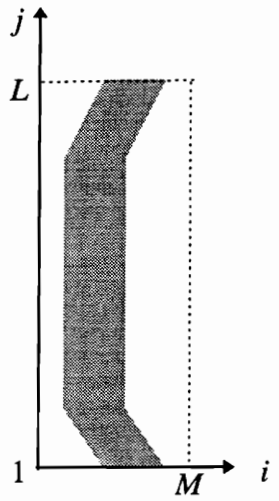

Figure 4-4. Thresholded profile image in a two dimensional space.

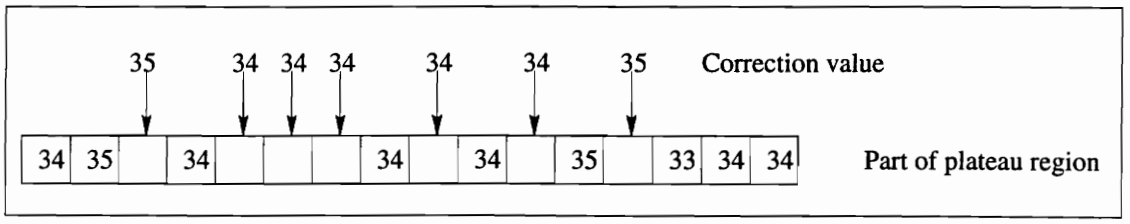

Figure 4-5. Replacement of dropout points. Each dropout point on the plateau takes its previous neighboring value as its replacement value.

4.4 Profile classification by template matching

Template matching is the simplest approach to many visual inspection tasks. A template is a small image representing an ideal view of the object under inspection. In this application, different templates have been obtained which represent profile curves. The unknown profile is then compared with all templates in the database, and the best match determines the profile code of the door.

4.4.1 Database

The database of profile classification contains 12 profile templates. These profile templates were obtained from camera images using the same preprocessing steps described in the previous section. We also considered generating profile templates from AutoCAD drawings, which would be ideal templates according to the designer. But before template matching can applied, these templates would have to be scaled and rotated according to the camera angle and position. This would require careful camera calibration and modeling, and was not attempted here.

4.4.2 Mathematical representation of template matching

Instead of using cross-correlation described in EQ. 3-3, another distance measure was used to reduce the computational cost. This is given by

$$d_{jk} = \sum_{i=1}^{N} \left| T_j(i) - p(i-k) \right|, \qquad (k = -3 \,..\, 3;\ j = 1 \,..\, 12) \tag{4-1}$$

where T_j is a template for style j, L is the number of points on the template, and p is the unknown profile. Considering the position variations, the profile is shifted by three pixels in both directions, as indicated by index k. The point-by-point difference between the template and the unknown profile is summed for each shift, and is represented by d_{jk}. Style j is assigned to profile p for the value of j that satisfies $d_j = min(d_{jk})$, where d_j is the minimum distance between p and all shifted templates. The value d_j is a similarity measurement for T_j and p. For a perfect match, d_j is 0.

EQ. 4-1 is applied to the unknown profile for all twelve templates. The smallest value of d_j indicates the best match of the profile with template j. A threshold value was carefully chosen to determine if the match is a "real" match, or if that profile should be classified as "unknown". The template matching method is summarized in Figure 4-6.

4.4.3 Summary

Classification using template matching did not perform as well as expected. Although it correctly classified styles F35, P, Q, R, Y8, E8, N8, T8, 3P, and 3S, it failed

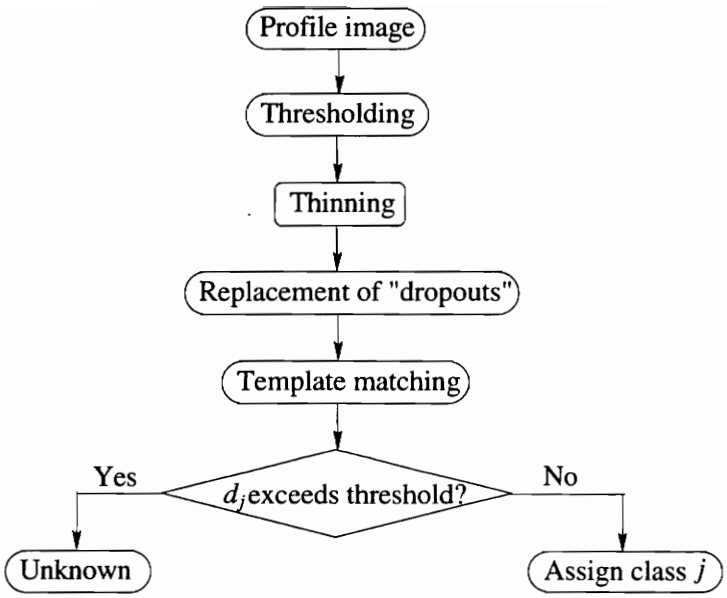

Figure 4-6. Profile processing and classification by template matching.

to classify most other styles. The reason for misclassification is that the template matching method is very sensitive to position change, and small manufacturing tolerances. A small variation or error in manufacturing, or some small change in the position of the camera and laser, can result a mismatch or an unknown style.

Template matching is simple, and easy to implement. The biggest advantage of template matching method is that it is easy to add new styles to the classification system. This can be done by preprocessing the new profile style, and then adding it to the profile style database. Unfortunately, the performance is not acceptable in this application

4.5 Feature based profile classification

In this section, a feature-based approach in profile classification is described. This method has been extensively tested, and has proved to work reliably for all known profile styles.

4.5.1 Features extraction

After careful analysis, we decided that the set of features illustrated in Figure 4-7 can distinguish the 12 existing profile styles. Features d_1 and d_2 are the distances from the left edge of the profile to the two plateau ends. Features d_3 and d_4 represent the height values of two points on the inside profile, and feature d_5 represents the height of the panel. Feature d_5 is also used to distinguish whether the panel is flat, raised, or empty for door frames.

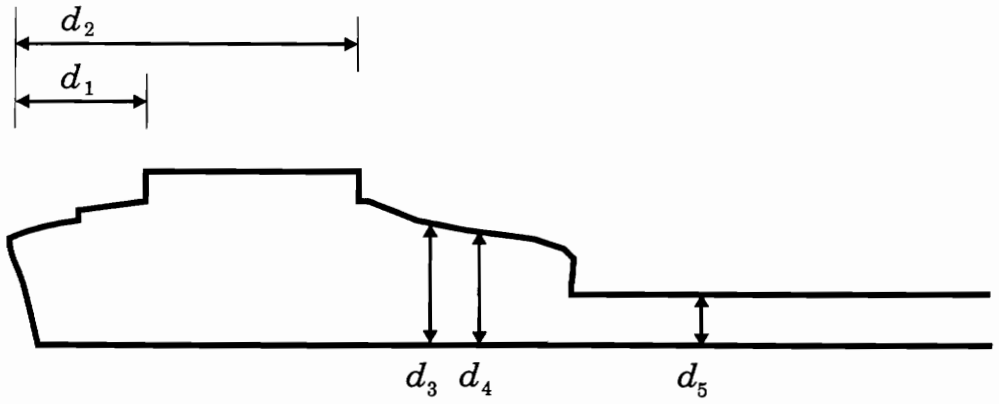

Figure 4-7. Features used for profile classification. The first two features on the left are most significant. They are sufficient to distinguish most of the door profiles shown in Figure 2-5.

Among the five features described above, features d_1 and d_2 are the most important. They can reliably distinguish all of the style groups except for the following:

{(1K, 1M), (Y1, E1, N1, T1), (Y2, E2, N2, T2)}

and

{(3T, 3U), (F35, L35)}.

In the first set, the corner locations are exactly the same according to the AutoCAD drawings, and therefore require additional processing. The only difference

between these three groups is the inside profile. After considering several alternatives, such as template matching or curve fitting on the inside profile, we decided that the height measurements of d_3 and d_4 can distinguish these three groups. The problem with the second set is that the plateau corner locations are too close to distinguish them consistently. Fortunately, the panel height for these two groups differs by 0.06". With a resolution of 0.01 inch/pixel, the profile camera can classify these two groups by measuring d_5.

The result of the preprocessing steps is a one-dimensional profile curve $p(i)$, where i is the row index of the original image. The index is now offset so that $i = 1$ references the first point on the curve. With this convention, features d_3, d_4, and d_5 are trivial to determine since they are simple height values of the profile array p for prestored values of i.

Features d_1 and d_2 are the distances from the left edge of the profile to the two plateau endpoints. Locating these endpoints is accomplished by performing edge detection on $p(i)$. Several edge detectors are evaluated in Chapter 5 with and without artificially added noise, and at several filter lengths. Because of processing speed, simplicity, and noise immunity, the filter [1 1 1 0 -1 -1 -1] has been implemented in the final system. This filter reliably detects plateau endpoints for most profile groups. An exception is style 1F, which does not have a plateau endpoint near the outside profile. This style is therefore recognized by the absence of a plateau endpoint. Filtering results for examples of all existing profiles are shown in Figure 4-8.

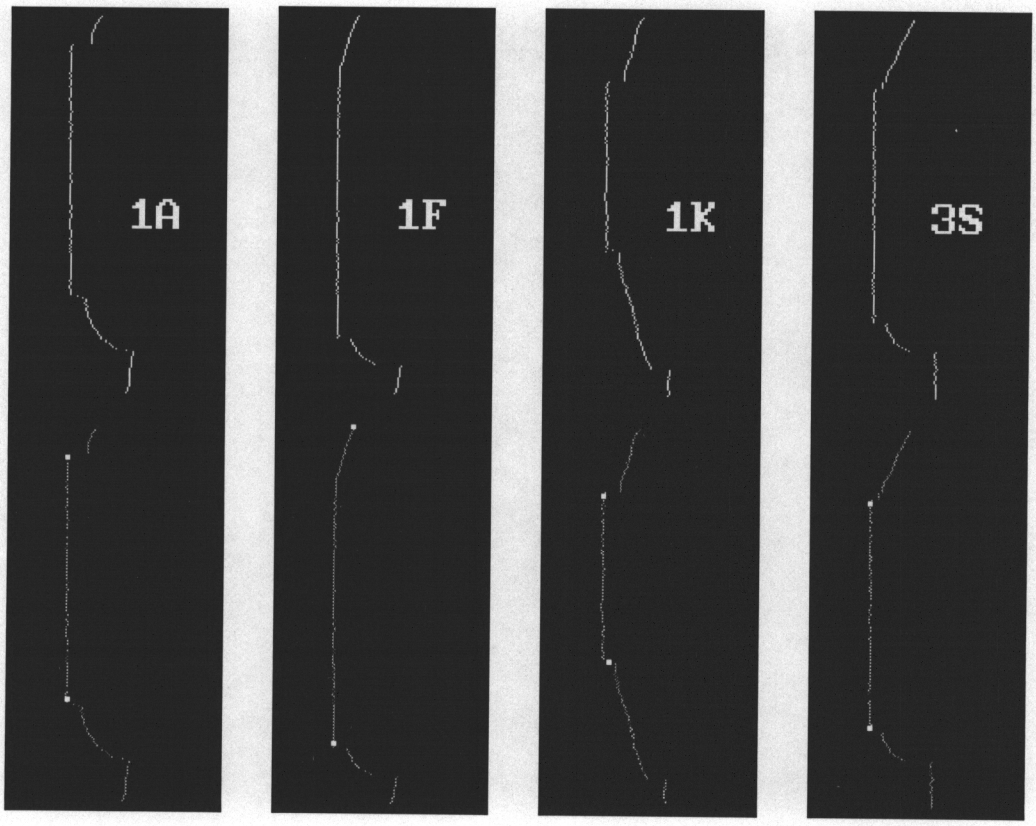

Figure 4-8. Twelve profile images currently in production. In each image, the curve shown at the top is preprocessed profile image. The curves shown at the bottom illustrate the result of edge detection. Detected plateau endpoints are indicated by the bright spots on the profile. The edge detector used here is [1 1 1 0 -1 -1 -1]. (Continued on next page).

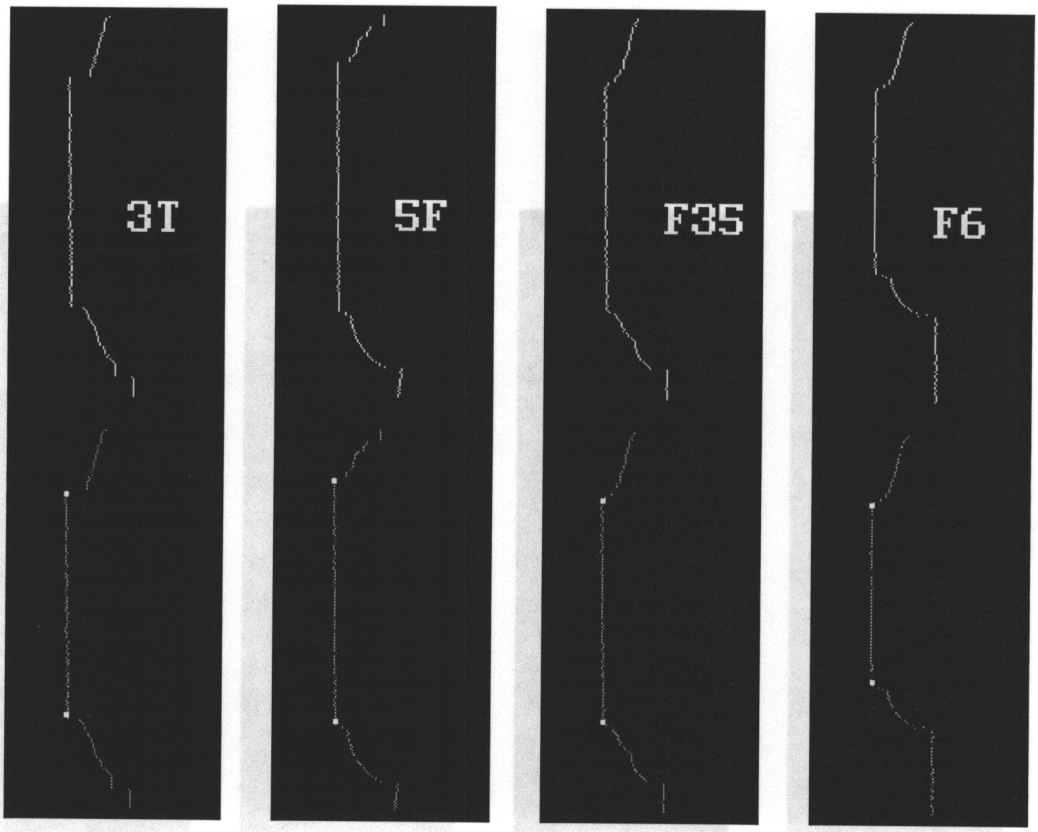

Figure 4-8. Continued.

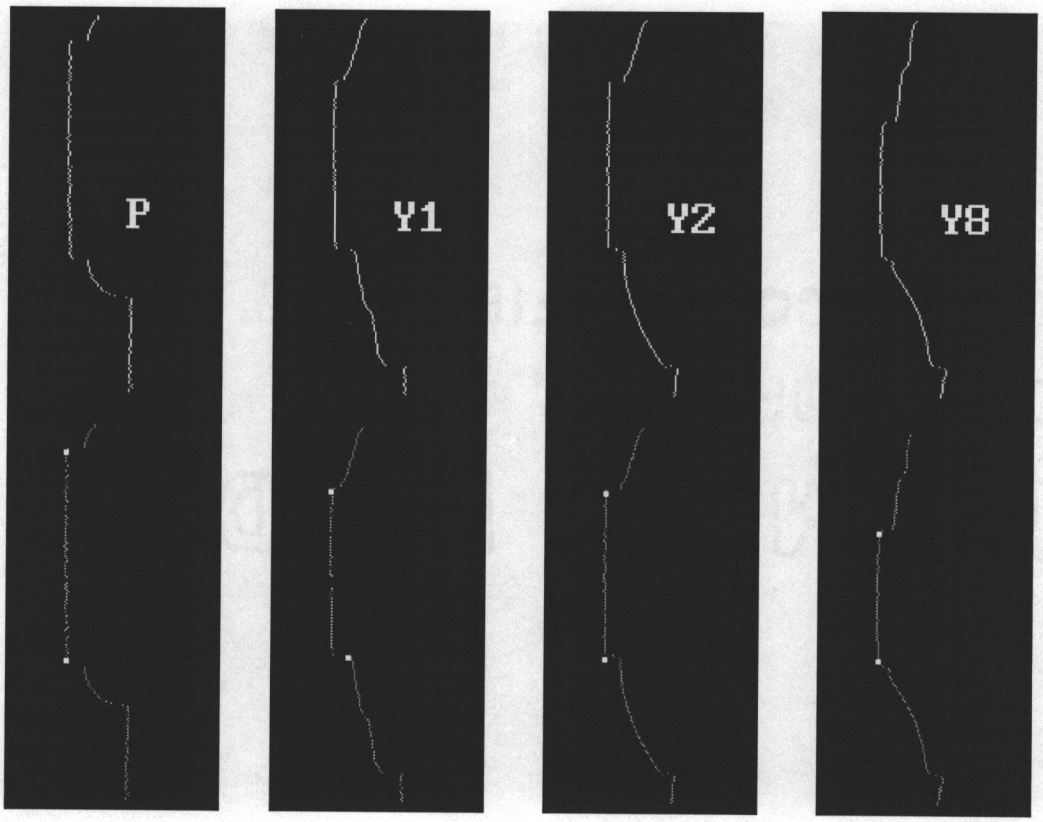

Figure 4-8. Continued.

4.5.2 Feature based profile classification

The result of profile processing is a feature vector $[d_1\ d_2\ d_3\ d_4\ d_5]^T$, with which it is possible to determine the profile code for the door. The approach we have adopted is a decision tree shown in Figure 4-9, encoded as a sequence of IF-THEN rules.

4.5.3 Summary

Feature based profile classification has been tested extensively. It is fast and reliable. Compared with the template matching approach, it requires less data storage. Instead of storing twelve thin profile arrays, it only needs to store features associated with each profile. On the other hand, the feature-based approach is also sensitive to position change, as discussed in Section 4.4.1. In addition, it is not as easy to add new styles to this system, as for template matching.

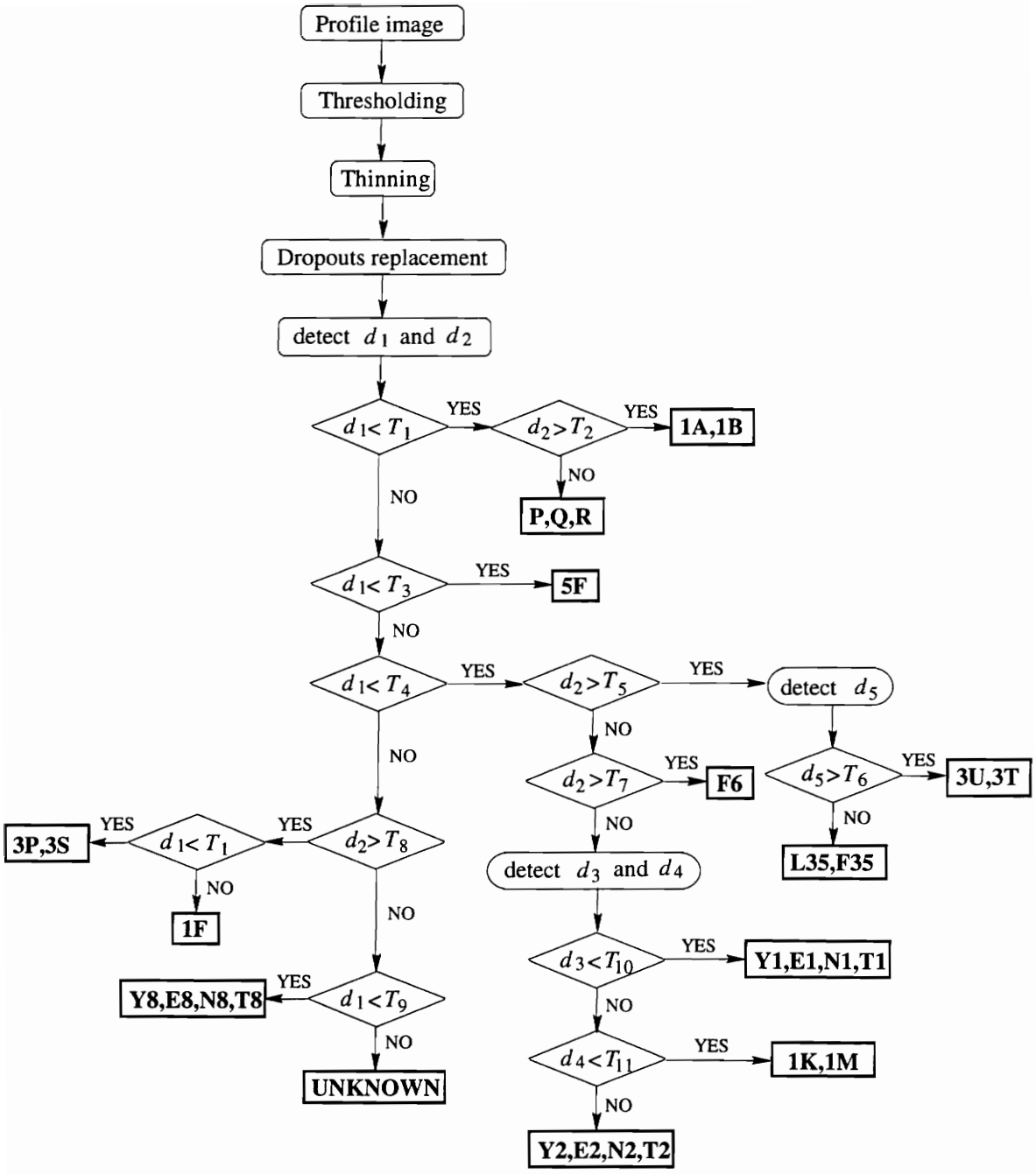

Figure 4-9. A decision tree for profile classification. Twelve profile groups can be distinguished by the locations of the plateau endpoints, two inside profile heights, and panel height. T_1 .. T_{11} are predetermined threshold values.

Chapter 5

Noise Sensitivity Analysis for Edge Detectors

Profile classification is a major processing step in door style classification. As described in Chapter 2, most of the profiles can be identified by determining the locations of plateau endpoints. One-dimensional edge detection can be used for this purpose, and it is very important for the edge operator to find the plateau edges correctly in the presence of noise.

The purpose of this chapter is to select a reliable edge detector for door profiles. Several linear edge detection filters are evaluated with and without artificially added Gaussian noise, and at several filter lengths. The main criteria in selecting a filter are localization accuracy, noise sensitivity, and processing speed. The resulting filter has been implemented in the final classification system.

5.1 Noise model and edge detection method

Edge detection can be viewed as a linear filtering process. A profile is convolved with the edge operator, and the absolute value of the result is then thresholded to obtain edge points. To test for noise sensitivity in the following analysis, additive Gaussian noise has been artificially introduced before processing. This is illustrated in Figure 5-1.

Let $p'(i)$ represent the original profile signal, let $n(i)$ represent additive Gaussian noise, let $p(i)$ represent the profile with noise, and let $h(i)$ represent the edge operator. N

is the length of the edge operator, and is assumed to be odd. L is the length of the profile signal. Then $p(i)$ is given by

$$p(i) = p'(i) + n(i) \tag{5-1}$$

The result of edge detection at each point is given by

$$e(i) = \sum_{j=-(N-1)/2}^{(N-1)/2} p(i-j)h(j), \quad \text{for } i = (N\text{-}1)/2 \text{ to } L - (N\text{-}1)/2 \tag{5-2}$$

The normalized result of a edge operator is given by

$$e_N(i) = \frac{e(i)}{\sum_{j=-(N-1)/2}^{(N-1)/2} |h(j)|}, \quad \text{for } i = (N\text{-}1)/2 \text{ to } L - (N\text{-}1)/2 \tag{5-3}$$

A point is assumed to be an edge point if

$$| e_N(i) | > T,$$

where T is the threshold value for an edge detector.

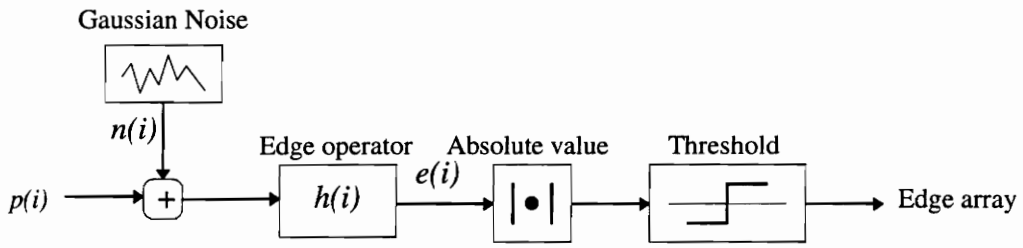

Figure 5-1. Processing steps in edge detection. The threshold value is different for each edge operator.

The goal of this processing is to detect plateau endpoints. Unfortunately, the method described above can result in many edges that are not part of the plateau. We determined experimentally that it is almost impossible to reliably detect only the two plateau endpoints for all the styles using a single edge operator.

One aspect of profile shapes makes it possible to detect only the plateau endpoints, however. If processing begins near the center of the plateau and works outward in both directions, the first edge points detected on both sides can be assumed to be plateau endpoints. By comparing the profiles for all styles, the region $[S_1, S_2]$ was determined to be on the plateau for all styles. By filtering a given profile in both directions, beginning at $(S_1 + (N-1)/2)$ and $(S_2 - (N-1)/2)$, and then moving left and right, respectively, false edge points on the inside and outside profile can be successfully ignored. This approach also has the advantage of reducing computational cost.

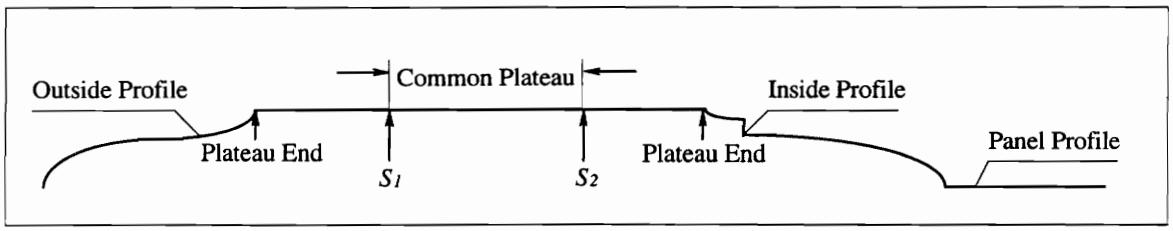

Figure 5-2 Example profile. By applying an edge detector in both directions from $S_1 + (N-1)/2$ and $S_2 - (N-1)/2$, the first edge point detected is considered to be plateau endpoint.

The rest of this section focuses on the selection of a reliable edge detector in the presence of noise, based on this bi-directional search method.

5.2 Edge detectors

Edge detection is a high-pass filtering process. The simplest one dimensional high-pass discrete filter is a difference operator, it is represented by [1 -1]. The simplest case with odd length is [1 0 -1]. For reasons of processing speed, a small filter size is essential, but because of noise, a larger filter is desirable. We concluded that a filter of length 7 represents the best compromise.

The filters we considered are

$h_1(i)$ = [1 1 1 0 -1 -1 -1]

$h_2(i)$ = [2 1.5 1 0 -1 -1.5 -2] (variation on h_1)

$h_3(i) = \frac{-i}{\sigma^2}\exp(\frac{-i^2}{2\sigma^2})$ (Canny operator)

The filter h_1 is the simplest of the three, a "difference-of-boxes" filter as discussed in Section 3.3.3. Filter h_2 is a variation of h_1. The final filter, h_3 is the first derivative of the Gaussian function, and is an approximation of the Canny edge detector[11]. This edge detector is known to have low error rates, and good localization in the presence of Gaussian noise. The tradeoff between detection and localization can be varied by changing the spatial width σ.

Ideally, the plateau region should be a straight line in the profile. In practice, the plateau will not be perfectly straight due to noise added during image acquisition. A typical profile is shown in Figure 5-3(a). Figure 5-3(b) is the same curve after artificially introducing additive Gaussian noise.

All three filters described here can be viewed as a combination of low-pass filtering and high-pass filtering. Low-pass filtering will reduce noise, and high-pass filtering will extract edge information.

Specially, the three edge detectors can be represented as

$h_1(i)$ = [1 2 3 3 2 1]*[1 -1]

$h_2(i)$ = [2 3.5 4.5 4.5 3.5 2]*[1 -1]

$h_3(i) = \frac{d}{di}(\exp(\frac{-i^2}{2\sigma^2}))$

where * represents convolution. This illustrates the fact that all three filters are a combination of low-pass and high-pass filtering.

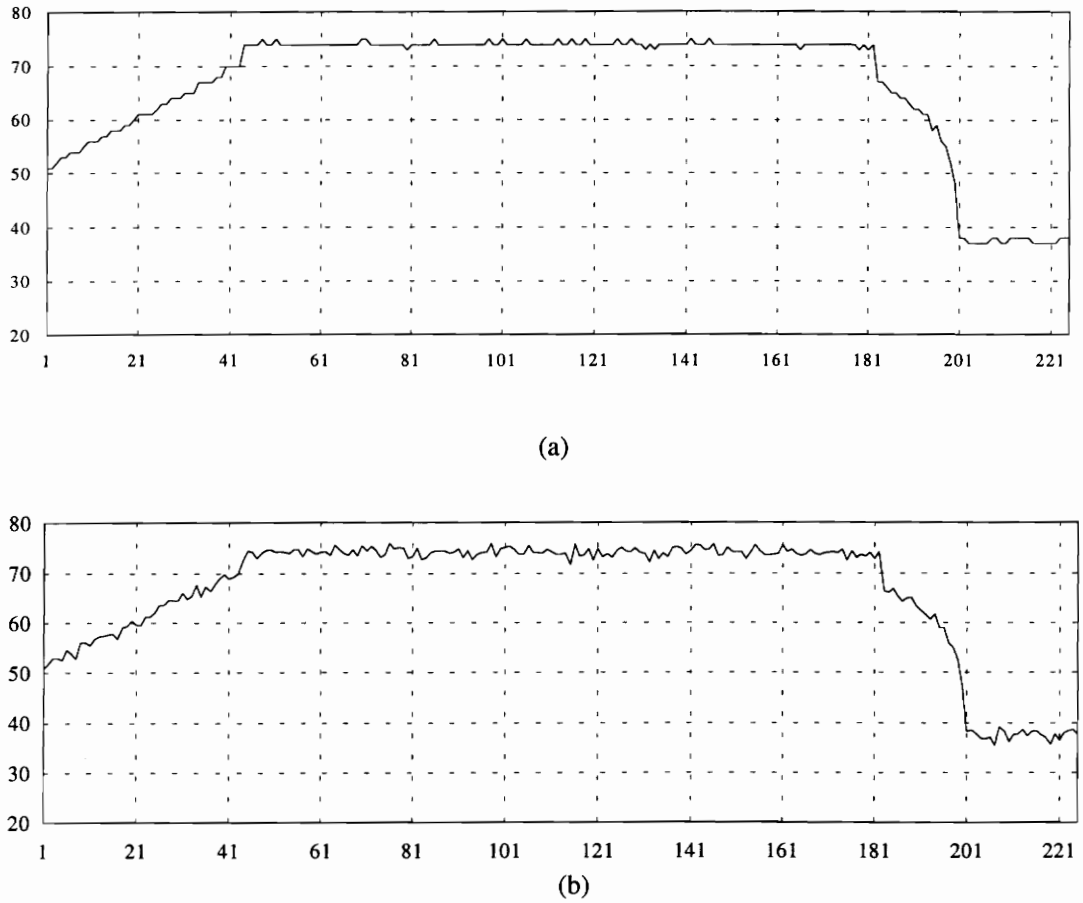

Figure 5-3. Example profile curve, style 3S. There are 225 data points. (a) Actual profile, obtained using the preprocessing steps of thresholding, thinning, and missing points correction. (b) The same profile with additive Gaussian noise, SNR = 25. In both cases, the horizontal axis corresponds to the row index of the original image, and the vertical axis represents the height value of the profile. For both axes, the units are pixels.

Figure 5-4 is a set of plots showing the effect of the low-pass portions of the three edge detectors. These are shown for the profile curve 3S with SNR = 25(Figure 5-3(b)). Figure 5-5 shows the results from the three edge detectors operating on the same profile. They can also be viewed as high-pass filtering of the smoothed curves shown in Figure 5-4.

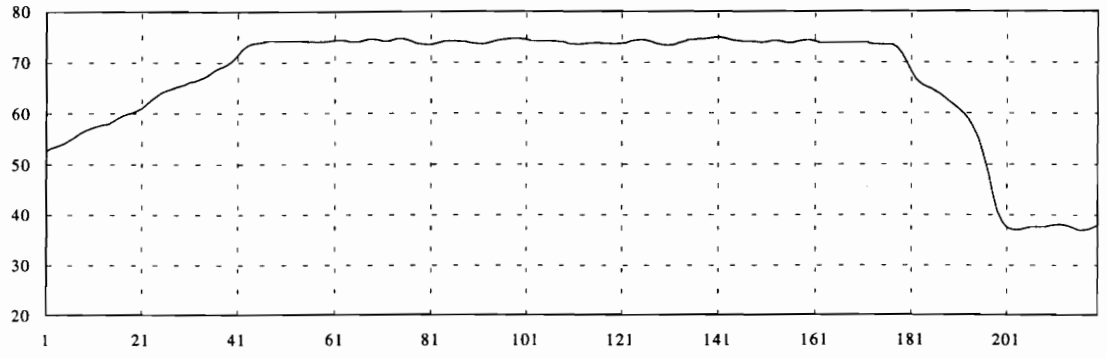

(a)

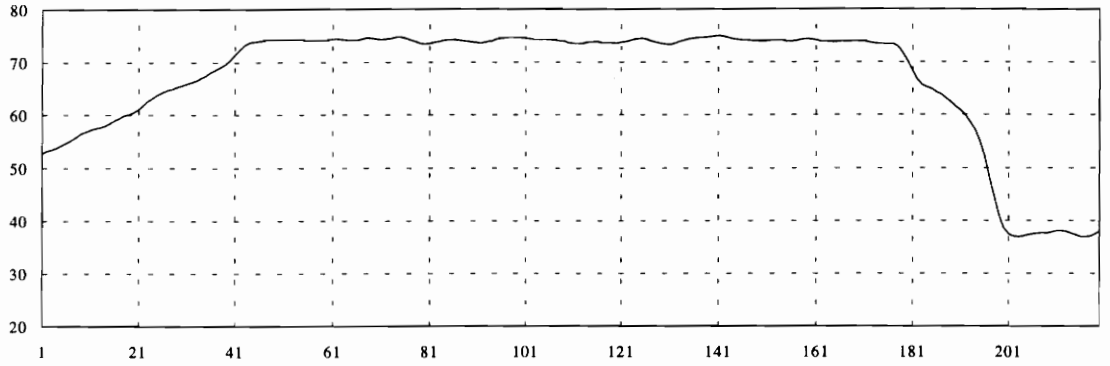

(b)

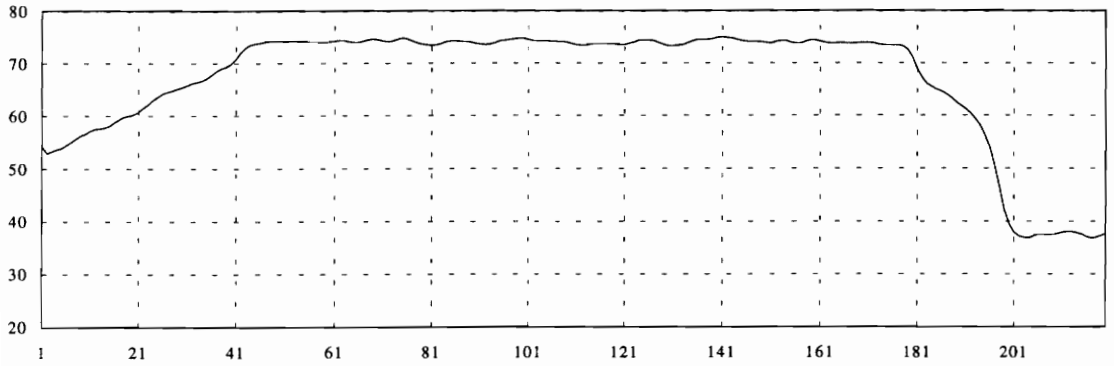

(c)

Figure 5-4. Results obtained by low-pass filtering the profile in Figure 5-3(b). (a) Results obtained using [1 2 3 3 2 1]. (2) Results obtained using [2 3.5 4.5 4.5 3.5 2]. (c) Results obtained using $\exp(\frac{-i^2}{2\sigma^2})$, with $\sigma^2 = 0.0002$.

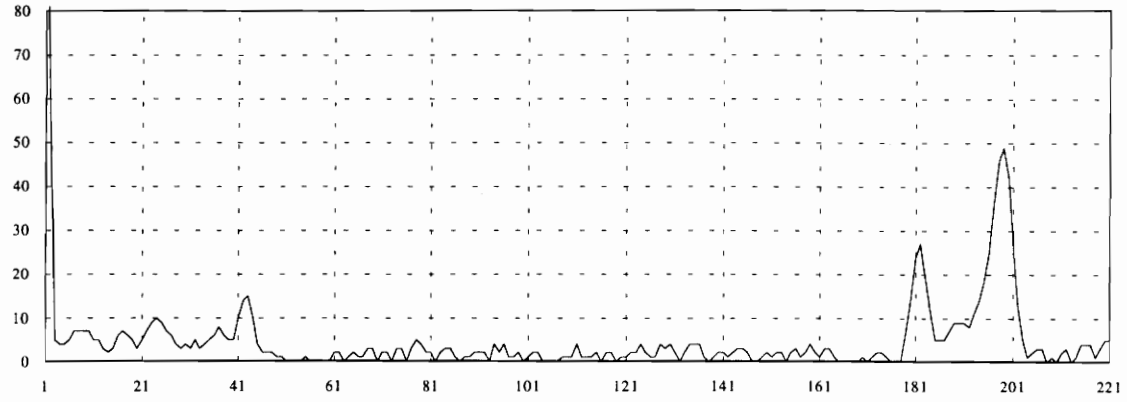

(a)

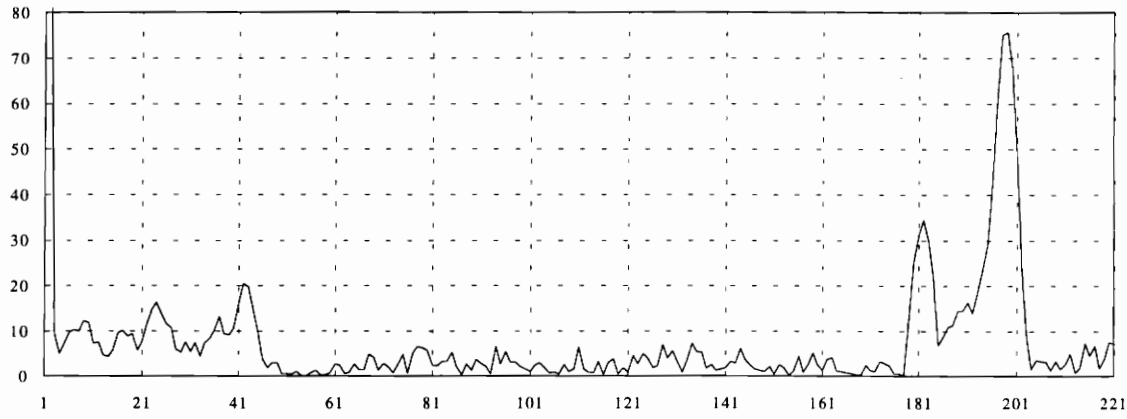

(b)

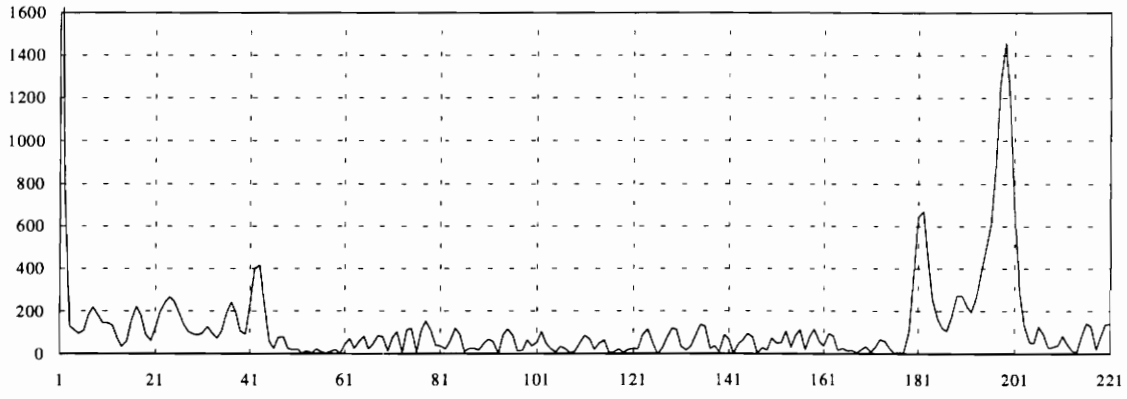

(c)

Figure 5-5. Results obtained by filtering the profile in Figure 5-3(b) using 7-point filters. These are the magnitudes of the filtered results. (a) Results obtained using h_1. (2) Results obtained using h_2. (c) Results obtained using h_3, the Canny edge detector with $\sigma^2 = 0.0002$.

Figure 5-5 shows that all three edge detectors can detect plateau endpoints on style 3S with an edge to non-edge ratio around 3. Here edge refers to the smaller value at the two plateau endpoints, and non-edge refers to the maximum value on the plateau region. However, we cannot decide which filter is the best by simply observing these plots. Further evaluation of these filters is discussed in the next section.

5.3 Noise sensitivity analysis

This section describes the experimental performance of the three edge detectors described in the previous section. Profiles of all styles were obtained using the classification station, with the conveyor belt moving at operational speed. Different levels of Gaussian noise have been added artificially. The results are presented in Table 5-1 for h_1, Table 5-2 for h_2, Table 5-3 for h_3 with $\sigma^2 = 0.00003$, and Table 5-4 for h_3 with $\sigma^2 = 0.0002$. The impulse responses for both Canny edge detectors with $\sigma^2 = 0.00003$ and $\sigma^2 = 0.0002$ are shown in Figure 5-6.

In Tables 5-1 to 5-4, N_{max} represents the maximum level observed on the non-edge, (plateau) region; C_{min} represents the smaller of the two outputs at the true plateau endpoints. The summary on the second to last row contains the maximum value of N_{max}, and the minimum value of C_{min} for all profiles. The last row in each table is most important: it represents the "detectability" of each detector, which is defined to be C_{min}/N_{max}. A higher value of edge to non-edge ratio means better detectability.

A special case is style 1F, which is marked by "*". The outside plateau corner of style 1F is curved, and can not be detected reliably by any of the three edge detectors. This is shown in Figure 2-5. This style is therefore detected by the absence of a sharp outside plateau edge.

These tables indicate that all of these of edge detectors can effectively detect plateau endpoints for SNR =∞, SNR = 30, and SNR = 25, since $C_{min} > N_{max}$, which indicates that a threshold value can be carefully chosen after observing filter responses for all 12 possible profiles. None of the edge filters performs well at SNR = 20. The edge to non-edge ratio for edge filter h_1 and h_2 is 1.0, which means that the maximum non-edge level and the minimum edge level is the same. The edge to non-edge ratio for the Canny edge detector at this noise level is less than 1 for $\sigma^2 = 0.00003$, and close to 1 for $\sigma^2 = 0.0002$. From the last row of the four tables, it can be concluded that edge filter h_1 has a better overall performance.

The Canny edge detector is a flexible edge detector, in that its performance can be adjusted by σ. From Tables 5-3 and 5-4, we see that the performance of the Canny edge detector with $\sigma^2 = 0.0002$ is much better, even though both of them are at filter length 7. Figure 5-6 contains plots for both of the Canny edge detectors. Figure 5-6(a) shows that the first and the seventh points of the Canny filter are almost zero, and the second and sixth points of the filter are close to zero, so that this filter is practically a filter with length 3. It is important to choose a σ carefully so that not only its filter length meets the requirement, but also to improve its performance. Figure 5-7 contains the results of both

Canny edge detectors applied to the profile shown in Figure 5-3(b). Figure 5-7(a) is the result of the Canny edge detector with $\sigma^2 = 0.00003$: its edge to non-edge ratio is about 1.5. Figure 5-7(b) is the result using $\sigma^2 = 0.0002$, and the resulting edge to non-edge ratio is about 2.0.

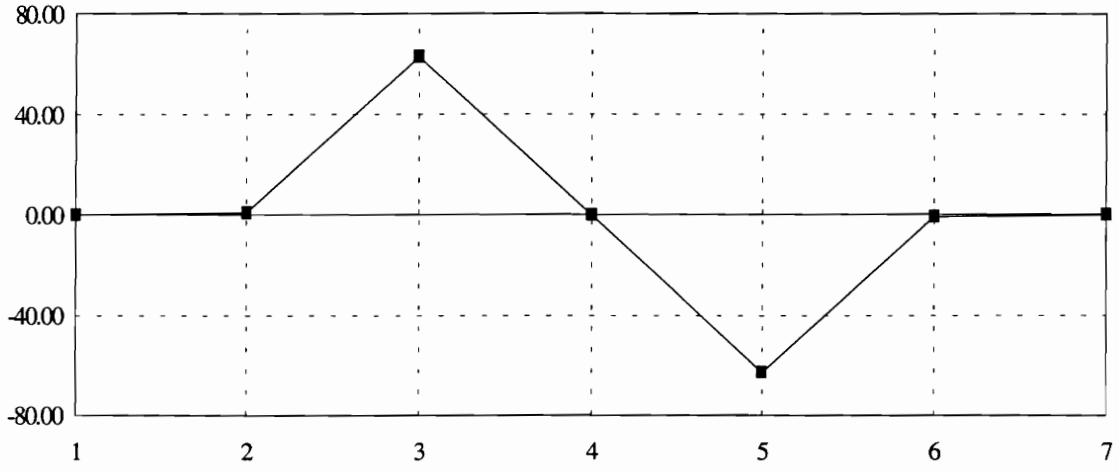

(a)

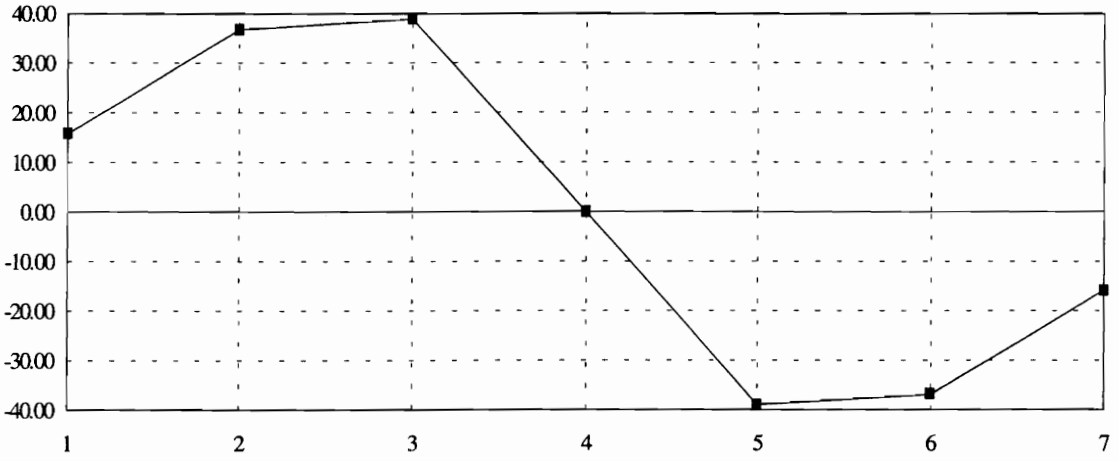

(b)

Figure 5-6. Canny edge detector with filter length 7. (a) $\sigma^2 = 0.00003$: the filter is [0.00 0.85 62.96 0 -62.96 -0.85 0.00]. (b) $\sigma^2 = 0.0002$: the filter is [15.81 36.79 38.94 0 -38.94 -36.79 -15.81].

Table 5-1. Non-normalized result using edge detector [1 1 1 0 -1 -1 -1]. Different levels of Gaussian noise were added to 12 profiles. N_{max} is the maximum magnitude within the plateau region, and C_{min} is the smaller value at the two edge locations. Edge to non-edge ratio is defined as C_{min}/N_{max}. Each style label may represent several styles as shown in Figure 2-5.

Filter 1		SNR = ∞		SNR = 30		SNR = 25		SNR = 20	
	style	*Nmax*	*Cmin*	*Nmax*	*Cmin*	*Nmax*	*Cmin*	*Nmax*	*Cmin*
$h_1(i)$	1A	3	>15	4	>15	6	>20	10	>20
	1F *	3	>15	3	>15	5	>20	10	>20
	5F	3	>15	5	>15	6	>20	8	>20
	F6	3	>15	6	>15	7	>20	8	>20
	1K	3	>15	3	>15	6	18	8	19
	L35	4	>15	6	>15	7	18	9	20
	P	3	>15	6	>15	6	>20	12	>20
	3S	3	12	4	13	6	16	9	14
	3U	3	>15	4	>15	8	>20	8	20
	Y1	3	>15	5	>15	6	17	9	20
	Y2	3	>15	4	>15	6	20	6	12
	Y8	3	>15	4	>15	4	17	7	16
Summary		4	12	6	13	8	16	12	12
Edge/non-edge		3.0		2.1		2.0		1.0	

Table 5-2. Non-normalized result using edge detector [2 1.5 1 0 -1 -1.5 -2].

Filter 2		SNR = ∞		SNR = 30		SNR = 25		SNR = 20	
	style	*Nmax*	*Cmin*	*Nmax*	*Cmin*	*Nmax*	*Cmin*	*Nmax*	*Cmin*
$h_2(i)$	1A	3	40	4	40	10	40	18	40
	1F *	4	36	5	38	8	36	12	38
	5F	5	37	6	37	8	32	16	30
	F6	3	37	6	37	5	35	12	38
	1K	4	28	4	30	8	30	15	33
	L35	7	28	8	28	5	30	18	28
	P	4	>40	6	>40	6	40	16	40
	3S	3	18	4	18	6	20	16	18
	3U	5	37	9	35	8	38	10	36
	Y1	4	28	7	28	6	20	12	28
	Y2	4	27	7	28	6	30	10	28
	Y8	3	27	5	32	8	26	18	34
Summary		7	18	9	18	10	20	18	18
Edge/non-edge		2.6		2.0		2.0		1.0	

Table 5-3. Non-normalized result of Canny edge detector, with $\sigma^2 = 0.00003$.

Canny Filter		SNR = ∞		SNR = 30		SNR = 25		SNR = 20	
	style	*Nmax*	*Cmin*	*Nmax*	*Cmin*	*Nmax*	*Cmin*	*Nmax*	*Cmin*
$h_3(i)$	1A	80	500	160	540	210	600	280	700
	1F *	110	400	180	400	200	400	280	380
	5F	110	320	120	400	200	360	340	440
	F6	80	400	130	380	180	400	360	400
	1K	80	260	100	300	180	320	360	380
	L35	110	310	180	360	180	380	300	320
	P	80	620	170	640	210	600	310	740
	3S	80	240	100	280	160	300	300	310
	3U	100	420	140	420	220	440	260	380
	Y1	80	380	110	400	180	480	240	500
	Y2	80	280	120	300	200	460	310	400
	Y8	80	310	100	300	180	310	360	360
Summary		110	240	180	280	220	300	360	320
Edge/non-edge		2.2		1.6		1.4		0.9	

Table 5-4. Non-normalized result of Canny edge detector, with $\sigma^2 = 0.0002$

Canny Filter		SNR = ∞		SNR = 30		SNR = 25		SNR = 20	
	style	*Nmax*	*Cmin*	*Nmax*	*Cmin*	*Nmax*	*Cmin*	*Nmax*	*Cmin*
$h_3(i)$	1A	90	800	100	750	160	780	300	680
	1F *	180	620	195	620	200	680	300	620
	5F	120	600	120	600	210	600	240	580
	F6	100	600	120	620	180	640	320	600
	1K	100	500	100	540	200	500	200	600
	L35	160	460	160	480	200	500	210	560
	P	100	900	100	880	210	900	380	900
	3S	90	380	110	390	180	410	300	420
	3U	160	680	170	680	210	650	260	700
	Y1	100	550	120	550	240	600	360	620
	Y2	100	500	110	480	120	520	300	620
	Y8	80	480	100	480	100	500	200	580
Summary		180	380	195	390	240	410	380	420
Edge/non-edge		2.1		2.0		1.7		1.1	

Several other σ^2 values were tested with "actual" filter lengths of 7, and their performance was very close to Table 5-4.

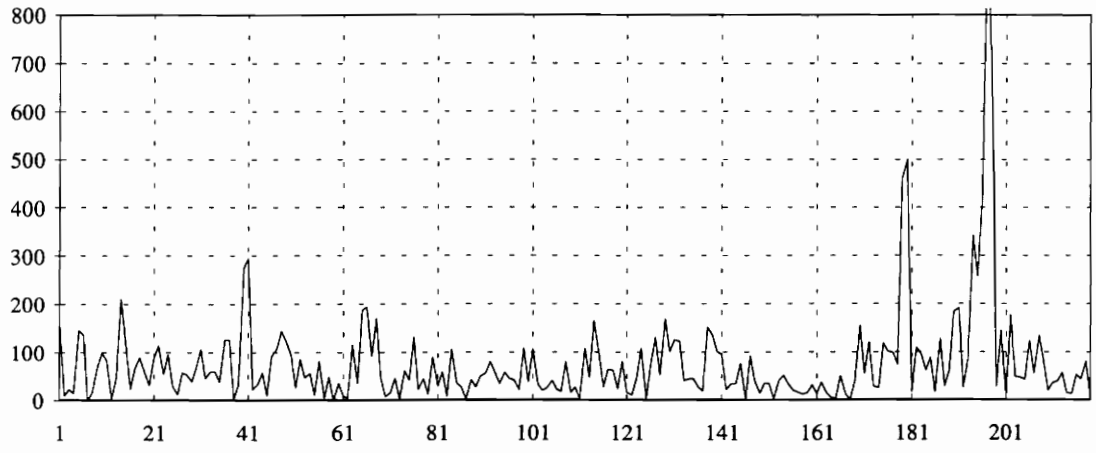

(a)

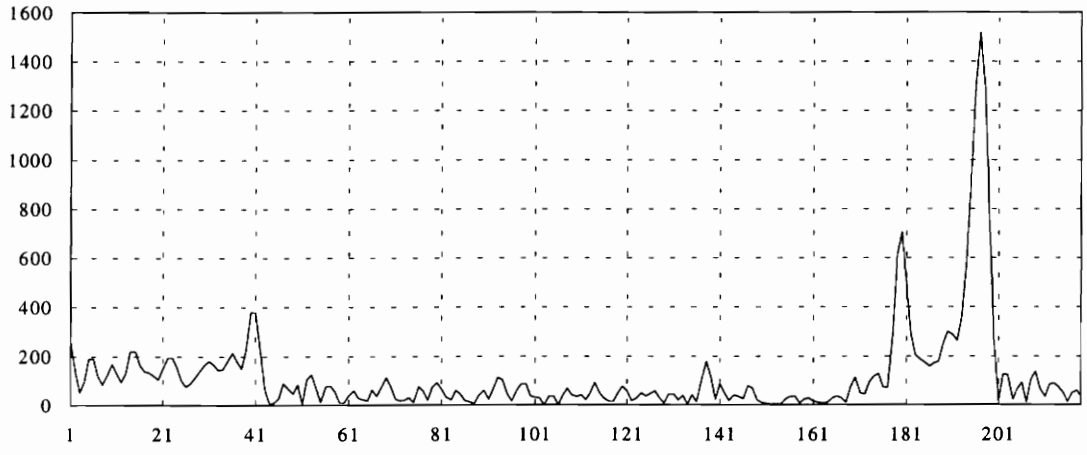

(b)

Figure 5-7. Result obtained from the Canny edge detector on the profile shown in Figure 5-3(b). (a) Result from the Canny edge detector with σ^2 = 0.00003. (b) Result from Canny detector with σ^2 = 0.0002.

5.4 Effect of filter length on edge detector performance

Further analysis has been performed using the Canny edge detector and the "difference-of-boxes" edge detector with filter length 19. Larger filter lengths will filter

out more noise, therefore have a higher edge to non-edge ratio. The Canny edge detector with length 19 and $\sigma^2 = 0.002$ is shown in Figure 5-8. Figure 5-9(a) is the result of edge filtering on the profile in Figure 5-3(b) using the Canny edge detector shown in Figure 5-8. Figure 5-9(b) is the result of difference-of-boxes filtering with length 19 on the same profile. For both edge detectors at this filter length, the edge to non-edge ratio is about 3.2, but we can see that the resulting curve at the plateau endpoints location obtained by the Canny edge detector is much sharper than that obtained by the difference-of-boxes filter. By adjusting σ, Canny edge detector not only has a good detectability, but also better localization. The difference-of-boxes filter cannot localize edges accurately at this filter length.

The tradeoff between localization and detection can also be varied with the length of the filter. This conclusion can be derived from the comparison between Figure 5-8(b) and Figure 5-7(b), or between Figure 5-8(c) and Figure 5-5(a). The edge to non-edge ratio is higher with bigger filter length, but edge filters with smaller filter length localize the edge better.

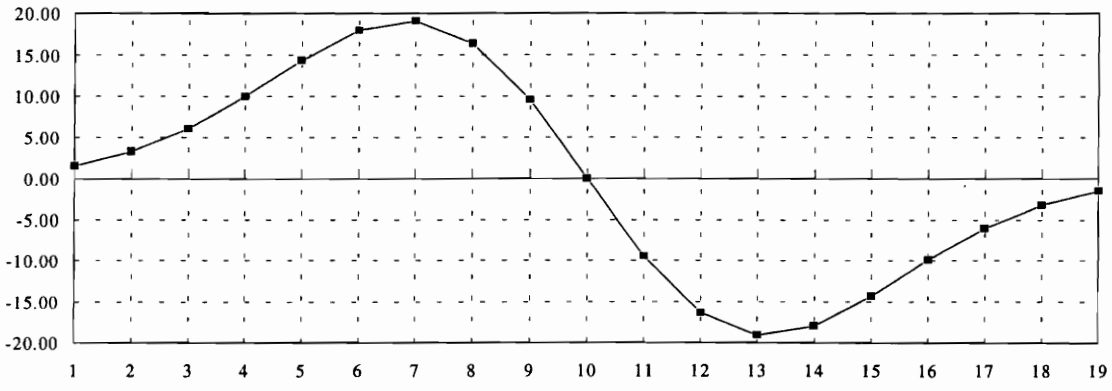

Figure 5-8. Canny edge detector with length 19, and $\sigma^2 = 0.001$.

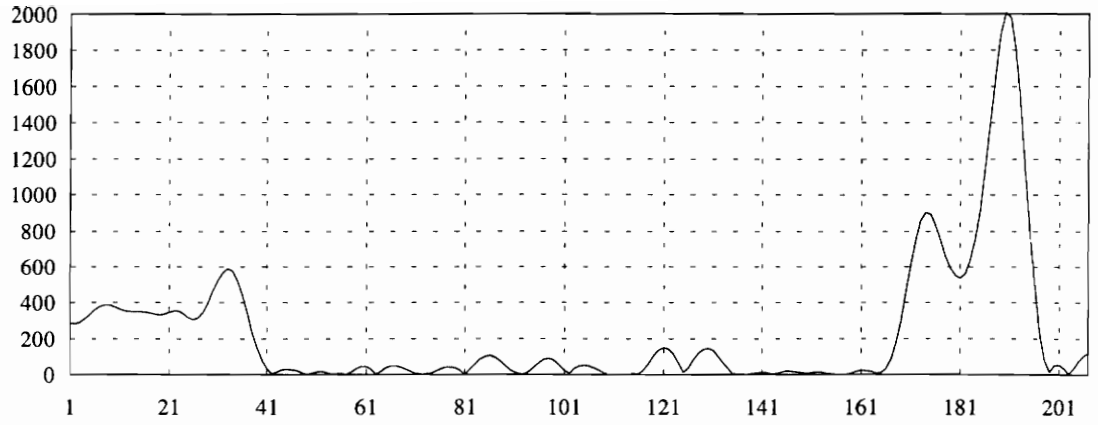

(a)

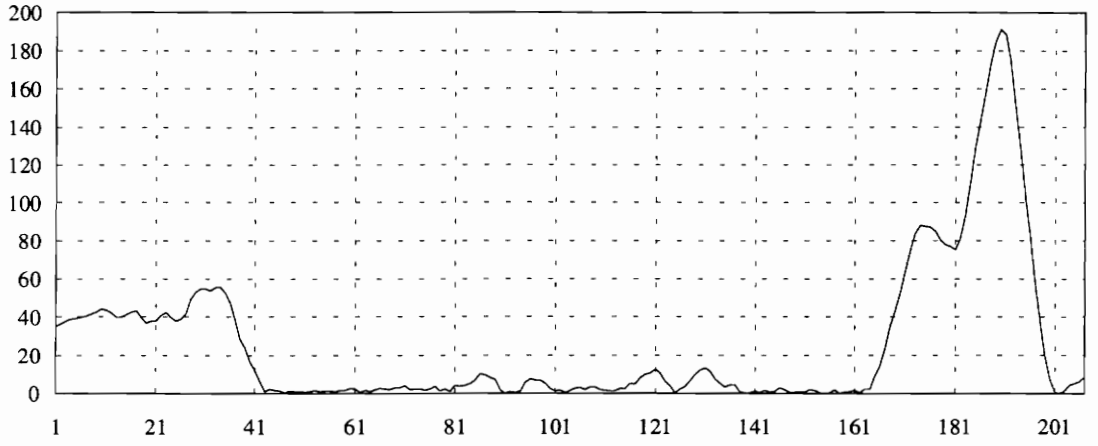

(b)

Figure 5-9. Comparison of Canny edge detector and difference-of-boxes filter with filter length 19. (a) Results obtained by applying the Canny edge detector on the profile curve shown in Figure 5-3(b). (b) Result obtained by applying the difference-of-boxes filter with length 19 on profile curve shown in Figure 5-3(b).

5.5 Conclusion

Several edge detectors have been analyzed in this chapter. The analysis has focused on different levels of noise being added to the profile, the detectability and localization of the filter, and the simplicity of the filter. Based on the experiments on twelve sample profiles, the filter h_1 = [1 1 1 0 -1 -1 -1] has been selected and implemented

in the final classification system. It is simple, accurate, and performs very well on all profiles of interest.

Chapter 6

Remaining Classification Tasks

6.1 Overview

As described in Chapter 2, doors are distinguished by style and size. Door style is determined by door profile, panel shape, and panel height. Door size is determined by width and height. The goal of this research is to detect all the features listed above, and then map these features to a unique ID code.

The last two chapters discussed the classification of door profiles only. Some door styles, such as 1F, F6, and 5F as illustrated in Figure 2-5, can be identified by profile classification alone. Others (such as P, Q, and R) have the same profile and need to be further distinguished by panel profile and panel shape. Fortunately, after identifying panel shape, only panel height is needed to distinguish all remaining styles. Although several panel profiles are possible, the height of the panel is sufficient to complete the classification.

This chapter describes the remaining tasks in door classification. Section 6.2 discusses the detection of all the features other than door profile, and includes ER-type doors. Section 6.3 describes the database for door code generation. Section 6.4 describes the final door classification station. Section 6.5 describes the classification procedures.

6.2 Remaining feature classification

6.2.1 Panel height

Panel height is given by d_5 as shown in Figure 4-7. It is simply the height value of the profile array at that location. It distinguishes raised panel, flat panel, or missing panel for door frames.

6.2.2 Door size

Door width is measured by the overview camera. Knowing that door widths range from 6.875" to 23.562", this camera observes distances of 6" to 25" from the alignment bar. This range of view, approximately 19", corresponds to 640 pixels in the image, so that the resolution is about 33 pixels per inch, or 0.03 inches per pixel.

Measurement of door height depends on the constant speed v of conveyor belt. A photoelectric sensor is used to detect the beginning and end of each door. An internal timer is programmed to run at 18.2 Hz, and a timer interrupt is enabled so that every 55 ms the microprocessor receives a timer interrupt. A counter is used to count the number of interrupts received by the microprocessor. It starts to count when the door blocks the sensor, and stops counting when the door leaves the sensor. The elapsed time t between the beginning and end of the door is given by

$$t = n \cdot \Delta t \qquad (6\text{-}1)$$

where n is the number of interrupts between the beginning and end of the door.

Then door height h is given by

$$h = v \cdot t = v \cdot n \cdot \Delta t \qquad (6\text{-}2)$$

From EQ. 6-2, we can see that the height measurement can be given by the number of interrupts n, since conveyor speed v and time Δt between two interrupts are constants. A lookup table based on the interrupt count n is used to measure the height.

6.2.3 Panel shape

6.2.3.1 Overview

The panel shape of cabinet doors can be square or cathedral. We have considered two different approaches to distinguish these shapes.

Figure 6-1 illustrates the difference between square and cathedral panels. The dimension h_1 is the width of the top horizontal bar on a square panel door, h_2 is the width of the bottom horizontal bar, and h_1' is the width of the top horizontal bar on a cathedral panel door, measured close to the vertical bar. The first difference between cathedral and square panels can be represented by

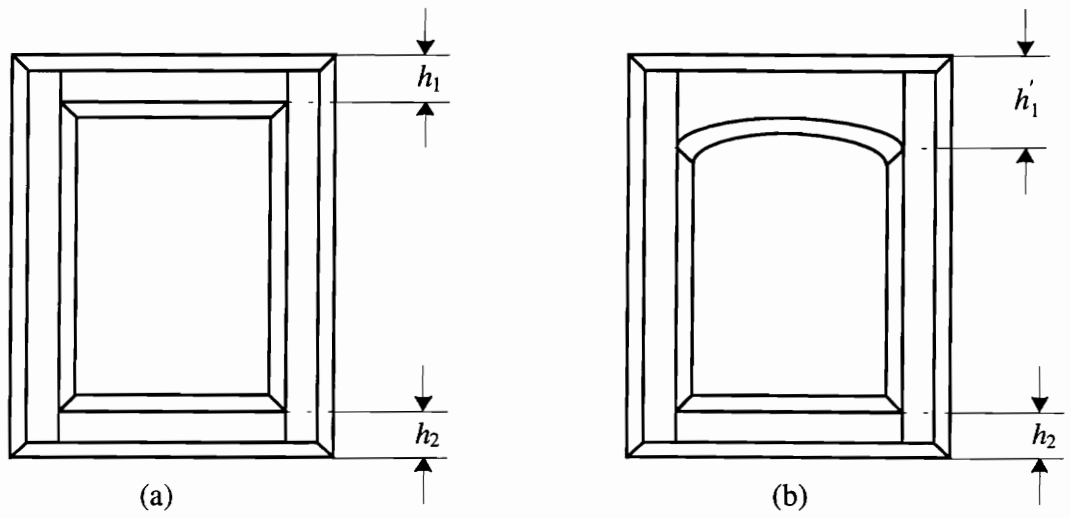

Figure 6-1. Classification of panel shape. (a) Square panel. (b) Cathedral panel. The difference between h_1 (or h_1') and h_2 can be used to distinguish square from cathedral panel.

$$h_1' > h_1 \qquad (6\text{-}3)$$

This expresses the fact that a cathedral panel door has a wider top horizontal bar. If a threshold value is carefully chosen, then both panel types can be distinguished by EQ. 6-3.

A second difference between cathedral and square panels is described in EQ. 2-4, and is shown in Figure 6-1. For a square panel, the vertical profile is symmetric. This is indicated by $h_1 = h_2$, but for a cathedral panel, $h_1' \neq h_2$, so that its vertical profile is not symmetric.

6.2.3.2 Classification of panel shape by top horizontal bar width

This approach is based on the first difference described above. It is attractive because it only involves the profile camera. As soon as the appearance of the door is detected, the profile camera begins to take images. The height value at a particular point (shown in Figure 6-2) is determined. This particular point is chosen just inside the vertical bar of the door along the alignment side. While the door is moving, and as images are continuously taken, the height value will have a sudden change when this point moves from the top horizontal bar to door panel. The total number of images taken until this moment is then used to determine the panel shape.

From Figure 6-2, we can see that after same number of image snaps, that particular point on Figure 6-2(b) has arrived at the door panel. However, that point shown in Figure 6-2(a) is still on the horizontal bar. Since $h_1' > h_1$, it takes longer for that particular point on the laser stripe to reach the door panel on a cathedral panel door.

This approach was the first that we attempted. It was successful for most cathedral panels. Unfortunately, for some narrow doors, which have a door width less than 12 inches, h_1' is very close to h_1. The result is that this method misclassifies them as square panels.

There are two limitations of this method. First, all the doors must travel top first; second, it depends heavily on the speed of image acquisition.

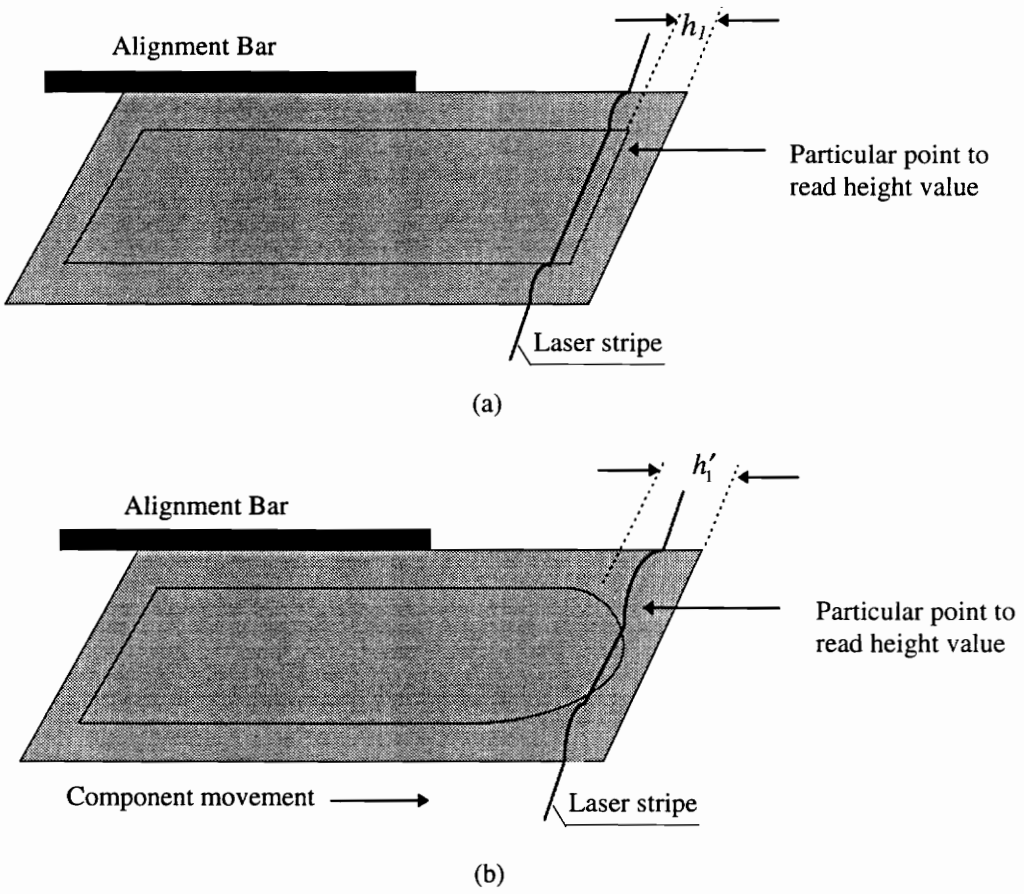

Figure 6-2. Illustration for panel shape analysis. After the same number of images have been taken from the profile camera, the laser stripe is different for (a) square and (b) cathedral panels. The values h_1' and h_1 are the widths of the top horizontal bar for cathedral and square panels, respectively.

Given a conveyor belt speed v of 6 inch/sec, the time delay Δt between two continuous snaps is 33 ms. The traveled distance s of the door between two consecutive snaps is

$$s = v \cdot \Delta t = 33(ms) \cdot 6(inch / \sec) = 0.2 \ (inch / snap)$$

In order to classify cathedral and square panel reliably, the distance between h_1 and h_1' in Figure 6-2 must be greater than $2s$, which is 0.4 inches. Unfortunately, some of the narrowest cathedral doors, such as 1K and 3T, do not meet this requirement. For this reason, this method was discarded.

6.2.3.3 Classification of panel shape by vertical profile

This approach is based on detecting asymmetric vertical profiles as described in section 2.3. This method calls for adding a third camera to the station, along with a second laser and a second photoelectric sensor. There are two motivations for this. The main reason is the need to handle narrow doors. The second reason is to accommodate ER-type doors, which can travel upside down on the conveyor, as described in the next section.

Figure 6-3 illustrates this approach. A second laser source generates a second laser line that is parallel to the direction of travel. The light stripe falls near the inside profile of doors that are aligned on the conveyor. A "panel camera" is positioned at the side of the conveyor to observe this new light stripe, which is approximately 6 inches long. Two photoelectric sensors are positioned at the side of the conveyor belt to trigger image acquisition. Both top and bottom images of the door are acquired. The panel camera

must be located in the middle of two sensors, so that the top and bottom images will appear symmetric for the square panel.

When the second sensor detects the presence of the door, the panel camera catches the first side-view image. This can be either the top or bottom portion of the door. When

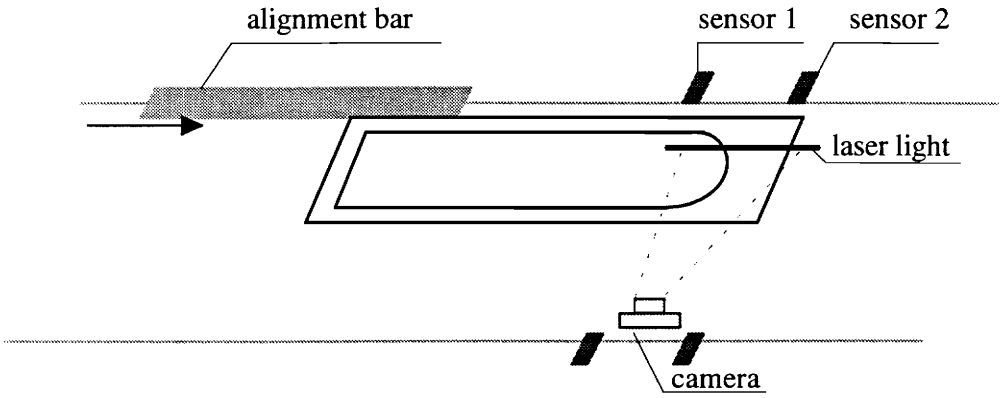

(a)

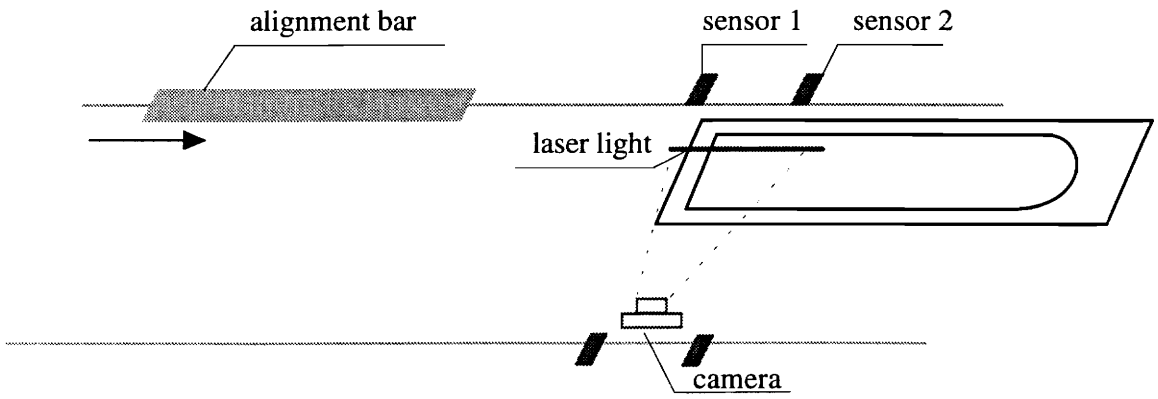

(b)

Figure 6-3. New approach for panel shape classification. (a) As soon as sensor 2 detects the presence of the door, an image is acquired using a third (panel) camera. (b) A second image is taken as soon as the sensor 1 detects the departure of the door. Sensor 1 is also used to measure the door height.

the first sensor detects the departure of the door, the second side-view image is taken by the panel camera. The system now uses information from both panel-camera images to determine the panel shape: If the panel shape is square, then the top and bottom portions of the door should be symmetric; otherwise it is classified as a cathedral panel.

Example images using this method are shown in Figure 6-4. These were obtained using the panel camera. Figure 6-4(a-b) are a pair of images of a cathedral-panel door. Figure 6-4(c-d) are a pair of images of a square-panel door. Notice that the profile of the square panel door appears symmetric. This method will work regardless of whether the door is long or short, and regardless of whether the door travels top-first or bottom-first. It has been verified to work well for all production doors.

6.2.4 ER-type doors

ER-type doors differ from normal doors in that the outside profile is not the same around the entire perimeter of the door. Instead, one vertical side of the door has a right-angle cut that we call a "square" profile.

In order to have the normal profile of ER doors visible to the profile camera, the normal profile needs to be placed against the alignment bar, even if this causes the door to travel bottom-first on the conveyor. The fact that some doors would be traveling upside down introduced a problem in classifying panel shape using the method described in section 6.2.3.2. After considering several alternatives, we decided to classify panel shape using vertical profile approach, which is described in section 6.2.3.3.

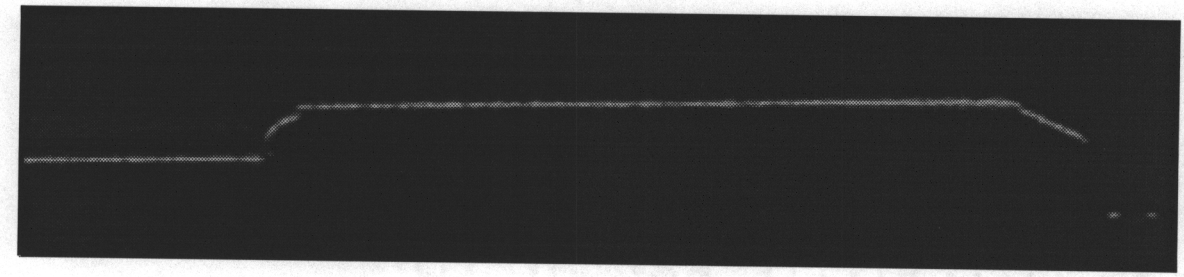

(a)

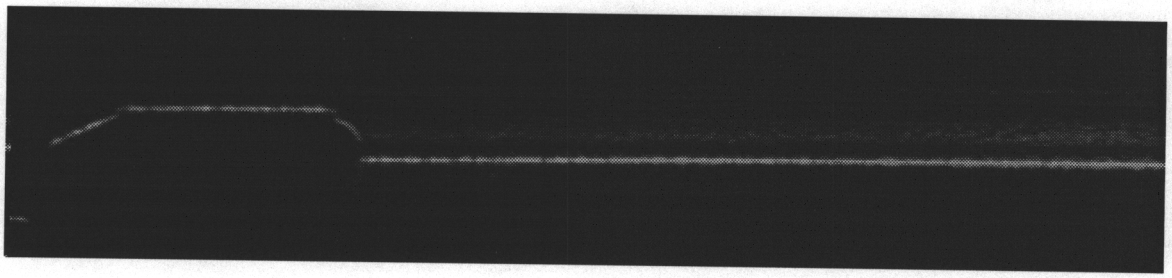

(b)

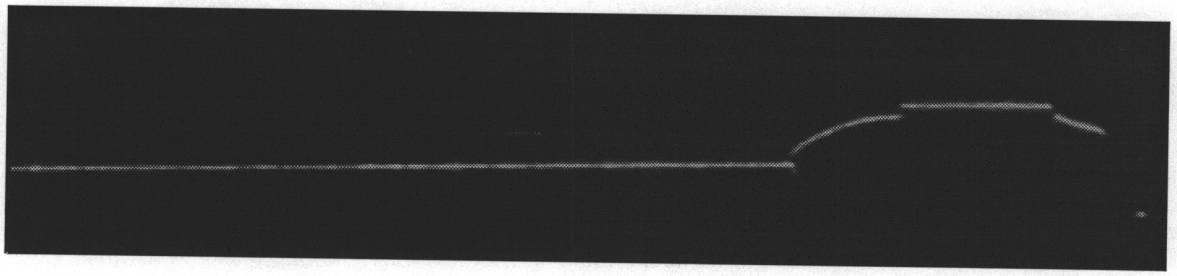

(c)

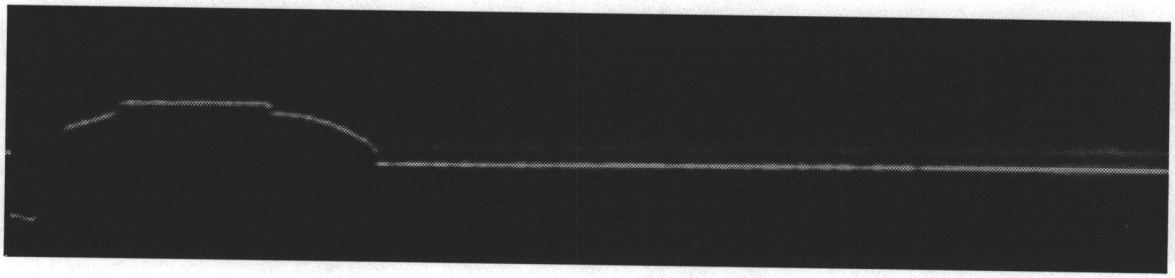

(d)

Figure 6-4. Sample images to illustrate panel shape classification. (a) Top portion of a cathedral panel. (b) Bottom portion of a cathedral panel. Notice that the plateau height is different in (a) and (b). (c) Top portion of a square panel. (d) Bottom portion of a square panel. The plateau lengths are nearly the same in two images.

The operator will place ER-type doors so that the "normal" outside profile is against the alignment bar. ER doors will travel either bottom-first or top-first, depending

on which side has the normal profile. The overview camera will observe the square profile side of ER doors, and the square profile can be detected by the sudden change in height map of laser stripe in overview image. Example overview images of ER-type and non ER-type doors are illustrated in Figure 6-5.

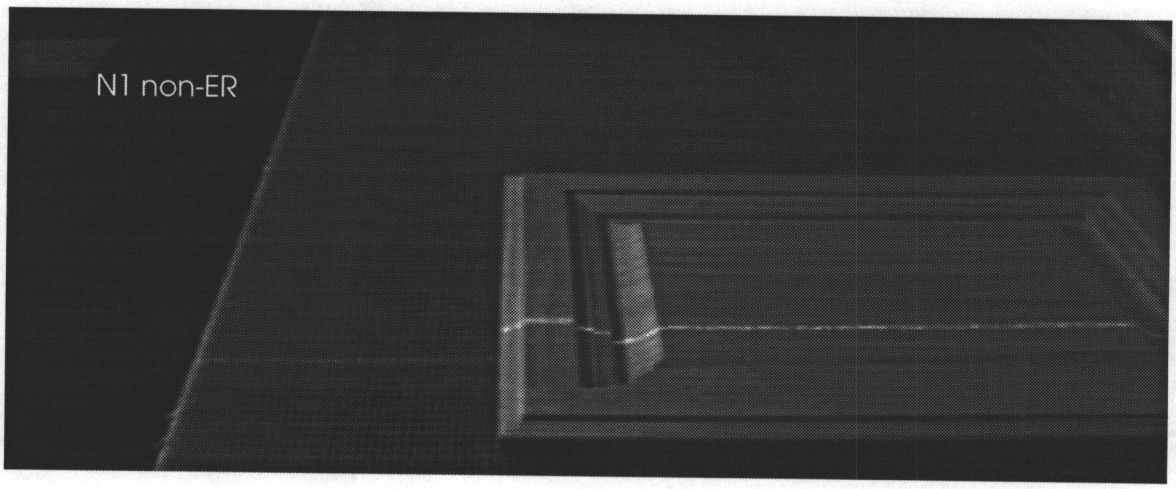

(a)

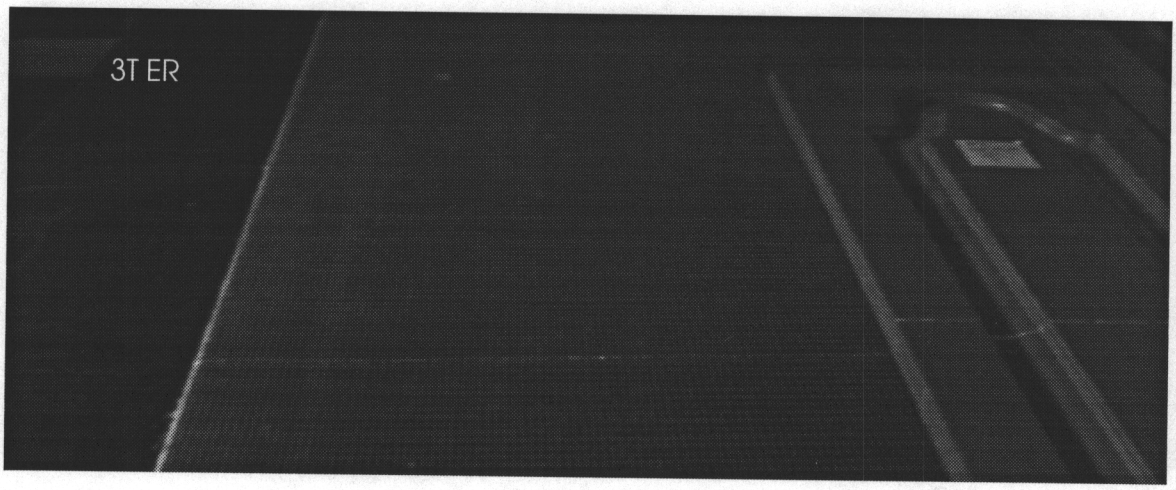

(b)

Figure 6-5. Sample image to illustrate classification of ER-type. Both images are taken from overview camera. (a) Non-ER type, N1 style. (b) ER type, 3T style.

6.3 Databases

A style database and a size database are maintained for door classification. The style database is organized as a three dimensional array, with each dimension representing profile style, panel height, and panel shape respectively. There are twelve profile styles as illustrated in Figure 2-5. Panel height refers to raised panel, flat panel, or empty panel for door frames. Panel shape refers to cathedral panel and square panel. ER-type is an independent feature, and is considered separately.

The size database includes door height and door width information. Door height is stored as a two dimensional array, with the first dimension representing door height measured in interrupt counts, and the second dimension represents the number of possible door widths within that height group. There is a Width_Code structure corresponding to each height group. The first element of this structure is an array of door widths, and the second is an array of door size code. The search algorithm is illustrated in Algorithm 6-1.

The algorithm searches for the door height first. Door height is classified into nineteen groups, with each representing the following heights in inches: 10, 11.5, 13, 14.5, 16, 17.5, 17.875, 20, 22.375, 23.875, 27, 28, 29.5, 34, 35.5, 40, 41.5, 47.75, and 49.25. These inch values correspond to interrupt counts in the database. Whenever a height group is detected, the number of possible door widths within that height group is given by the database. The algorithm then searches for door width corresponding to that height group. If there is a match for width, then a size code is generated for that match.

Algorithm 6-1. Search algorithm for size code

```
int     Height[Number_of_possible_height_group][2];
typedef  struct Width_Code {
        int     Width[Max_num_of_width_within_height_group];
        char    Code[Max_num_of_width_within_height_group][Max_len_of_code];
} Width_Code[Number_of_possible_height_group];


height_group_index = 100;           /* no more than 100 possible height group*/
door_size_code = "UNKNOWN";


FOR i = 0 to Number_of_possible_height_group
        IF  height equal to Height[i][0]
                height_group_index = i;
                break;
        END IF
END  FOR


IF      height_group_index equal to 100
        exit;
END IF


FOR j = 0 to Height[height_group_index][1]
        IF width equal to Width_Code[height_group_index].Width[j]
                door_size_code = Width_Code[height_group_index].Code[j];
                break;
        END IF
END  FOR
```

The system will generate a style code and size code for each door passing through the classification station. If there is no match in the database for either style or size code, then an "unknown" ID is assigned to that door. Otherwise, if it is an ER-type door, then code "ER" will also be specified. An example result from the classification system is "3T 1512", where 3T is a style code, and 1512 is size code. Since ER is not specified, this is a non-ER type door. Another example is "F5 FR 1230 ER", where F5 is a style code, 1230 is a size code, FR indicates that this is a door frame, and ER indicates that this door is ER-type.

6.4 Door classification station

The door style classification station is shown in Figure 6-6. It has been implemented and extensively tested, and performs very well for all styles and sizes currently in production. The station has three video cameras, two photoelectric sensors, and two lasers. All of this equipment is mounted above the conveyor belt.

Door must be aligned against the alignment bar as shown, and can travel either top-first or bottom-first. ER-type doors must be aligned so that the normal profile is against the alignment bar.

Laser stripe I is perpendicular to the direction of movement. It covers the entire door width, from the alignment bar to the maximum door width of about 25" inches. Laser stripe II is parallel to the moving direction. It covers the area within the two photoelectric sensors.

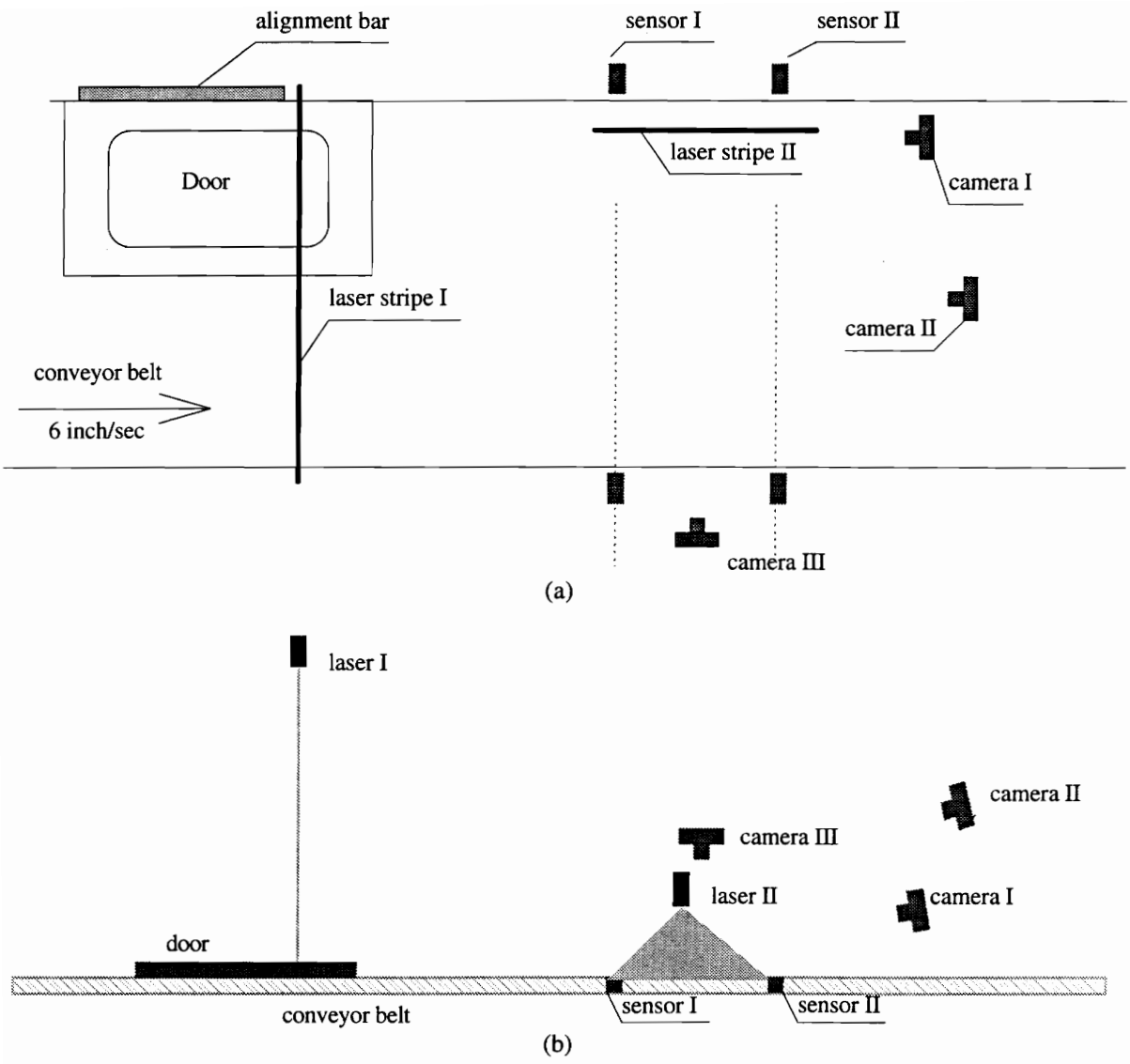

Figure 6-6. Door style classification station. (a) Top view. (b) Side view. Camera I (profile camera) provides a close-up view of the profile. Camera II (overview camera) is used to measure width and detect ER types. Camera III (sideview camera) looks from the side to detect panel shape.

Camera I is known as the "profile camera". It captures a close-up view of laser stripe I on the profile of a door near the alignment bar. Its field of view is approximately 3.5", and its resolution is approximately 0.01 inch/pixel. Camera II is called the "overview

camera", and it has a wider field of view. Measured from the alignment bar, it observes distances of approximately 6" to 25" for the door width. The overview image is also used to determine whether the door is ER-type. Camera III is known as the "side camera". It is positioned in the middle of two pairs of sensors, provides a view of vertical profile obtained by laser stripe II. The side-view images taken from camera III are used to determine panel shape. Its field of view is approximately 7".

6.5 Door classification procedure

The following list describes the sequence of events that are involved in classifying the style of one door.

1) The system is initialized. It immediately begins to acquire images from camera I and check for the appearance of a door.

2) An operator places a door against the alignment bar, and the door begins to move toward laser stripe I. Doors must be separated by at least 24" along the conveyor. (This is limited by the current classification system speed.) Non-ER doors may travel top or bottom first. ER-type doors must travel with the normal profile side against the alignment bar.

3) The door enters the field of view for camera I. As soon as the door is detected, the system waits a predetermined amount of time, and then acquires a profile image and an overview image from camera I and II for later processing. The time delay is needed so that the true profile image will have time to come into view.

4) The door soon breaks the light path of sensor I. The timer interrupt is enabled, and interrupts are generated every 1/18.2 second. The timer interrupt is disabled by the departure of the door detected by sensor I. This will be used to measure height by counting the number of interrupts during that period.

5) The door soon breaks the light path of sensor II, and the system acquires an image from camera III. This will be one of the side-view images used to determine panel shape.

6) As soon as the door leaves the light path of sensor I, a second side-view image is taken from camera III. Also, the duration of sensor I being activated is used to compute door height.

7) The system processes the image from camera I to obtain the style code. The system processes the image from camera II to determine the door's width, and whether it is a ER type. Width and height are used together to determine the appropriate size code. The system processes the images from camera III to determine whether the panel shape of the door is cathedral or square. The final classification result including style code and size code are printed on the video monitor.

These processing steps are summarized graphically in Figure 6-7.

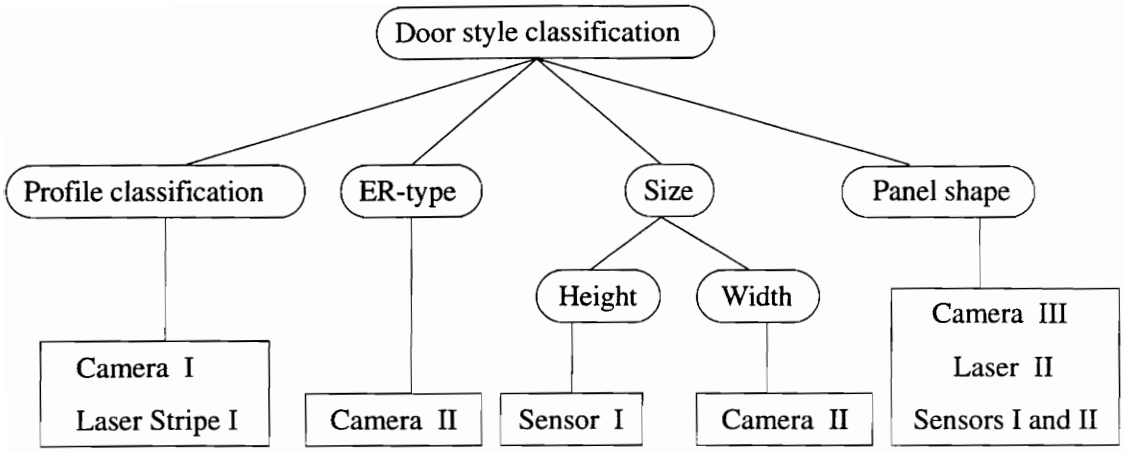

Figure 6-7. Classification of door styles and sizes. The ovals represent the features used in door classification. The rectangles represent the equipment associated with the detection of the feature.

Chapter 7

Performance and Future Enhancement

7.1 Classification system performance

The final classification system described in this thesis has been proved to be successful and reliable. During laboratory tests, it has achieved 99% accuracy at full operational speed for all styles and for most sizes. It was tested by passing 175 sample doors through the system 6 times. There are no unexplainable misclassifications and no "unknowns." The misclassifications are described below.

The most sensitive classification involves distinguishing the Y1, Y2, and 1K profile groups. These three profile groups have the same plateau corner locations, and the only difference among them on the inside profile. As described in section 4.5.1, the system distinguishes these three profile groups by height measurements at two particular locations on the inside profile. This method is very sensitive to position changes, since the profile camera has a resolution of 0.01 inch/pixel. During the experiments, we observed that misclassification of these groups occurs on narrowest doors or widest doors only. The reason for this is illustrated in Figure 7-1. The misclassification is due to a curved conveyor belt. Any curvature in the conveyor belt surface can cause a difference of several pixels in the profile image. The narrowest doors and widest doors are both tilted on the curved conveyor, causing a height change at the two points of interest.

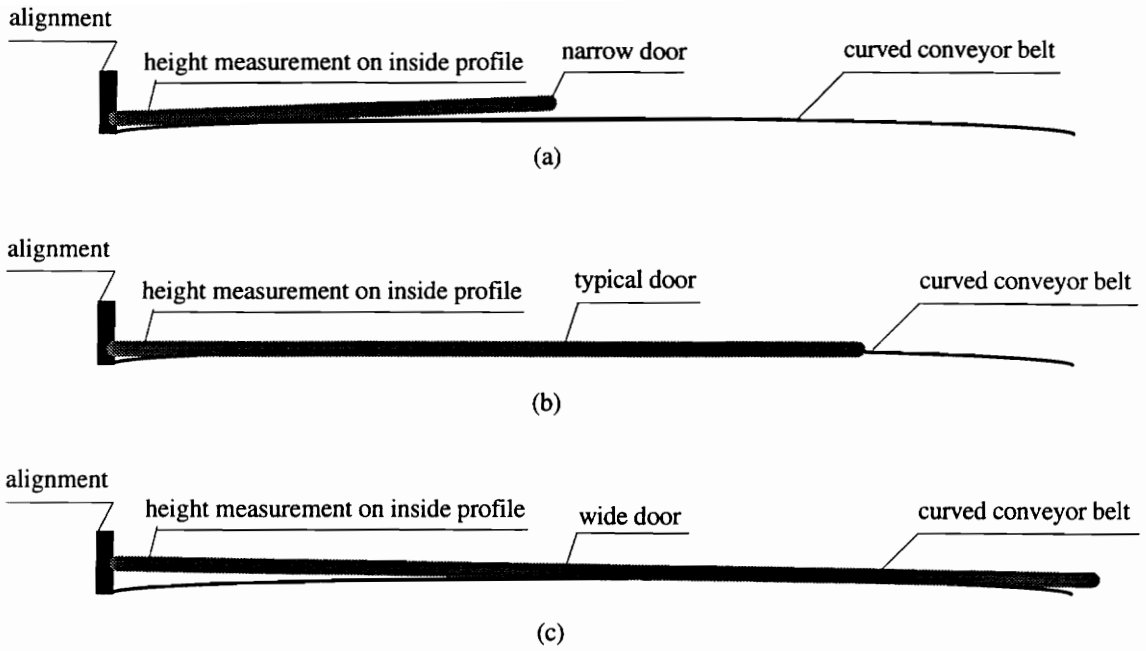

Figure 7-1. Illustration of misclassification among profile groups 1K, Y1, and Y2. (a) A narrow door tilts on the alignment side. This lowers the height measurement on the inside profile, and misclassification occurs. (b) A normal-width door, which is not tilted on the conveyor belt. The current classification method can identify the style correctly. (c) A wide door also tilts on the curved conveyor. This causes an increment in height measurement on the inside profile, and misclassification occurs.

Another misclassification is failure to mark some square panel doors as "unknowns". This is caused by the limitation of panel shape classification method. As described in Chapter 6, the final classification station assumes that vertical profiles are symmetric for square panels. Normally, the vertical profile should be symmetric for all square panel doors currently produced. However, as shown in Figure 7-2, a few samples of square panel doors do not have same top and bottom horizontal bar, so that their vertical profile is not symmetric. In this case, the classification system will misclassify them as cathedral panels instead of marking them as "unknown".

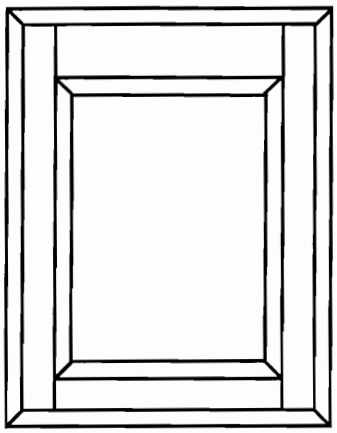

Figure 7-2. An "unknown" square panel door. Notice that the widths of the top and bottom horizontal bars are different. With the current panel shape classification method, it is misclassified as a cathedral panel door.

7.2 Future enhancement

Several performance enhancements are suggested here. These would reduce the sensitivity of profile classification, improve the method of panel shape analysis, increase the classification speed, and simplify the process of adding new styles and deleting old styles.

Door profile shapes are designed using lines and circular arcs. Plateau corner detection is a major step for segmenting a door profile into inside profile, plateau, and outside profile. The current height measurement method is not only sensitive to position change, but is also very limited. It is not guaranteed to work if profile groups cannot be separated by the plateau corner locations. Features that are unique to the profile style such as curvature, inflection points, and discontinuity points will differentiate subtle changes in profile design better. However, the detection of these features will increase the

computational complexity. A least-squares curve fitting method is suggested for this, and is presented in Appendix A. We have experimented with the inside profile of the 1K, Y1, and Y2 group. It is concluded that second or third order polynomial curve fitting can be used to classify these three profile groups.

The current panel shape classification method depends on the symmetric property of vertical profiles for square panels. One alternative is to add another laser source that generates a laser stripe close to and parallel to laser stripe II, so that the curvature on the cathedral panel can be detected by the difference in two vertical profiles. A drawback is that this approach will increase cost and processing difficulty.

The current classification system runs at the full speed specified in a factory environment, but it requires a spacing of two feet between doors to provide enough processing time. It is desirable to reduce the required spacing. Possibly, improvements in program efficiency can be used to reduce the spacing. Another approach is to reduce the image acquisition time. This can possibly be accomplished by modifying the equipment spacing on the classification station, or by changing the order of image acquisitions to reduce the waiting period between acquisitions.

Adding or deleting a profile is not easy with the current algorithm. It requires detailed feature analysis before updating the source code. One alternative to avoid updating the source is to use a profile database to provide IF .. ELSE statements to the program code. The profile database could include the number of profile currently in

production, a set of plateau corner locations, and other features necessary. Developing an analysis program to automatically collect these features is recommended.

Chapter 8

System installation and calibration

8.1 Overview

The station for door classification includes a host computer with a video digitizer, three cameras, two lasers, and two photoelectric sensors. These equipment items are listed in Table 8-1. The three cameras are referred to as the profile camera (camera I), the overview camera (camera II), and the sideview camera (camera III). Two lasers generate fan-shaped light planes, and these light planes intersect the components on the conveyor belt to form a horizontal profile and a vertical profile of each door. As shown in Figure 8-1, laser stripe I forms horizontal profiles observed by camera I and camera II, and laser stripe II generates vertical profiles observed by camera III. Sensor I and sensor II are used to trigger image acquisition. In addition, sensor I is used to provide a height measurement of the door.

As described in Chapter 4 and Chapter 6, placement of this equipment is critical to door classification tasks. Profile classification and panel height measurement depend on the location of the laser stripe in the image, and are very sensitive to camera positions. Door height measurement depends on knowledge of the conveyor belt speed, which must be controlled to within a certain range. Therefore, system calibration before classification is important. In this chapter, we describe an installation procedure for the final

classification system, a camera alignment algorithm, and a calculation of tolerance of conveyor belt speed.

Table 8-1. Equipment list.

Equipment	Quantity	Description	Manufacture & model
Host computer	1	This system serves as the overall controller of the system. It initiates image acquisition, controls image-processing operations, provides a user interface.	IBM PC. ValuePoint 486 DX2 66 MHz
Video digitizer	1	This plugs into one slot of the AT bus of the PC. It acquires and stores images up to 1024 rows by 1024 columns in size.	Imaging Technology, Inc. AFG (Advanced Frame Grabber)
Cameras	3	This is a well-known CCD camera that produces black and white images of size 640x480.	Pulnix, Inc. TM-7CN
Lenses	2 1	25 mm (camera I and III) 16 mm (camera II)	
Photoelectric sensors (transmitter, receiver)	2	Two of these 18 mm photoelectric sensors are mounted near the top of the conveyor to detect the presence of a component, and to trigger image acquisition.	Honeywell CP18RDND2 CP18EDX2
Laser	2	These are solid-state laser sources with fan-shaped beam, 45-degree fan angle, 30mW, 115 VAC transformer.	Lasiris, Inc. SNF-512

8.2 Installation procedure

This section describes the installation procedure for the door classification stand. Dimensions and measurements of cameras, lasers, and sensors are illustrated in Figure 8-2. The following symbols are defined to simplify the description.

d_z(object): The vertical distance between object and conveyor belt.

d_y(object): The horizontal distance between the object and alignment bar, perpendicular to the direction of travel.

d_x(object): The horizontal distance between the object and laser stripe I, along the direction of travel.

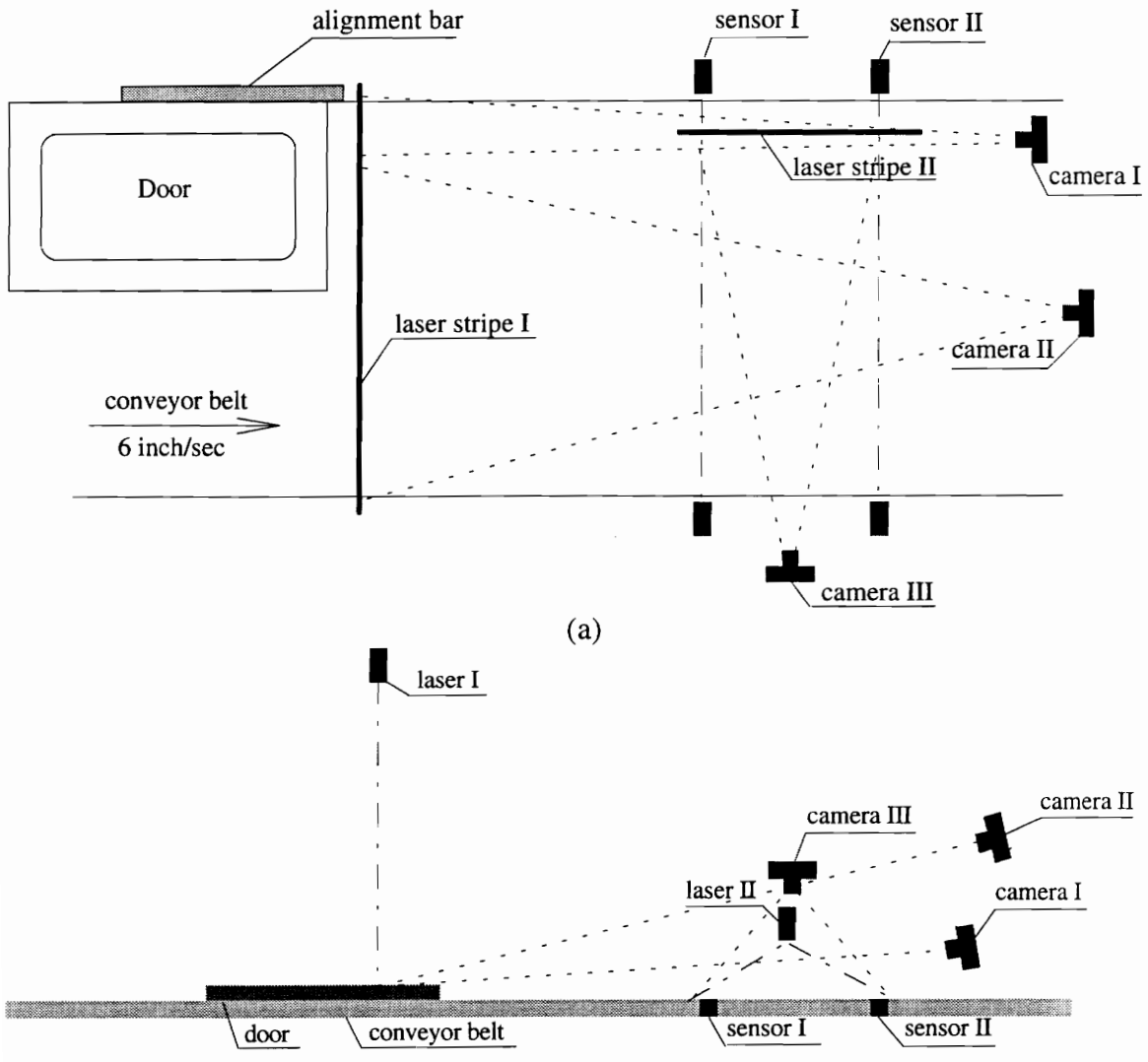

Figure 8-1. Door classification stand. (a) Top view. (b) Side view. Camera I is the profile camera, camera II is the overview camera, and camera III is the sideview camera. Their fields of view are indicated by dotted lines. Laser stripe I generates a horizontal profile viewed by camera I and camera II. Laser stripe II generates a vertical profile, which is observed by camera III. Sensor I and sensor II trigger image acquisition, and sensor I measures door height.

This coordinate system is illustrated in Figure 8-2. Coordinate x and y, shown in Figure 8-2(a), describe top view dimensions. Coordinate x and z, shown in Figure 8-2(b), describe side view dimensions.

Step 1. Installation of laser I

Laser I should be mounted 38 inches above the conveyor belt, so that d_z(laser I) = 38 inches. Laser stripe I is perpendicular to the moving direction of the conveyor belt. The length of laser stripe I is about 30 inches long, and must cover the entire door width beginning at the alignment bar.

Step 2. Installation of sensor I and sensor II

As shown in Figure 8-1(a), dash-dot lines illustrate the emitted light from both photoelectric sensors. They are parallel to laser stripe I.

$$d_x(\text{sensor I}) \approx 15 \text{ (inch)}$$

$$d_x(\text{sensor II}) \approx 22 \text{ (inch)}$$

Step 3. Installation of laser II

Laser stripe II is parallel to the moving direction of conveyor belt. The distance between laser stripe II and the alignment bar is about 2.4 inches. It covers the area between sensor I and sensor II. It is placed approximately 13.5 inches above the conveyor belt, with an 8-inch light stripe visible on the conveyor belt.

$$d_y(\text{laser II}) \approx 2.4 \text{ (inch)}$$

$$d_z(\text{laser II}) \approx 13.5 \text{ (inch)}$$

Step 4. Installation of cameras

Cameras are independent of each other. It is not required to install them in order. The following parameters define the dimension of the three cameras, as shown in Figure 8-2. Camera III must be located half way between the two photoelectric sensors.

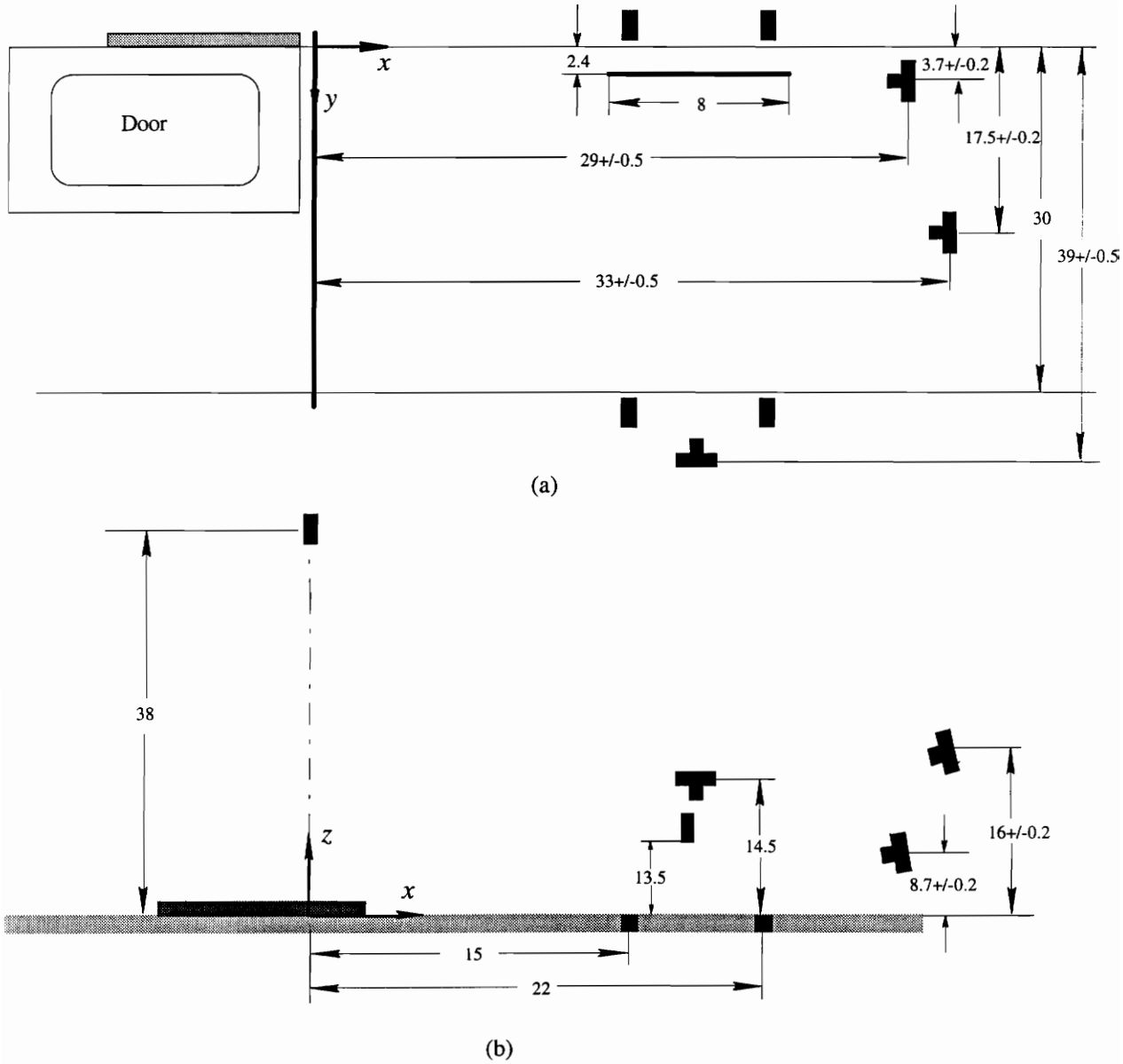

Figure 8-2. Equipment locations. All dimensions are in inches. (a) Top view. (b) Side view.

d_z(camera I) = 8.7 ± 0.2 (inch),

d_x(camera I) = 29± 0.5 (inch)

d_y(camera I) = 3.7± 0.2 (inch)

d_z(camera II) = 16± 0.2 (inch)

d_x(camera II) = 33± 0.5 (inch)

d_y(camera II) = 17.5± 0.2 (inch)

d_z(camera III) = 14.5± 0.2 (inch)

d_y(camera III) = 39 ± 0.5 (inch)

8.3 Camera alignment

Door classification is very sensitive to the orientation of cameras. This is especially true for the profile camera. After installation, the careful alignment of all three cameras is necessary for the system to work reliably.

A separate program has been written to assist in this for the profile and overview cameras. A sample door is used as a template. It can be any cabinet door. Both profile and overview images of this door are saved in a file as template images. Whenever calibration is necessary, the operator will put this sample door on the conveyor belt against alignment bar, and the calibration program will load the template images into memory. The program grabs profile images of the door, and displays both the template and the current image on the screen. The operator then adjusts the camera until both images line up. After aligning the profile camera, the overview camera is adjusted in the same way.

Figure 8-3 is a flow chart of this calibration program. Example images of profile camera calibration are shown in Figure 8-4.

Camera III (sideview camera) is positioned in the middle of sensor I and sensor II. It is use to capture the top and bottom images for panel shape classification. The method for panel shape classification is not very sensitive to camera position. It only requires that the plateau region of both top and bottom images should be horizontal. Example images are shown in Figure 8-5.

8.4 Tolerance of conveyor belt speed

Door height measurement depends on the speed of conveyor belt. Speed variation can cause a misclassification in door height. As described in section 6.2.1, the given speed v of conveyor belt is 6 inch/sec, and the time Δt between interrupts is 1/18.2 second. Door height can be measured by the number of interrupts n, which are counted while the door passes through the sensor.

Let h represent the correct height measurement at speed v, and let h' represent the incorrect height measurement at speed v'. Let n' represent the interrupt count at speed v'. Then we can express the measured heights as

$$h = n' \cdot \Delta t \cdot v' \qquad (8\text{-}1)$$

$$h' = n' \cdot \Delta t \cdot v \qquad (8\text{-}2)$$

Notice that instead of using the changed conveyor speed v' in EQ. 8-2, our program still calculates door height based on the original conveyor speed v. This will certainly cause an

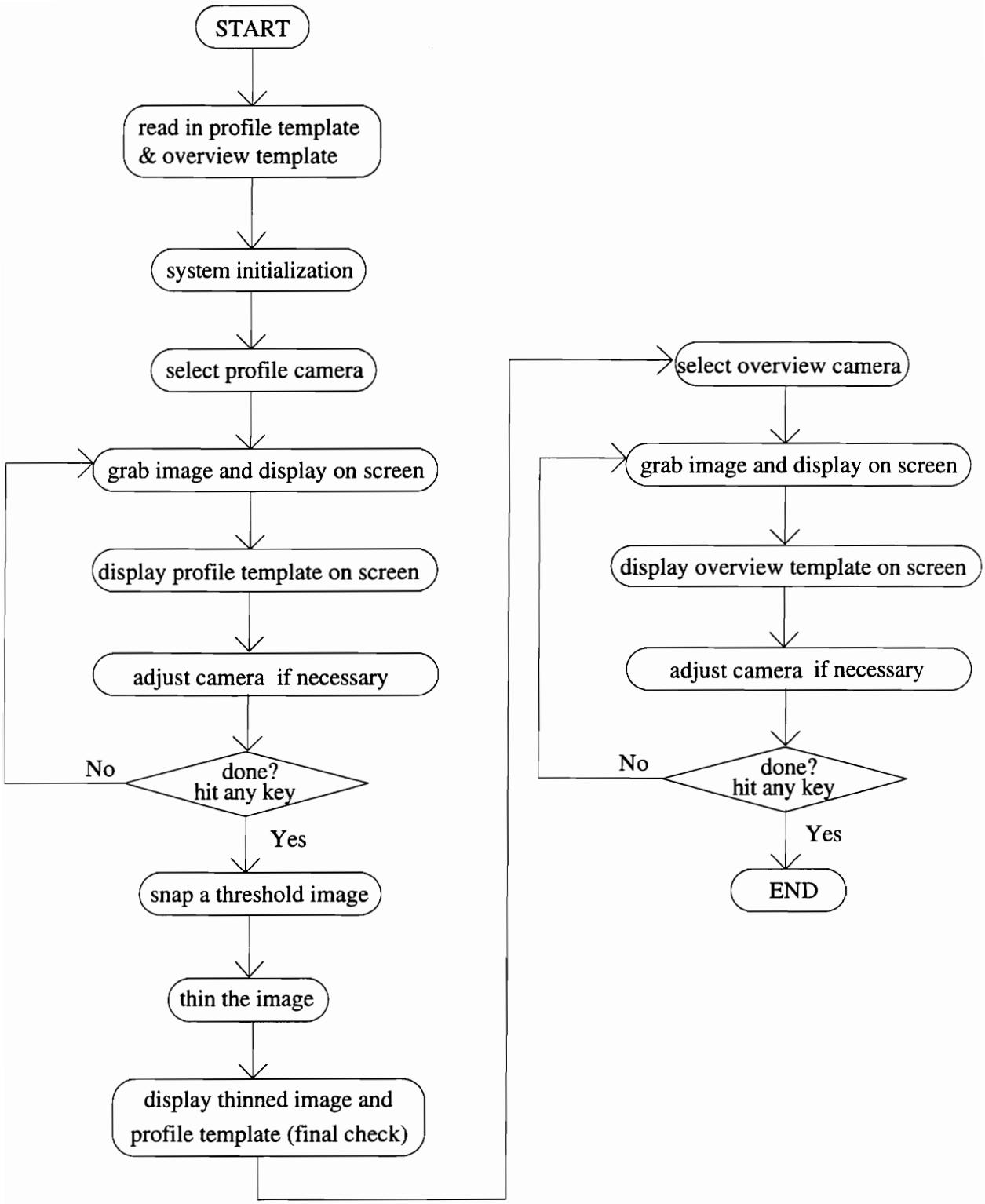

Figure 8-3. Flow chart of alignment program for profile camera and overview camera. This assists the operator in adjusting the camera orientation so that the classification program will operate properly.

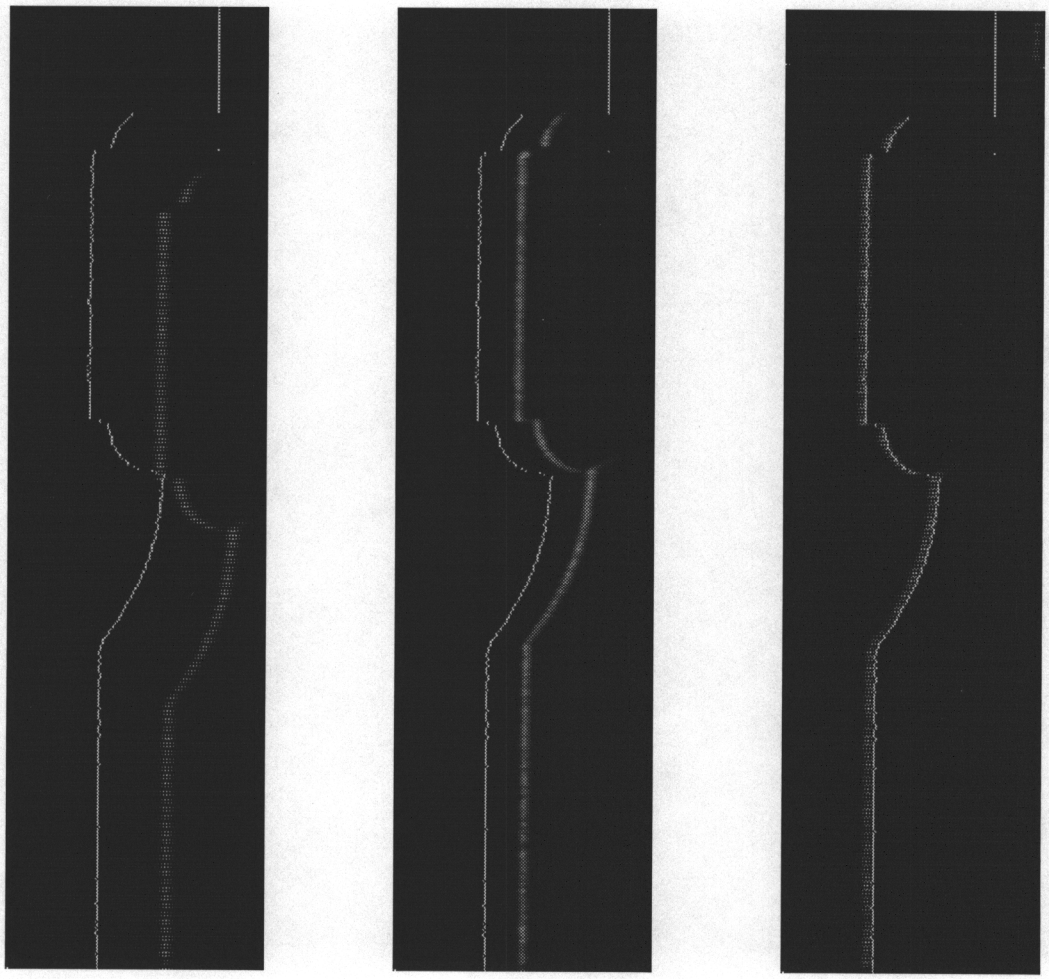

(a) (b) (c)

Figure 8-4. Example images during calibration of profile camera. (a) Images taken at the beginning of calibration. (b) Calibration in progress. (c) Overlap of template and current image, with calibration completed.

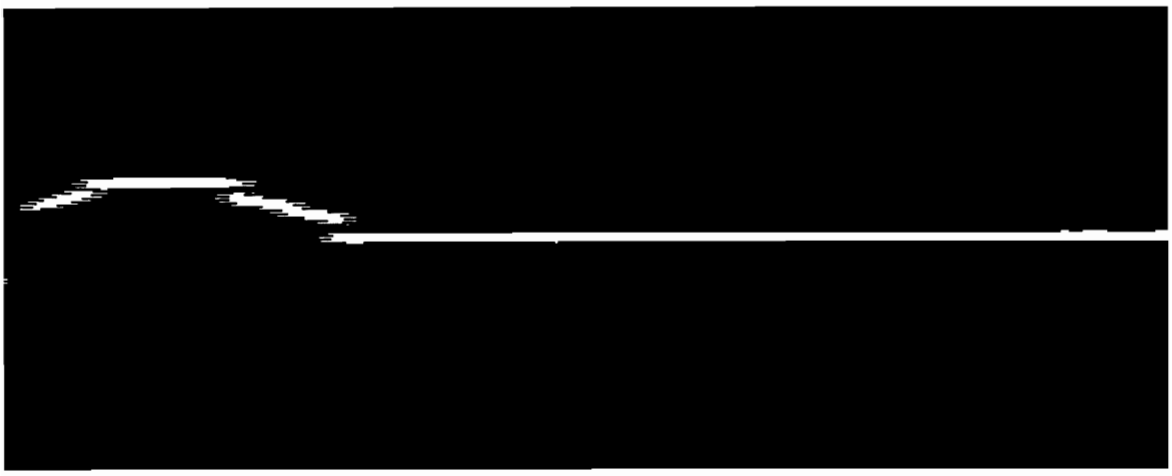

(a)

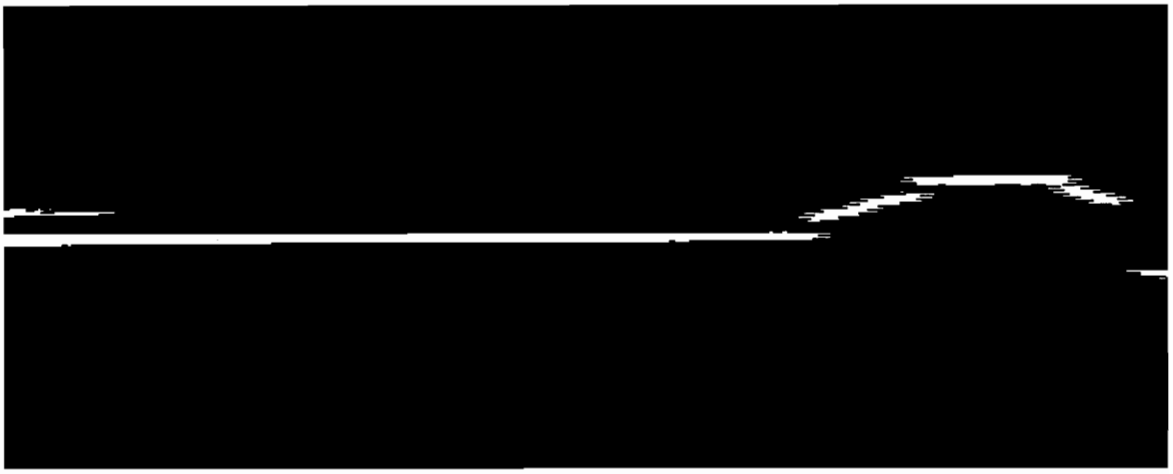

(b)

Figure 8-5. Example images from camera III (sideview camera). (a) Top image. (b) Bottom image. The plateau region of both images must be horizontal. If camera III is in the middle of the two photoelectric sensors, which are used to trigger image captures, then these images appear symmetric for a square panel (as shown).

error in height measurement. The error in height measurement Δh is

$$\Delta h \stackrel{\Delta}{=} h - h' \tag{8-3}$$

Substituting EQ. 8-1 and 8-2 into EQ. 8-3, we have

$$\Delta h = n' \cdot \Delta t \cdot \Delta v \tag{8-4}$$

where $\Delta v = v' - v$. This expresses the fact that an increase in belt speed by Δv will cause a decrease in measured height.

From EQ. (8-1) we have

$$n' = \frac{h}{v' \cdot \Delta t} = \frac{h}{(v + \Delta v) \cdot \Delta t} \tag{8-5}$$

Substituting EQ. 8-5 into EQ. 8-4, we have

$$\Delta h = \frac{h \cdot \Delta v}{v + \Delta v}$$

which can be rearranged as

$$\frac{\Delta v}{v} = \frac{\frac{\Delta h}{h}}{1 - \frac{\Delta h}{h}} \tag{8-6}$$

The largest door height is h = 49.25 inches, and within each size group the smallest height difference is 1.5 inches. According to sampling theorem, the maximum error in height measurement (Δh) caused by speed variation must be less than half of the smallest height difference, so that $\Delta h \leq 0.75$ inch. Substituting these values in EQ. 8-6, we obtain a tolerance of conveyor belt speed of

$$\frac{\Delta v}{v} \approx 0.015 = 1.5\%$$

For the current operational speed of the conveyor belt, we conclude that the conveyor belt speed must be 6.00 ± 0.09 inch/sec for reliable height measurement.

Chapter 9

Conclusion

This thesis has described a classification system that has been developed for manufacturing automation. The system uses structured light and computer vision techniques to classify components on a conveyor. It is capable of correctly classifying the styles and sizes of all doors and door frames currently being produced by American Woodmark Corporation. Development of this system has been motivated by a significant increase in the number of component types being produced at the manufacturing facility. The system exists in prototype form, and has been tested with a large number of samples. It is expected that this system will replace the current manual process, and increase productivity significantly.

References

1. Boyer, K.L., and Kak, A.C., "Color-encoded structured light for rapid active ranging", *IEEE transactions on Pattern Analysis and Machine Intelligence*, Vol. PAMI-9, No. 1, Jan. 1987, pp. 14-28.

2. Nakagawa, Y., "Automatic visual inspection of solder joints on printed circuit boards", *Proceedings of SPIE, Intelligent Robots and Computer Vision,* Vol. 336, 1982, pp. 121-127.

3. Zimmerman, N.J., Scherboom, P.L., Steenvoorden, G.K., and Groen, F.C.A., "Automatic visual inspection system for hybrid circuits", *Workshop on Industrial Applications of Machine Vision*, Research Triangle Park, NC, May 1982, pp. 55-61.

4. Wilder, J., "Industrial applications of machine vision", *Issues on Machine vision*, Wien, New York, Springer-Verlag, 1989, pp. 331-334.

5. Jang, B.K., and Chin, R.T., "One-Pass Parallel Thinning: Analysis, Properties, and Quantitative Evaluation", *IEEE Transactions on Pattern Analysis and Machine Intelligence*, Vol. PAMI-14, No. 11, Nov. 1992, pp. 1129-1140.

6. Ballard, D.H., and Brown, M.C., *Computer Vision*, Prentice-Hall, Inc., 1982.

7. Chin, R.T., and Wan, H.K., "A One-Pass Thinning Algorithm and its Parallel Implementation", *Computer Graphics, and Image Processing*, Vol. 40, 1987, pp. 30-40.

8. Marr, D., and Hildreth, E., "Theory of edge detection", *Proceedings of the Royal Society of London*, Vol. B207, 1980, pp. 187-217.

9. Tan, H.L., Gelfand, S.B., and Delp, E.J., "A cost minimization approach to edge detection using simulated annealing", *IEEE Transactions on Pattern Analysis and Machine Intelligence*, Vol. PAMI-14, No.1, Jan. 1991, pp. 3-18.

10. Hancock, E.R., and Kittle, J., "Discrete relaxation", *Pattern Recognition*, Vol. 23, 1990, pp. 711-733.

11. Canny, J., "A computational approach to edge detection", *IEEE Transactions on Pattern Analysis and Machine Intelligence*, Vol. PAMI-8, No. 6, Nov. 1986, pp. 679-697.

12. Franz L. Alt, "Digital Pattern Recognition by Moments", *Journal of Association of Computing Machinery*, Vol. 11, No. 2, 1962, pp. 240-258.

13. Zakaria, M.F., Vroomen, L.J., Zsomber-Murray P.J.A., and Van-Kessel, J.M.H.M., "Fast Algorithm for the Computation of Moment Invariants", *Pattern Recognition*, Vol. 20, 1987, pp. 639-643.

14. Dai, M., Baylou, P., and Najim, M., "An Efficient Algorithm of Computation of Shape Moments from Run-length Codes or Chain Codes", *Pattern Recognition*, Vol. 25, 1992, pp. 1119-1128.

15. Duda, R.O., and Hart, P.E., *Pattern Classification and Scene Analysis*, Wiley, 1973.

16. Anisimov, V.A., and Gorsky, N.D., "Fast Hierarchical Matching of an Arbitrarily Oriented Template", *Pattern Recognition Letters*, Vol. 14, 1993, pp. 95-101.

17. Ventura, J.A., and Chen, J.M., "Segmentation of Two Dimensional Curve Contours", *Pattern Recognition*, Vol. 25, 1992, pp. 1129-1140.

18. Pei, S.C., and Lin, C.N., "The Detection of Dominant Points on Digital Curves by Scale-Shape Filtering", *Pattern Recognition*, Vol. 25, 1992, pp. 1307-1314.

19. Teh, C.H., and Chin, R.T., "On Detection of Dominant Points on Digital Curves", *IEEE Transactions on Pattern Analysis and Machine Intelligence*, Vol. PAMI-11, No. 8, 1989, pp. 859-872.

20. Ciccotelli, J. and Portala, J.-F., "Applications of artificial vision in the wood industry,", *Industrial Metrology*, Vol. 2, No. 3 and 4, May 1992, pp. 185-194.

21. Pölzleitner, W. and Schwingshakl, G., "Real-time surface grading of profiled wooden boards," *Industrial Metrology*, Vol. 2, No. 3 and 4, May 1992, pp. 283-298.

22. Cho, T. H., Conners, R. W., and Araman, P. A., "A computer vision system for automatic grading of rough hardwood lumber using a knowledge-based approach," *Proc. IEEE International Conference on Systems, Man, and Cybernetics,* Nov. 1990, pp. 345-350.

Appendix A

Profile classification using curve fitting

As we described in Chapter 4, most profile groups shown in Figure 2-5 can be classified by the location of plateau endpoints. But the location of plateau endpoints for profile group 1K, Y1, and Y2 are exactly the same. The only difference among these three groups is the inside profile. The method that we used to distinguish them is the height measurement at two particular points on the inside profile. As discussed in Chapter 7, this method is very sensitive to position change, so that any variation in placement or curvature on conveyor belt surface may cause a misclassification of these three groups.

One possible approach to classify their inside profiles is using curve fitting. This appendix describes least-squares curve fitting, and experiment result of classification using curve fitting on the inside profiles.

A-1 Least Squares Fitting of a polynomial

Let us attempt to fit a polynomial of fixed degree m

$$y = a_0 + a_1 x + \cdots + a_m x^m \qquad \text{(A-1)}$$

to n points

$$(x_1, y_1), (x_2, y_2), \ldots\ldots, (x_n, y_n)$$

Substituting these n values of x and y into (A-1) yields the n equations:

$$y_1 = a_0 + a_1 x_1 + \cdots + a_m x_1^m$$

$$y_2 = a_0 + a_1 x_2 + \cdots + a_m x_2^m$$

. . . .

. . . .

. . . .

$$y_n = a_0 + a_1 x_n + \cdots + a_m x_n^m$$

This can be represented in vector form

$$Y = M\,V \qquad \text{(A-2)}$$

where

$$Y = \begin{bmatrix} y_1 \\ y_2 \\ \vdots \\ y_n \end{bmatrix},$$

$$M = \begin{bmatrix} 1 & x_1 & \cdots & x_1^m \\ 1 & x_2 & \cdots & x_2^m \\ \vdots & \vdots & \vdots & \vdots \\ 1 & x_n & \cdots & x_n^m \end{bmatrix},$$

$$V = \begin{bmatrix} a_0 \\ a_1 \\ \vdots \\ a_n \end{bmatrix}$$

If $n > m$ and if not all of the n data points are on the mth order curve, it is impossible to find a vector V to satisfy (A-2). In this case, we define the error vector between the actual points as

$$E = Y - MV$$

$$\stackrel{\Delta}{=} [e_1 \; e_2 \; .... \; e_n]^T \qquad \text{(A-3)}$$

Our objective will be to find a vector V that minimizes E, which is equivalent to minimizing the sum of squares $\sum e_i^2$.

If V^* is such a minimizing vector, $V^* = [a_0^* \; a_1^* \; ... \; a_m^*]^T$, then

$$V^* = (M^T M)^{-1} M^T Y \qquad \text{(A-4)}$$

The standard deviation of the fitting error is used to describe degree of fitness, given by

$$\sqrt{\frac{1}{n-1}\sum_{i=1}^{n}(e_i - \bar{e})^2} \qquad \text{(A-5)}$$

where $\bar{e}$ is the mean of e_i, which is given by

$$\bar{e} = \frac{1}{n}\sum_{i=1}^{n} e_i \qquad \text{(A-6)}$$

A-2 Experiment and result

The following tables are the curve fitting results for the *inside profile* only of 1K, Y1, and Y2. Four images for each style were obtained using the classification station. Second, third, and fourth order polynomials have been fit to these curves using EQ. A-4.

A standard deviation of fitting error is calculated, and shown in the last column of Tables A-1 to A-3.

Table A-1. Results from second-order polynomial curve fitting. Style designations are at the left. The last column of the table is the standard deviation of fitting error.

	a_0	a_1	a_2	a_3	a_4	**STD**
Y1	60.7147	-0.2325	-0.0007	N/A	N/A	1.0418
	60.3157	-0.2103	-0.0006			1.0405
	61.4271	-0.2058	-0.0008			0.9387
	61.8549	-0.2609	-0.0001			1.0615
Y2	65.1459	-0.0071	-0.0058	N/A	N/A	0.5588
	66.4844	-0.0173	-0.0058			0.6091
	67.1735	-0.0264	-0.0052			0.6165
	64.1116	-0.0043	-0.0053			0.5679
1K	70.2115	-0.2398	-0.0006	N/A	N/A	0.6839
	70.8886	-0.2302	-0.0009			0.8076
	67.5005	-0.2202	-0.0011			0.8986
	67.7324	-0.2109	-0.0012			0.6512

Table A-2. Results from third-order polynomial curve fitting.

	a_0	a_1	a_2	a_3	a_4	**STD**
Y1	59.3395	0.0084	-0.0098	0.0001	N/A	0.9258
	59.1299	-0.0056	-0.0082	0.0001		0.9553
	60.6003	-0.0631	-0.0061	0.0001		0.8936
	60.4397	-0.0130	-0.0094	0.0001		0.9408
Y2	65.0950	-0.0165	-0.0062	0.0000	N/A	0.5585
	66.7090	-0.0209	-0.0044	0.0000		0.6041
	67.4877	-0.0799	-0.0032	0.0000		0.6067
	64.6641	-0.0970	-0.0020	0.0000		0.5342
1K	70.8219	-0.3452	0.0033	-0.0000	N/A	0.6501
	71.8345	-0.3912	0.0049	-0.0001		0.7374
	68.5006	-0.3904	0.0051	-0.0001		0.8284
	68.5271	-0.3442	0.0036	-0.0000		0.5894

Table A-3. Results from fourth-order polynomial curve fitting.

	a_0	a_1	a_2	a_3	a_4	STD
Y1	57.9314	0.4077	-0.0365	0.0007	-0.0000	0.8323
	59.3385	0.2993	-0.0304	0.0006	-0.0000	0.8858
	59.8080	0.1585	-0.0207	0.0004	-0.0000	0.8639
	58.2744	0.2336	-0.0240	0.0004	-0.0000	0.9929
Y2	64.7082	0.1247	-0.0133	0.0002	-0.0000	0.5472
	64.3073	0.0001	-0.0082	0.0001	-0.0000	0.5241
	67.0694	0.0355	-0.0107	0.0002	-0.0000	0.5945
	66.2478	0.1063	-0.0127	0.0002	-0.0000	0.5892
1K	69.6895	-0.0285	-0.0176	0.0004	-0.0000	0.5620
	67.4174	-0.0424	-0.0158	0.0004	-0.0000	0.4938
	66.3301	-0.0282	-0.0338	0.0008	-0.0000	0.5405
	70.2901	-0.0347	-0.0228	0.0006	-0.0000	0.5867

A-3 Conclusion

From Table A-1 to A-3, we draw following conclusions:

1) Y1 can be distinguished by cofficient a_0 from the second, third, and fourth order least square curve fitting.

2) Y2 and 1K can not be separated by fourth order curve fitting. However, they can be separated by a_1 and a_2 in third order polynomial curve fitting; or by a_1 in second order polynomial curve fitting.

3) Second and third order polynomials are sufficient to fit the inside profile of Y1, Y2, and 1K. Orders higher than that are not necessary, and will not guarantee good result.

VITA

Bin Yuan was born on September 9, 1967, in Shanghai, China. She graduated from Fu-Xin High School, Shanghai, China, in 1985. She attended Zhejiang University in China and received a Bachelor of Engineering degree in Biomedical Engineering in 1990. She received a Master of Science degree in Electrical Engineering from Virginia Polytechnic Institute and State University in 1994.